ROBUST REPETITIVE CONTROL AND APPLICATION TO A CD PLAYER

Chak Hong Lee

Trinity Hall
Cambridge

A dissertation submitted for
the degree of Doctor of Philosophy

February 1998

To my parents, my brothers, my sister and Fion

Abstract

Repetitive control (RC) has been used in various industrial applications. The aim of RC is to asymptotically track/reject periodic references/disturbances. Typically, these signals are of known fundamental period but unknown amplitudes and phase. A main focus of the dissertation is the robustness of RC schemes to plant model uncertainty. In particular, the trade-offs and limitations imposed by robustness requirements on steady state disturbance response and transient performance are investigated. Controller designs and implementations are also considered.

In this dissertation, robustness is measured using the gap metric. A linear control approach to RC is first investigated. An expression for the optimal gap metric robustness margin subject to the requirement of asymptotic rejection of periodic disturbances is derived. This shows the interaction between robustness and RC requirements. As a complement to this, the optimal achievable steady state attenuation for a prescribed robustness level is also given. For the transient state, a *power-energy induced measure* is defined. This measure describes the energy of the worst transient output corresponding to periodic inputs with unit power. The relation between this transient measure and robustness is examined. A CD player control design problem is considered both theoretically and experimentally. Two design approaches are considered, one of which is implemented in real-time on a CD player experimental rig. Finally, the dissertation considers nonlinear RC. It is pointed out that complete asymptotic rejection of a periodic disturbance is not achievable robustly with a linear controller in the case that the periodic signal has infinitely many non-zero harmonics. It is shown that nonlinear control can achieve robust asymptotic disturbance rejection for a specific waveform, e.g. for a triangular waveform disturbance.

Keywords: Repetitive Control, Periodic Signals, Robust Stability, Disturbance Rejection, Steady State Attenuation, Transient Performance, Triangular Waveforms, Gap Metric, $\mathcal{H}_\infty$ Loop Shaping, Closed-loop Pole Placement.

Acknowledgements

It is a great pleasure to express my gratitude to my supervisor Dr. Malcolm C. Smith for his constant guidance and encouragement during the past three years. He has been offering his precious time generously with me to communicate ideas and provide helpful advice. I would also like to thank Professor Keith Glover, Dr. Jan Maciejowski, Dr. Glenn Vinnicombe and Dr. Gunnar Hillerström, from whom I have learnt much about engineering and control theory.

I am also grateful to my colleagues, past and present, in the Cambridge University Engineering Department (CUED) Control Group for creating a relaxed and supportive working environment. I would like to sincerely thank Dr. Thomas Fliegner, Miss Olivia Kwong and Miss Mabel Wong for spending evenings in proofreading various chapters of the manuscript. Many thanks also go to my friends in Cambridge and in Hong Kong for sharing their happiness, joy and burdens.

I am greatly indebted to my parents, my brothers, my sister and my relatives for their non-stop encouragement and support during my years in Cambridge. I wish to thank Miss Fion Chui for her care and concern during the completion of my Ph.D.

This work has been financially supported by the Overseas Research Student Award and the Cambridge Commonwealth Trust (CCT). Travel grants for conference attendance was also received from CCT, Cambridge Philosophical Society, CUED and Trinity Hall. The overrun funding was granted by CCT and CUED.

I would also like to declare that I am the author R.C.H. Lee appeared in the Bibliography of this dissertation.

As required by University Statute, I hereby declare that this dissertation is not substantially the same as any that I have submitted for a degree or other qualification at any other University. This dissertation is the result of my own work and includes nothing which is the outcome of work done in collaboration.

C.H. Lee
Trinity Hall
Cambridge
February 1998

Contents

List of Figures

List of Tables

Notations

Symbols	**Page**	**Descriptions**
$\in$		is an element of
$\mathbb{R}$	3	field of real numbers
$\mathbb{R}_+$	3	set of non-negative real numbers
$\mathbb{Z}$	3	ring of integers
$\mathbb{Z}_+$	3	set of non-negative integers
$\mathbb{C}$	3	field of complex numbers
$\Re(\cdot)$	3	real part of $(\cdot)$
$f(s)^*$	3	complex conjugate transpose function of $f(s)$
$\sigma_{\max}(\cdot)$	3	maximum singular value of $(\cdot)$
$\sigma_{\min}(\cdot)$	3	minimum singular value of $(\cdot)$
$\lambda_{\max}(\cdot)$	3	maximum eigenvalue of $(\cdot)$
$\\|\cdot\\|_{\mathrm{H}}$	3	maximum Hankel singular value
$\mathscr{L}_2(\mathbb{R}_+)$	4	space of all (Lebesgue measurable) functions on $\mathbb{R}_+$ with finite energy
$\mathscr{H}_2$	4	Laplace transform of functions in $\mathscr{L}_2(\mathbb{R}_+)$
$\mathscr{L}_{2e}(\mathbb{R}_+)$	5	extended space of $\mathscr{L}_2(\mathbb{R}_+)$
$\mathscr{L}_\infty(\mathbb{R}_+)$	5	space of all essentially bounded functions on $\mathbb{R}_+$
$\\|\cdot\\|_{\mathscr{P}}$	5	power of a signal
$\mathcal{L}_\infty$	9	a Banach space
$\mathcal{RL}_\infty$	9	set of all real-rational functions in $\mathcal{L}_\infty$
$\mathcal{H}_\infty$	9	set of all stable $\mathcal{L}_\infty$ functions, a Hardy space
$\mathcal{RH}_\infty$	9	set of all real-rational functions in $\mathcal{H}_\infty$
$\mathcal{L}_2$	9	a Hilbert space
$\mathcal{RL}_2$	9	set of all real-rational functions in $\mathcal{L}_2$
$\mathcal{H}_2$	10	set of all stable $\mathcal{L}_2$ functions
$\mathcal{RH}_2$	10	set of all real-rational functions in $\mathcal{H}_2$

Symbols	**Page**	**Descriptions**
$M,\ N,\ \tilde{M},\ \tilde{N}$	10	coprime factors
$[\mathbf{P},\mathbf{C}]$	11	feedback loop in Figure 2.1
$\mathcal{G}_{\mathbf{P}},\ \mathcal{G}_{\mathbf{C}}$	11	graphs of causal mappings **P** and **C**
$\Pi_{\mathcal{G}_{\mathbf{P}}//\mathcal{G}_{\mathbf{C}}},\ \Pi_{\mathcal{G}_{\mathbf{C}}//\mathcal{G}_{\mathbf{P}}}$	16	parallel projections
$\vec{\delta}(\mathcal{X},\mathcal{Y})$	16	directed gap between two sets $\mathcal{X}$ and $\mathcal{Y}$
$\delta(\mathcal{X},\mathcal{Y})$	16	gap between two sets $\mathcal{X}$ and $\mathcal{Y}$
$b_{\mathbf{P},\mathbf{C}},\ b_{P,C}$	16	gap metric robustness margin
$\Omega_n,\ \Omega_\infty$	25	set of frequencies under consideration
$\mathcal{S}_n,\ \mathcal{S}_\infty$	25	set of signals (expressed in Fourier series) under consideration
$b_{\mathrm{opt}}(P,\Omega_n)$	26	constrained optimal robustness margin in rejecting frequencies in Ω_n
$\Vert G\Vert_{\mathrm{tr}\leftarrow\mathcal{S}_n}$	32	power-energy induced measure of transient output of a stable system G excited by periodic signals in $\mathcal{S}_n$
R_{error}, RE	41	electrical radial error signals
$\mathcal{T}(\omega_0)$	52	class of triangular signals with fundamental frequency ω_0

Acronyms	**Page**	**Descriptions**
RHP	3	open right half plane
SISO	6	single-input single-output
MIMO	6	multi-input multi-output
LTI	7	linear time-invariant
LCF	10	left-coprime factorization
RCF	10	right-coprime factorization
GM	18	gain margin
PM	18	phase margin
IMP	22	internal model principle
DSP	42	digital signal processor

1

Introduction

1.1 Overview

One of the main concerns in feedback system analysis is to achieve some prescribed performance requirements. Mathematical optimization techniques, such as Linear Quadratic Gaussian theory, have been used as the basic tools in controller designs. However, some design approaches are not able to deal with robustness question directly in the design process. The discrepancies between mathematical models and real systems are inevitable in nature and they may cause serious effects on performance or even instability in the feedback loop. In the past couple of decades, the issue of robustness to uncertainties and plant variabilities has been addressed with development of new methods. $\mathcal{H}_\infty$ control has been shown to be a systematic, effective and reliable method in obtaining robust controllers. This method has also been proved to be efficient and accurate in practical designs, especially with the help of sophisticated computation softwares, such as MATLAB.

The research on repetitive control began in 1980s. The aim of repetitive control is to achieve tracking/rejection of periodic references/disturbances and internal stability. This area has been studied extensively and is found to have many applications in industry.

This dissertation raises the issue of robustness in repetitive control. The research was motivated by an undergraduate CD player control experiment at Cambridge University, which investigates the d.c. disturbance rejection and stabilization of the CD player rig using proportional-integral (PI) lead-lag controller design. This control system has relatively good gain and phase margins. However, it does not reject completely periodic disturbances arising from imperfections in a CD. The general question of achieving such a requirement with a robust controller was a starting point for this dissertation.

This research is principally concerned with understanding the trade-offs and limitations imposed by robustness requirements on steady state disturbance response and transient performance for periodic signals. The gap metric is adopted as a measure of robustness. Practical controller design methods, with applications to a CD player, for repetitive control of some general periodic signals are also illustrated. It can be seen that a linear control approach has limitations to robust stability and is not applicable to some repetitive control problems. An extension of the theory using a nonlinear control approach is given as a feasible solution to them.

1.2 Outline of the Dissertation

A general outline of the contents of this dissertation is as follows.

Chapter 2 Some general mathematical preliminaries relevant to robust control and repetitive control are described in this chapter and mathematical notations are fixed. The standard feedback configuration which will be used throughout is introduced.

Chapter 3 This chapter contains a literature survey and some theories of repetitive control. It also contains some results of linear repetitive control concerning robust stability, steady state behaviour, transient performance and design methods.

Chapter 4 Some descriptions of a CD player and controller designs are given. Practical issues on controller design and real-time implementation results are also presented.

Chapter 5 This chapter investigates the nonlinear theory of repetitive control in certain cases where linear repetitive control fails.

Chapter 6 This is a brief concluding chapter summarizing the main contributions of this dissertation and making some recommendations for future research in this area.

Appendices Proofs and side materials which are complementary to the main context are given.

2

Preliminaries

This chapter outlines some notations and mathematical tools in modern control theory which will be used throughout this dissertation. It is neither complete nor self-contained, as readers are assumed to have some basic knowledge of modern control theory. Propositions in this chapter are stated without proof. Instead, full references are given. The definitions and results in this chapter are valid in a multi-dimensional setting, though corresponding dimensions are suppressed in the notations. Moreover, all signals and systems under consideration are supposed to be continuous-time.

Some general mathematical notations are listed in Section 2.1. Definitions and basic properties of signals and systems are recalled in Section 2.2 and Section 2.3, respectively. Some aspects of modern robust control theory such as coprime factorizations (Section 2.3.3), graph of a system (Section 2.3.4), feedback and stability (Section 2.4), plant uncertainties (Section 2.5), gap metric (Section 2.6) are reviewed. Finally, two controller design methods are recapitulated in Section 2.7.

2.1 General Definitions

Denote the field of real numbers by $\mathbb{R}$ and the subset of all non-negative real numbers $\{x : x \geq 0\}$ by $\mathbb{R}_+$. Similarly, $\mathbb{Z}$ and $\mathbb{Z}_+$ refer to the ring of all integers and the subset $\{n \in \mathbb{Z} : n \geq 0\}$, respectively. $\mathbb{C}$ stands for the field of all complex numbers, with $j := \sqrt{-1}$. The real part of a complex number s is denoted by $\Re(s)$. RHP represents the open right half plane $\{s \in \mathbb{C} : \Re(s) > 0\}$. If $f(s)$ is a matrix function of s, $f(s)^* := \overline{f(-\overline{s})}^T$. The maximum singular value, the minimum singular value and the maximum eigenvalue of a matrix A are denoted by $\sigma_{\max}(A)$, $\sigma_{\min}(A)$ and $\lambda_{\max}(A)$, respectively. $\|G\|_{\mathrm{H}}$ refers to the maximum Hankel singular value of a transfer function G [ZDG96].

2.2 Signals

Definition 2.2.1. *A (continuous-time) signal is a Lebesgue measurable function that maps* $\mathbb{R}_+$ *into* $\mathbb{C}^r$*.*

The class of all signals forms a linear space with addition and scalar multiplication defined in the usual way.

Definition 2.2.2. *The* 2*-norm (or energy) of a signal* f *is defined as the Lebesgue integral*

$$\|f\|_2 := \left(\int_0^\infty |f(t)|^2\, dt\right)^{\frac{1}{2}}.$$

Denote the set of all signals f *with finite energy by* $\mathscr{L}_2(\mathbb{R}_+)$ *(or simply* $\mathscr{L}_2$*), i.e.*

$$\mathscr{L}_2(\mathbb{R}_+) := \{f : \|f\|_2 < \infty\}.$$

Remark 2.2.3. *We denote the set of Laplace transforms of elements in* $\mathscr{L}_2(\mathbb{R}_+)$ *as*

$$\mathscr{H}_2 := \{\hat{f} : f \in \mathscr{L}_2(\mathbb{R}_+)\}$$

with the 2*-norm in this space defined as*

$$\|\hat{f}\|_{\mathscr{H}_2} := \left(\frac{1}{2\pi}\int_{-\infty}^{\infty} |\hat{f}(j\omega)|^2\, d\omega\right)^{\frac{1}{2}}.$$

For background material on Laplace transforms, see e.g. [GL95].

Remark 2.2.4. *The* 2*-norm of an* $\mathscr{L}_2$ *function* f *can also be computed in the frequency domain (Parseval's identity) [ZDG96, GL95]*

$$\|f\|_2 = \|\hat{f}\|_{\mathscr{H}_2}$$

where $\hat{f}$ *is the Laplace transform of* f*.*

For simplicity, the Laplace transform $\hat{f}(j\omega)$ will be denoted by $f(j\omega)$ as well if no ambiguity can result. We will sometimes use $\mathscr{L}_2(\mathbb{R}_+)$ and $\mathscr{H}_2$ interchangeably to represent the same set of signals. Similar abuse of notations will also be found for some systems (see Section 2.3).

Definition 2.2.5. *Define the truncation operator* $\mathbf{T}_{t_0}$ *as*

$$(\mathbf{T}_{t_0}f)(t) = \begin{cases} f(t) & 0 \le t \le t_0, \\ 0 & \textit{otherwise}, \end{cases}$$

where f *is a signal and* $t_0 \ge 0$*.*

Definition 2.2.6. *The shift operator* $\mathbf{S}_{t_0}$ *is defined as*

$$(\mathbf{S}_{t_0} f)(t) = \begin{cases} f(t-t_0) & \text{when } t \geq t_0, \\ 0 & \text{otherwise,} \end{cases}$$

for any signal f *and* $t_0 \geq 0$.

Definition 2.2.7. *Define the extended* 2*-space* $\mathscr{L}_{2e}(\mathbb{R}_+)$ *as*

$$\mathscr{L}_{2e}(\mathbb{R}_+) = \{f : \mathbf{T}_{t_0} f \in \mathscr{L}_2(\mathbb{R}_+) \text{ for all } t_0 \geq 0\}.$$

Definition 2.2.8. *The (essential) supremum norm of a signal* f *is defined as*

$$\|f\|_\infty := \operatorname*{ess\,sup}_{t \in \mathbb{R}_+} |f(t)|.$$

Denote the space of all essentially bounded signals as

$$\mathscr{L}_\infty(\mathbb{R}_+) := \{f : \|f\|_\infty < \infty\}$$

(or simply $\mathscr{L}_\infty$*).*

We next introduce a third measure (besides the 2-norm and the supremum norm) for signals, which turns out to be useful in some circumstances, especially when dealing with some signals having infinite 2-norms.

Definition 2.2.9. *The average power (or simply power) of a signal* f *is defined as*

$$\|f\|_{\mathscr{P}} := \left(\lim_{\gamma \to \infty} \frac{1}{\gamma} \int_0^\gamma |f(t)|^2 \, dt \right)^{\frac{1}{2}}$$

if the limit exists.

Remark 2.2.10. *Every* $\mathscr{L}_2(\mathbb{R}_+)$ *signal has zero power [DFT92].*

In the sequel, a *signal space* can be either $\mathscr{L}_2(\mathbb{R}_+)$, $\mathscr{L}_{2e}(\mathbb{R}_+)$ or $\mathscr{L}_\infty(\mathbb{R}_+)$.

Definition 2.2.11. *A function* $f : \mathbb{R}_+ \to \mathbb{C}^r$ *is said to be periodic with period* T *if* $f(t+T) = f(t)$ *for all* $t \in \mathbb{R}_+$.

Remark 2.2.12. *If* f *is periodic with period* T *and with finite power, the power can be computed by the formula*

$$\|f\|_{\mathscr{P}} = \left(\frac{1}{T} \int_0^T |f(t)|^2 \, dt \right)^{\frac{1}{2}}.$$

For instance, the power of a unit step is unity and the power of a unit amplitude sinusoid is $1/\sqrt{2}$.

Constant functions, sinusoids, triangular waves and square waves are examples of periodic functions. The following definition describes a useful tool in analysing periodic signals.

Definition 2.2.13. *Suppose a function $f : \mathbb{R}_+ \to \mathbb{C}^r$ is periodic with period T and (Lebesgue) integrable over $[0, T]$. The series*

$$\sum_{k=-\infty}^{\infty} a_k \, e^{j\frac{2\pi}{T}kt}$$

is called the Fourier series of f where

$$a_k := \frac{1}{T}\int_0^T f(t)e^{-j\frac{2\pi}{T}kt}\, dt$$

are called the complex Fourier coefficients of f.

If f is real-valued, the Fourier coefficients satisfy the relations $a_{-k} = \overline{a}_k$ for $k \geq 0$. Denote the partial sum of the Fourier series as

$$S_N^f(t) := \sum_{k=-N}^{N} a_k \, e^{j\frac{2\pi}{T}kt}.$$

A function f defined on an interval I is said to be piecewise C^1 on I if f and its first derivative(s) are piecewise continuous on I. We have the following convergence result:

Proposition 2.2.14. *[Fol92] If $f : \mathbb{R}_+ \to \mathbb{C}^r$ is periodic with period T and piecewise C^1 on $\mathbb{R}_+$, then*

$$\lim_{N\to\infty} S_N^f(t) = \frac{1}{2}\left[f(t-) + f(t+)\right]$$

for every $t > 0$. In particular, f will be equal to its Fourier series if f is also continuous.

2.3 Systems

Definition 2.3.1. *A (continuous-time) system is a mapping $\mathbf{G}$ from the input signal space (e.g. $\mathscr{L}_2(\mathbb{R}_+)$) to the output signal space (e.g. $\mathscr{L}_2(\mathbb{R}_+)$).*

The class of all systems (having the same input signal space and output signal space) forms a linear space with addition as parallel connection and scalar multiplication defined in the usual way. A system is said to be *single-input single-output* (SISO) if the input signals and the output signals are scalar-valued. Otherwise, it is called *multi-input multi-output* (MIMO).

Definition 2.3.2. *A system $\mathbf{G}$ is called causal if for any input and any $t_0 \in \mathbb{R}_+$, the output up to t_0 does not depend on the input for time $t > t_0$.*

$\mathbf{G}$ is causal if $\mathbf{T}_{t_0}\mathbf{G}\mathbf{T}_{t_0} = \mathbf{T}_{t_0}\mathbf{G}$ for all $t_0 \geq 0$, where the equation means both sides are equal when acting on any input signal.

Definition 2.3.3. *Let $w(\cdot)$ be an input signal of a system $\mathbf{G}$ and $z_w(\cdot)$ the corresponding output. If $z_{\mathbf{S}_{t_0}w}(\cdot) = \mathbf{S}_{t_0} z_w(\cdot)$ for any $t_0 \in \mathbb{R}_+$ and any input $w(\cdot)$, the system is said to be time-invariant.*

Definition 2.3.4. *A system $\mathbf{G}$ is said to be linear if*

$$\mathbf{G}(\alpha w_1 + \beta w_2) = \alpha \mathbf{G}(w_1) + \beta \mathbf{G}(w_2)$$

for all scalars α, β and for all input signals w_1, w_2.

Definition 2.3.5. *A causal linear system $\mathbf{G}$ is said to be $\mathscr{L}_2$-stable if $z = \mathbf{G}w$ is in $\mathscr{L}_2(\mathbb{R}_+)$ whenever w is in $\mathscr{L}_2(\mathbb{R}_+)$ and*

$$\sup\left\{\frac{\|\mathbf{G}w\|_2}{\|w\|_2} : w \neq 0,\ w \in \mathscr{L}_2(\mathbb{R}_+)\right\} < \infty.$$

Similar definitions of stability on other signal spaces will be given in Section 2.4.2.

The space of all linear systems (having the same input signal space and output signal space) forms an algebra under addition (parallel connection) and composition (series connection). Many linear systems can be represented by the integral operator

$$z(t) = \int_0^\infty G(t,\tau) w(\tau)\, d\tau.$$

Using this representation, a system is causal if and only if $G(t,\tau) = 0$ for all $\tau > t$ and is time-invariant if $G(t,\tau) = G(t-\tau, 0)$ for all t, τ. These linear time-invariant (abbreviated as LTI) systems may be represented as a convolution integral

$$z(t) = \int_0^\infty G(t-\tau) w(\tau)\, d\tau, \tag{2.1}$$

where $G(t-\tau)$ stands for $G(t-\tau, 0)$.

2.3.1 Linear Time-invariant Systems and Frequency Domain

One way of representing some LTI systems is by using frequency domain representation. Taking the Laplace transform of (2.1), we have (with abuse of notation)

$$z(s) = G(s) w(s),$$

in which

$$G(s) := \int_0^\infty G(t) e^{-st}\, dt.$$

The Laplace transform $G(s)$ is called the *transfer function* of the system. *In this dissertation, G denotes the transfer function, if it exists, of the system* $\mathbf{G}$. In the $\mathscr{L}_2(\mathbb{R}_+)$ case, stable causal LTI systems can be represented as left multiplications by $\mathcal{H}_\infty$ functions [Wei91, GS93]. (Similar results on general spaces $\mathscr{L}_p(\mathbb{R}_+)$ can be found in [Wei91].)

Define, for any $R > 0$, the subset in $\mathbb{C}$

$$\Theta_R := \left\{ s = re^{j\theta} : r \geq R,\, \theta \in \left[-\frac{\pi}{2}, \frac{\pi}{2} \right] \right\}.$$

A matrix function $F(s)$ is said to be *proper* (respectively *strictly proper*) if $\sup_{s \in \Theta_R} \sigma_{\max}(F(s))$ exists and is finite for sufficiently large R (respectively tends to zero as $R \to \infty$) [GS93]. We say that a system $\mathbf{G}$ is *proper* (respectively *strictly proper*) if it has a transfer function representation and the same is true for its transfer function G. A *rational* matrix function $F(s)$ (i.e. each entry of $F(s)$ is a rational function) is proper (respectively strictly proper) if $\lim_{s\to\infty} F(s)$ exists and is finite (respectively $\lim_{s\to\infty} F(s) = 0$).

Many LTI systems can be described by a set of linear finite dimensional ordinary differential equations:

$$\begin{aligned} \dot{x}(t) &= Ax(t) + Bu(t), \quad x(t_0) = x_0 \in \mathbb{R}^n \\ y(t) &= Cx(t) + Du(t), \end{aligned} \tag{2.2}$$

where the dimensions of the state x, input u and output y are n, m and p, respectively, and the matrices A, B, C, D are appropriately sized. The corresponding transfer function $G(s)$, with zero initial condition $x_0 = 0$, can be computed as

$$G(s) = D + C(sI - A)^{-1}B.$$

We call this transfer function description a *state-space* form. State-space systems are causal and rational. They are always proper. They are strictly proper if and only if $D = 0$. Given a pair (C, A) with stable A, the (symmetric) matrix solution L_o of the Lyapunov equation

$$A^* L_o + L_o A + C^* C = 0$$

is called the *observability Gramian.* It is known [ZDG96] that

$$L_o = \int_0^\infty e^{A^* t} C^* C e^{At}\, dt$$

and $L_o \geq 0$ (or > 0) if and only if $C^* C \geq 0$ (or > 0).

2.3.2 System Spaces

For the analysis of systems in frequency domain, it is convenient to introduce some normed function spaces [ZDG96]:

- The space $\mathcal{L}_\infty(j\mathbb{R})$

  $\mathcal{L}_\infty(j\mathbb{R})$ (or simply $\mathcal{L}_\infty$) is the Banach space of functions that are essentially bounded on $j\mathbb{R}$ with norm

  $$\|F\|_{\mathcal{L}_\infty} := \operatorname*{ess\ sup}_{\omega\in\mathbb{R}\bigcup\{\pm\infty\}} \sigma_{\max}(F(j\omega)).$$

  The subspace of all real-rational functions, denoted by $\mathcal{RL}_\infty(j\mathbb{R})$ (or simply $\mathcal{RL}_\infty$), consists of all real-rational and proper functions with no poles on the imaginary axis.

- The space $\mathcal{H}_\infty(j\mathbb{R})$

  $\mathcal{H}_\infty(j\mathbb{R})$ (or simply $\mathcal{H}_\infty$) is the (closed) subspace of $\mathcal{L}_\infty$ consisting of functions that are analytic and bounded in RHP. For $F \in \mathcal{H}_\infty$, the $\mathcal{H}_\infty$ norm is defined as

  $$\|F\|_{\mathcal{H}_\infty} := \sup_{\Re(s)>0} \sigma_{\max}(F(s)) = \operatorname*{ess\ sup}_{\omega\in\mathbb{R}\bigcup\{\pm\infty\}} \sigma_{\max}(F(j\omega)).$$

  The second equality can be proved using the Maximum Modulus Principle [Rud87], if the $\mathcal{H}_\infty$ norm is finite. The subspace of all real-rational functions, denoted by $\mathcal{RH}_\infty(j\mathbb{R})$ (or simply $\mathcal{RH}_\infty$), consists of all stable, real-rational and proper functions.

- The space $\mathcal{L}_2(j\mathbb{R})$

  $\mathcal{L}_2(j\mathbb{R})$ (or simply $\mathcal{L}_2$) is the Hilbert space of matrix-valued functions F on $j\mathbb{R}$ for which the integral

  $$\int_{-\infty}^{\infty} \mathrm{Trace}\,[F^*(j\omega)F(j\omega)]\,d\omega$$

  is finite. The inner product for this Hilbert space is defined as

  $$\langle F, G\rangle := \frac{1}{2\pi}\int_{-\infty}^{\infty} \mathrm{Trace}\,[F^*(j\omega)G(j\omega)]\,d\omega$$

  for $F, G \in \mathcal{L}_2$, and the norm induced by this inner product is given by

  $$\|F\|_{\mathcal{L}_2} := \sqrt{\langle F, F\rangle}.$$

  The set of all real-rational and strictly proper transfer functions with no poles on the imaginary axis forms a subspace (not closed) of $\mathcal{L}_2$ which is denoted by $\mathcal{RL}_2(j\mathbb{R})$ or simply $\mathcal{RL}_2$.

- The space $\mathcal{H}_2(j\mathbb{R})$

  $\mathcal{H}_2(j\mathbb{R})$ (or simply $\mathcal{H}_2$) is a (closed) subspace of $\mathcal{L}_2$ with matrix functions analytic in RHP such that

  $$\|F\|_{\mathcal{H}_2}^2 := \sup_{\sigma>0}\left\{\frac{1}{2\pi}\int_{-\infty}^{\infty}\text{Trace}\left[F^*(\sigma+j\omega)F(\sigma+j\omega)\right]d\omega\right\} < \infty.$$

  For $F \in \mathcal{H}_2$, the $\mathcal{H}_2$ norm can also be expressed by

  $$\|F\|_{\mathcal{H}_2}^2 = \frac{1}{2\pi}\int_{-\infty}^{\infty}\text{Trace}\left[F^*(j\omega)F(j\omega)\right]d\omega.$$

  The subspace of all real-rational functions, denoted by $\mathcal{RH}_2(j\mathbb{R})$ (or simply $\mathcal{RH}_2$), consists of all stable, real-rational and strictly proper transfer functions.

The above function spaces are essential in studying robust control theory. For instance, the $\mathscr{L}_2$-*induced gain* and the energy of the impulse response of a stable proper LTI system, represented by a transfer function, are the $\mathcal{H}_\infty$ norm and the $\mathcal{H}_2$ norm of the transfer function, respectively [DFT92, ZDG96]. For simplicity, $\|\cdot\|_\infty$ is sometimes used to represent both $\|\cdot\|_{\mathcal{L}_\infty}$ and $\|\cdot\|_{\mathcal{H}_\infty}$ and, similarly, $\|\cdot\|_2$ for $\|\cdot\|_{\mathcal{L}_2}$ and $\|\cdot\|_{\mathcal{H}_2}$.

2.3.3 Coprime Factorizations

Coprime factorizations are central to many aspects of robust control theory, especially in converting robustness optimizations into tractable $\mathcal{H}_\infty$ optimizations.

Definition 2.3.6. *[ZDG96] Two matrix functions $M, N \in \mathcal{RH}_\infty$ are right-coprime over $\mathcal{RH}_\infty$ if they have the same number of columns and if there exist matrix functions $X_r, Y_r \in \mathcal{RH}_\infty$ such that*

$$\begin{bmatrix} X_r & Y_r \end{bmatrix}\begin{bmatrix} M \\ N \end{bmatrix} = X_rM + Y_rN = I.$$

Similarly, two matrix functions $\tilde{M}, \tilde{N} \in \mathcal{RH}_\infty$ are left-coprime over $\mathcal{RH}_\infty$ if they have the same number of rows and if there exist matrix functions $X_l, Y_l \in \mathcal{RH}_\infty$ such that

$$\begin{bmatrix} \tilde{M} & \tilde{N} \end{bmatrix}\begin{bmatrix} X_l \\ Y_l \end{bmatrix} = \tilde{M}X_l + \tilde{N}Y_l = I.$$

Let $P(s)$ be a real-rational and proper matrix function. A *right-coprime factorization (RCF)* of P is a factorization $P = NM^{-1}$ where $M, N \in \mathcal{RH}_\infty$ are right coprime. Similarly, a *left-coprime factorization (LCF)* of P has the form $P = \tilde{M}^{-1}\tilde{N}$ where $\tilde{M}, \tilde{N} \in \mathcal{RH}_\infty$ are left coprime. *Normalized* coprime factorizations of P, i.e. factorizations satisfying $N^*N + M^*M = I$ and $\tilde{N}\tilde{N}^* + \tilde{M}\tilde{M}^* = I$, are often considered.

A state-space form of the normalized coprime factorizations can be obtained by solving two algebraic Riccati equations given a stabilizable and detectable realization of the transfer function [ZDG96].

2.3.4 Graph of a System

We treat a plant and a controller as causal mappings from their input signal spaces to their output signal spaces. It is fruitful to think of a system in terms of its *graph*.

Definition 2.3.7. *[GS93, GS97] Given signal spaces $\mathcal{U}$ and $\mathcal{Y}$. Let $\mathbf{P} : \mathcal{U} \to \mathcal{Y}$ and $\mathbf{C} : \mathcal{Y} \to \mathcal{U}$ be causal mappings. The graph of $\mathbf{P}$ is defined as*

$$\mathcal{G}_{\mathbf{P}} := \left\{ \begin{pmatrix} u \\ \mathbf{P}u \end{pmatrix} : u \in \mathcal{U}, \mathbf{P}u \in \mathcal{Y} \right\} \subset \mathcal{W} := \mathcal{U} \times \mathcal{Y}$$

and the graph of $\mathbf{C}$ (or the inverse graph) is defined as

$$\mathcal{G}_{\mathbf{C}} := \left\{ \begin{pmatrix} \mathbf{C}y \\ y \end{pmatrix} : \mathbf{C}y \in \mathcal{U}, y \in \mathcal{Y} \right\} \subset \mathcal{W}.$$

$\mathcal{G}_{\mathbf{P}}$ and $\mathcal{G}_{\mathbf{C}}$ are linear subspaces of $\mathcal{W}$ if $\mathbf{P}$ and $\mathbf{C}$ are linear.

2.4 Feedback and Stability

Recall that a plant and a controller are treated as *causal systems* $\mathbf{P} : \mathcal{U} \to \mathcal{Y}$ and $\mathbf{C} : \mathcal{Y} \to \mathcal{U}$, where $\mathcal{U}$ and $\mathcal{Y}$ are appropriate signal spaces. Suppose $\mathbf{P}0 = 0$ and $\mathbf{C}0 = 0$. Form a closed loop, denoted by $[\mathbf{P}, \mathbf{C}]$, as the standard feedback control configuration in Figure 2.1. Here, u_0 is the

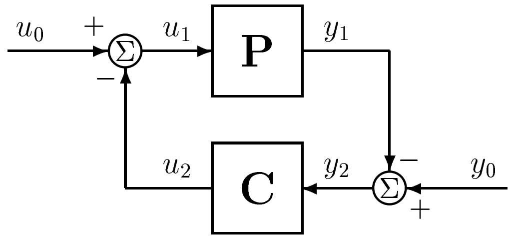

Figure 2.1 *Standard Feedback Configuration.*

plant input disturbance and y_0 the reference tracking signal. The controller has to be designed so that "closed-loop stability" is guaranteed.

Definition 2.4.1. *[Wil71, DV75, GS97] The feedback system in Figure 2.1 is said to be well-posed if for any $(u_0, y_0) \in \mathcal{U} \times \mathcal{Y} =: \mathcal{W}$, there exist unique signals $u_1, u_2 \in \mathcal{U}$ and $y_1, y_2 \in \mathcal{Y}$ such* *that the following feedback equations hold*

$$\begin{aligned} u_0 &= u_1 + u_2, \\ y_0 &= y_1 + y_2, \\ y_1 &= \mathbf{P}u_1, \\ u_2 &= \mathbf{C}y_2, \end{aligned} \tag{2.3}$$

and moreover

$$\mathbf{H}_{\mathbf{P},\mathbf{C}} : \mathcal{W} \to \mathcal{W} \times \mathcal{W} : \begin{pmatrix} u_0 \\ y_0 \end{pmatrix} \mapsto \left(\begin{pmatrix} u_1 \\ y_1 \end{pmatrix}, \begin{pmatrix} u_2 \\ y_2 \end{pmatrix} \right)$$

is causal.

It can be shown that the feedback system in Figure 2.1 is well-posed if the product of instantaneous gains of $\mathbf{P}$ and $\mathbf{C}$ is less than 1 [Wil71]. Let $\mathcal{X}_i$ $(i = 1, 2)$ be signal spaces or subsets of such spaces. Some definitions on stability are given below.

Definition 2.4.2. *[Wil71, DV75, GS97] A causal operator* $\mathbf{F} : \mathcal{X}_1 \to \mathcal{X}_2$ *is said to be stable if* $\mathbf{F}0 = 0$ *and*

$$\|\mathbf{F}|_{\mathcal{X}_1}\| := \sup \left\{ \frac{\|\mathbf{T}_\tau \mathbf{F} x\|}{\|\mathbf{T}_\tau x\|} : x \in \mathcal{X}_1, \tau > 0, \|\mathbf{T}_\tau x\| \neq 0 \right\} < \infty$$

where $\mathbf{T}_\tau$ *is the truncation operator defined in Definition 2.2.5.*

Definition 2.4.3. *[Wil71, DV75, GS97] The feedback system in Figure 2.1 is said to be internally stable (or closed-loop stable or stable) if the operator* $\mathbf{H}_{\mathbf{P},\mathbf{C}}$ *is stable in the sense of Definition 2.4.2.*

Definition 2.4.4. *[Wil71, DV75, GS97] A causal operator* $\mathbf{F} : \mathcal{X}_1 \to \mathcal{X}_2$ *is said to be incrementally stable if* $\mathbf{F}0 = 0$ *and*

$$\|\mathbf{F}|_{\mathcal{X}_1}\|_\triangle := \sup \left\{ \frac{\|\mathbf{T}_\tau(\mathbf{F}x_1 - \mathbf{F}x_2)\|}{\|\mathbf{T}_\tau(x_1 - x_2)\|} : x_1, x_2 \in \mathcal{X}_1, \tau > 0, \|\mathbf{T}_\tau(x_1 - x_2)\| \neq 0 \right\} < \infty.$$

Proposition 2.4.5. *[Wil71, DV75] The feedback configuration in Figure 2.1 is internally stable if* $\mathbf{P}$ *and* $\mathbf{C}$ *are incrementally stable and satisfy* $\|\mathbf{P}\|_\triangle \cdot \|\mathbf{C}\|_\triangle < 1$.

When the input space $\mathcal{U}$ and the output space $\mathcal{Y}$ are taken to be $\mathscr{L}_2(\mathbb{R}_+)$ and $\mathbf{P}$ and $\mathbf{C}$ are causal and LTI, internal stability holds if and only if $H_{P,C} \in \mathcal{H}_\infty$ (where $H_{P,C}$ is the transfer function of $\mathbf{H}_{\mathbf{P},\mathbf{C}}$). The following proposition characterizes all the real-rational and proper stabilizing controllers for the closed loop $[\mathbf{P}, \mathbf{C}]$ when the plant is real-rational and proper.

Proposition 2.4.6. *[Vid85, Fra87] Let* P *be a real-rational and proper matrix function in Figure 2.1 and denote its normalized coprime factorizations by* $P = NM^{-1} = \tilde{M}^{-1}\tilde{N}$. *Then there exist* $U, V, \tilde{U}, \tilde{V} \in \mathcal{RH}_\infty$ *such that the Bezout identity*

$$\begin{bmatrix} \tilde{V} & -\tilde{U} \\ -\tilde{N} & \tilde{M} \end{bmatrix} \begin{bmatrix} M & U \\ N & V \end{bmatrix} = \begin{bmatrix} M & U \\ N & V \end{bmatrix} \begin{bmatrix} \tilde{V} & -\tilde{U} \\ -\tilde{N} & \tilde{M} \end{bmatrix} = \begin{bmatrix} I & 0 \\ 0 & I \end{bmatrix}$$

is satisfied. All real-rational and proper stabilizing controllers of P can be parameterized in the form

$$C = (U + MQ_r)(V + NQ_r)^{-1} = (\tilde{V} + Q_l\tilde{N})^{-1}(\tilde{U} + Q_l\tilde{M})$$

for some Youla parameter $Q_r, Q_l \in \mathcal{RH}_\infty$ where $\det(I + V^{-1}NQ_r)(j\infty) \neq 0$ and $\det(I + Q_l\tilde{N}\tilde{V}^{-1})(j\infty) \neq 0$.

2.5 Plant Uncertainties and Small Gain Theorem

Analysis and design in control theory are based on mathematical models (i.e *nominal* models). There will always be some discrepancies (e.g. due to parameter variations, unmodelled structures) between a mathematical model and a real physical system. These may lead to closed-loop instability or deteriorating performance. For simplicity, systems in this section are assumed to be LTI and have transfer function representations; unless otherwise stated. Various ways to represent possible discrepancies (or uncertainties) are described below [ZDG96]:

Additive Uncertainties. The model uncertainty is represented by an additive perturbation

$$\tilde{P} = P + W_1\Delta W_2$$

where $\Delta \in \mathcal{H}_\infty$.

Multiplicative Uncertainties. The model uncertainty is represented as

$$\tilde{P} = (I + W_1\Delta W_2)P$$

with $W_1, W_2, \Delta \in \mathcal{H}_\infty$.

Coprime Factor Uncertainties. Consider normalized coprime factorizations $P = NM^{-1} = \tilde{M}^{-1}\tilde{N}$. The model uncertainty is represented as

$$\tilde{P} = (N + \Delta_N)(M + \Delta_M)^{-1}$$

or

$$\tilde{P} = (\tilde{M} + \tilde{\Delta}_M)^{-1}(\tilde{N} + \tilde{\Delta}_N)$$

with $\Delta_M, \Delta_N, \tilde{\Delta}_M, \tilde{\Delta}_N \in \mathcal{H}_\infty$.

Robust stability criteria under these uncertainties can be derived from the *Small Gain Theorem.* Consider the interconnected system in Figure 2.2 with $w_1, w_2 \in \mathscr{L}_2(\mathbb{R}_+)$, and $G \in \mathcal{H}_\infty$.

Proposition 2.5.1. *[ZDG96] [Small Gain Theorem] Suppose $G \in \mathcal{H}_\infty$ and let $\gamma > 0$. Then the interconnected system shown in Figure 2.2 is well-posed and internally stable for all $\Delta \in \mathcal{H}_\infty$ with*

1. *$\|\Delta\|_\infty \leq 1/\gamma$ if and only if $\|G\|_\infty < \gamma$;*

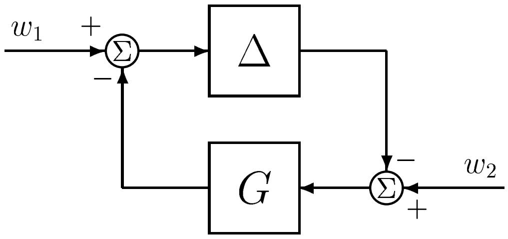

Figure 2.2 *Small Gain Theorem.*

2. $\|\Delta\|_\infty < 1/\gamma$ *if and only if* $\|G\|_\infty \leq \gamma$.

Define the sensitivity function and the complementary sensitivity function as $S := (I - PC)^{-1}$ and $T := I - S = -PC(I - PC)^{-1}$. Expressing the perturbed plant $\tilde{P}$ in terms of the nominal plant P and applying the small gain theorem, we obtain robust stability tests for the aforementioned uncertainties, listed in Table 2.1. It is noteworthy that [ZDG96]

$$\begin{aligned} & \|M^{-1}(I - CP)^{-1}(-C, I)\|_{\mathcal{H}_\infty} \\ = & \left\| \begin{pmatrix} -C \\ I \end{pmatrix} (I - PC)^{-1}\tilde{M}^{-1} \right\|_{\mathcal{H}_\infty} \\ = & \left\| \begin{pmatrix} I \\ P \end{pmatrix} (I - CP)^{-1}(I, -C) \right\|_{\mathcal{H}_\infty}. \end{aligned}$$

The 2×2 block matrix in the last expression corresponds to the four closed-loop transfer functions from external inputs to internal signals in Figure 2.1. In other words, good robust stability in the coprime factor uncertainties results in good performance of the closed loop.

A stronger notion of stability, other than internal stability, is defined when the plant and the controller are LTI.

Definition 2.5.2. *[GS93] A parameterized family of operators* $\{\mathbf{I}_\rho, \rho > 0\}$ *is called an approximate identity if for any* ρ, $\mathbf{I}_\rho$ *has the transfer function* $I_\rho \in \mathcal{H}_\infty$ *satisfying* $\|I_\rho\|_{\mathcal{H}_\infty} = 1$ *for all* ρ *and*

$$\left\| \big(I_\rho(s) - I\big)\frac{1}{s+1} \right\|_{\mathcal{H}_\infty} \to 0$$

as $\rho \to 0$.

Typical examples of approximate identities are $\frac{1}{\rho s+1}I$ and $e^{-\rho s}I$.

Definition 2.5.3. *[GS93] Let* $\mathbf{P}$, $\mathbf{C}$ *be LTI systems. The feedback system* $[\mathbf{P}, \mathbf{C}]$ *in Figure 2.1 is said to be w-stable if for any approximate identities* $\mathbf{I}_\rho$ *and* $\mathbf{J}_\sigma$, *there exists* $\alpha > 0$ *such that* $[\mathbf{I}_\rho\mathbf{P}, \mathbf{J}_\sigma\mathbf{C}]$ *is internally stable for all* ρ, σ *in* $(0, \alpha)$.

$W_1, W_2, \Delta \in \mathcal{H}_\infty$, $\lVert\Delta\rVert_\infty \le \gamma$	
Uncertainty Type	Robust Stability Tests
$\tilde{P} = P + W_1 \Delta W_2$	$\lVert W_2 CSW_1 \rVert_\infty < 1/\gamma$
$\tilde{P} = (I + W_1 \Delta W_2)P$	$\lVert W_2 T W_1 \rVert_\infty < 1/\gamma$
$\tilde{P} = (N + \Delta_N)(M + \Delta_M)^{-1}$, $\Delta = \begin{bmatrix} \Delta_N \\ \Delta_M \end{bmatrix}$	$\lVert M^{-1}(I - CP)^{-1}(-C, I) \rVert_\infty < 1/\gamma$
$\tilde{P} = (\tilde{M} + \tilde{\Delta}_M)^{-1}(\tilde{N} + \tilde{\Delta}_N)$, $\Delta = \begin{bmatrix} \tilde{\Delta}_N & \tilde{\Delta}_M \end{bmatrix}$	$\left\lVert \begin{pmatrix} -C \\ I \end{pmatrix} (I - PC)^{-1} \tilde{M}^{-1} \right\rVert_\infty < 1/\gamma$

Table 2.1 *Robust Stability Tests for Various Plant Uncertainties.*

w-stability allows perturbations to have time delays and high frequency roll-offs in each channel. It can be seen from the following proposition that w-stability is not much stronger than the usual internal stability for some plants and controllers.

Proposition 2.5.4. *[GS89, GS93] Let* $\mathbf{P}$, $\mathbf{C}$ *be LTI systems with closed graphs and* P, C *the respective transfer functions. Then* $[\mathbf{P}, \mathbf{C}]$ *is* w*-stable if and only if the following two conditions are satisfied:*

1. $[\mathbf{P}, \mathbf{C}]$ *is stable,*
2. $\mathbf{P}$, $\mathbf{C}$ *are proper and satisfy*

$$\sup_{s \in \Theta_R} \sigma_{\max}\big(P(s)\big)\sigma_{\max}\big(C(s)\big) < 1$$

for some sufficiently large $R > 0$. *In particular, when* P, C *are rational, the last inequality is reduced to*

$$\sigma_{\max}\big(P(\infty)\big) \cdot \sigma_{\max}\big(C(\infty)\big) < 1.$$

For a stable closed loop where the plant and the controller are proper, it is w-stable if one of them is strictly proper.

2.6 Gap Metric

In the study of robust stability in the feedback system, the following pair of parallel projections plays a central role [GS97]. Using the notion of graphs defined in Section 2.3.4, we define the parallel projection operators as:

$$\Pi_{\mathcal{G}_\mathbf{P}//\mathcal{G}_\mathbf{C}} := \Pi_1 \mathbf{H}_{\mathbf{P},\mathbf{C}} \text{ and } \Pi_{\mathcal{G}_\mathbf{C}//\mathcal{G}_\mathbf{P}} := \Pi_2 \mathbf{H}_{\mathbf{P},\mathbf{C}}$$

where $\Pi_i : \mathcal{W} \times \mathcal{W} \to \mathcal{W}$ denotes the natural projection onto the ith component ($i = 1, 2$) of $\mathcal{W} \times \mathcal{W}$. These parallel projection operators[1] represent the mappings, in Figure 2.1, from the external inputs to the input and output of $\mathbf{P}$ and the output and input of $\mathbf{C}$, respectively. The "distance" between two systems can be measured by the "distance" between their corresponding graphs. Here comes the definition of the gap between two graphs.

Definition 2.6.1. *[GS97] Let $\mathcal{X}, \mathcal{Z}$ be nonempty subsets of an ambient space $\mathcal{W} := \mathcal{U} \times \mathcal{Y}$. The directed gap and the gap between $\mathcal{X}$ and $\mathcal{Z}$ are defined as*

$$\vec{\delta}(\mathcal{X}, \mathcal{Z}) := \begin{cases} \inf\{\, \|(\mathbf{\Phi} - \mathbf{I})|_{\mathcal{X}}\| : \mathbf{\Phi} \textit{ is a causal, bijective mapping} \\ \qquad \textit{from } \mathcal{X} \textit{ onto } \mathcal{Z} \textit{ with } \mathbf{\Phi}0 = 0\} \\ \infty \textit{ if no such operator } \mathbf{\Phi} \textit{ exists} \end{cases}$$

and

$$\delta(\mathcal{X}, \mathcal{Z}) := \max\left\{\vec{\delta}(\mathcal{X}, \mathcal{Z}), \vec{\delta}(\mathcal{Z}, \mathcal{X})\right\}$$

respectively. In the linear case, this definition coincides with the usual definition.

The following proposition gives a sufficient condition on the closed-loop stability when there are uncertainties in the plant and the controller, measured by the gap metric.

Proposition 2.6.2. *[GS97] Consider the feedback system in Figure 2.1. Let $\mathbf{H}_{\mathbf{P},\mathbf{C}}$ be stable. If*

$$\vec{\delta}(\mathcal{G}_\mathbf{P}, \mathcal{G}_{\mathbf{P}'}) \|\Pi_{\mathcal{G}_\mathbf{P}//\mathcal{G}_\mathbf{C}}\| + \vec{\delta}(\mathcal{G}_\mathbf{C}, \mathcal{G}_{\mathbf{C}'}) \|\Pi_{\mathcal{G}_\mathbf{C}//\mathcal{G}_\mathbf{P}}\| < 1$$

then $\mathbf{H}_{\mathbf{P}',\mathbf{C}'}$ is stable and

$$\|\Pi_{\mathcal{G}_{\mathbf{P}'}//\mathcal{G}_{\mathbf{C}'}}\| \le \frac{\|\Pi_{\mathcal{G}_\mathbf{P}//\mathcal{G}_\mathbf{C}}\| \, (1 + \vec{\delta}(\mathcal{G}_\mathbf{P}, \mathcal{G}_{\mathbf{P}'}))}{1 - \vec{\delta}(\mathcal{G}_\mathbf{P}, \mathcal{G}_{\mathbf{P}'}) \|\Pi_{\mathcal{G}_\mathbf{P}//\mathcal{G}_\mathbf{C}}\| - \vec{\delta}(\mathcal{G}_\mathbf{C}, \mathcal{G}_{\mathbf{C}'}) \|\Pi_{\mathcal{G}_\mathbf{C}//\mathcal{G}_\mathbf{P}}\|}.$$

The quantity $b_{\mathbf{P},\mathbf{C}} := \|\Pi_{\mathcal{G}_\mathbf{P}//\mathcal{G}_\mathbf{C}}\|^{-1}$ is called the *gap metric robustness margin* for the closed-loop system $[\mathbf{P}, \mathbf{C}]$. We remark that this definition of $b_{\mathbf{P},\mathbf{C}}$ depends on the choice of the underlying signal spaces. If $\mathcal{U} = \mathcal{Y} = \mathscr{L}_2(\mathbb{R}_+)$ and $\mathbf{P}$ and $\mathbf{C}$ are rational and proper, then this definition coincides with the definition in [GS90]. Related material will be given in the following subsection.

[1] In the linear case, the parallel projections become

$$\Pi_{\mathcal{G}_\mathbf{P}//\mathcal{G}_\mathbf{C}} = \begin{pmatrix} I \\ P \end{pmatrix} (I - CP)^{-1}(I, -C)$$

and

$$\Pi_{\mathcal{G}_\mathbf{C}//\mathcal{G}_\mathbf{P}} = \begin{pmatrix} C \\ I \end{pmatrix} (I - PC)^{-1}(-P, I).$$

2.6.1 Gap Metric Robustness Margin in the Linear Case

Suppose the plant **P** and the controller **C** are LTI and have transfer functions P, C respectively. The parallel projection operator $\Pi_{\mathcal{G}_{\mathbf{P}}//\mathcal{G}_{\mathbf{C}}}$ can easily be shown to have transfer function

$$\begin{pmatrix} I \\ P \end{pmatrix} (I - CP)^{-1}(I, -C)$$

and thus the gap metric robustness margin is

$$b_{\mathbf{P},\mathbf{C}} = b_{P,C} := \begin{cases} \left\| \begin{pmatrix} I \\ P \end{pmatrix} (I - CP)^{-1}(I, -C) \right\|_{\infty}^{-1}, & \text{if } [\mathbf{P}, \mathbf{C}] \text{ is stable} \\ 0, & \text{otherwise,} \end{cases}$$

when $\mathcal{U} = \mathcal{Y} = \mathscr{L}_2(\mathbb{R}_+)$. As a consequence, optimization in the gap metric is equivalent to the optimization for normalized coprime factor uncertainty (see Table 2.1). We define the optimal robustness margin of **P** as

$$b_{\text{opt}}(P) := \sup_{C \text{ stblz}} b_{P,C}.$$

Using the Bezout identity and the Youla parameterization (see Proposition 2.4.6), we have

$$\begin{pmatrix} I \\ P \end{pmatrix} (I - CP)^{-1}(I, -C) = \begin{pmatrix} M \\ N \end{pmatrix} (\tilde{V} + Q\tilde{N}, -(\tilde{U} + Q\tilde{M}))$$

for some $Q \in \mathcal{RH}_\infty$. Again, using the normalization property of the coprime factors of P and the Bezout identity, $b_{P,C}$ can be re-written as

$$\begin{aligned} b_{P,C} &= \left\| \begin{pmatrix} M \\ N \end{pmatrix} (\tilde{V} + Q\tilde{N}, -(\tilde{U} + Q\tilde{M})) \right\|_{\mathcal{H}_\infty}^{-1} \\ &= \left\| (\tilde{V} + Q\tilde{N}, -(\tilde{U} + Q\tilde{M})) \right\|_{\mathcal{H}_\infty}^{-1} \\ &= \left\| (\tilde{V} + Q\tilde{N}, -(\tilde{U} + Q\tilde{M})) \begin{pmatrix} M & -\tilde{N}^* \\ N & \tilde{M}^* \end{pmatrix} \right\|_{\mathcal{L}_\infty}^{-1} \\ &= \left\| (I, -(\tilde{U}\tilde{M}^* + \tilde{V}\tilde{N}^* + Q)) \right\|_{\mathcal{L}_\infty}^{-1} \\ &= \frac{1}{\sqrt{\left\| \tilde{U}\tilde{M}^* + \tilde{V}\tilde{N}^* + Q \right\|_{\mathcal{L}_\infty}^2 + 1}}. \end{aligned} \tag{2.4}$$

Thus, from (2.4), this optimization can be converted into the standard Nehari problem form:

$$b_{\text{opt}}(P)^{-2} = \inf_{Q \in \mathcal{RH}_\infty} \left\| \tilde{U}\tilde{M}^* + \tilde{V}\tilde{N}^* + Q \right\|_{\mathcal{L}_\infty}^2 + 1. \tag{2.5}$$

Convenient formulas for the computation of $b_{\text{opt}}(P)$ can be found in [MG90, ZDG96]:

$$b_{\text{opt}}(P) = \sqrt{1 - \left\| \begin{bmatrix} \tilde{N} & \tilde{M} \end{bmatrix} \right\|_{\text{H}}^{2}},$$

where $\tilde{N}, \tilde{M}$ are the normalized LCF of P and $\|\cdot\|_{\text{H}}$ denotes the maximum Hankel singular value. In practice, it would be necessary to consider a weighted robustness measure: $b_{WP,CW^{-1}}$, for some weighting function fixed in advance, where $W, W^{-1} \in \mathcal{RH}_\infty$, to take into account scaling or to reflect an *a priori* view on the frequency weighting of uncertainties. This weighted robustness optimization problem is considered in the $\mathcal{H}_\infty$ loop shaping design [MG90, BDG+94].

The linear gap metric robustness margin $b_{P,C}$ can be related to the classical *gain margin* (GM) and *phase margin* (PM) [FPEN94, Vin93, Vin98]. It turns out that the GM and PM can be bounded in terms of $b_{P,C}$ and that a good $b_{P,C}$ results in good GM and PM. Given a SISO plant $\mathbf{P}$ and a SISO controller $\mathbf{C}$ with transfer functions P, C respectively. For a stable feedback $[\mathbf{P}, \mathbf{C}]$, we define the gain margin and the phase margin as follows [Vin93, Vin98]:

If $PC(j\omega) \in \mathbb{R}_+$ for some ω, then

$$\text{GM}(\mathbf{P}, \mathbf{C}) := \min \left\{ k \in \mathbb{R} : k \geq 1, kPC(j\omega) = 1 \text{ or } PC(j\omega)/k = 1 \text{ for some } \omega \right\},$$

otherwise $\text{GM}(\mathbf{P}, \mathbf{C}) := \infty$. If $|PC(j\omega)| = 1$ for some ω, then

$$\text{PM}(\mathbf{P}, \mathbf{C}) := \min \left\{ \theta \in \mathbb{R} : \theta \geq 0, e^{j\theta} PC(j\omega) = 1 \text{ or } e^{-j\theta} PC(j\omega) = 1 \text{ for some } \omega \right\},$$

otherwise $\text{PM}(\mathbf{P}, \mathbf{C}) := \infty$.

We have the following proposition giving lower bounds on GM and PM in terms of $b_{P,C}$.

Proposition 2.6.3. *[Vin93, Vin98] Consider the feedback configuration in Figure 2.1 where the plant and the controller have transfer functions P, C respectively. If $[\mathbf{P}, \mathbf{C}]$ is stable, then*

$$GM(\mathbf{P}, \mathbf{C}) \geq \frac{1 + b_{P,C}}{1 - b_{P,C}}$$

and

$$PM(\mathbf{P}, \mathbf{C}) \geq 2 \arcsin(b_{P,C}).$$

A gap metric robustness margin of value 0.3 generally indicates a good robustness margin. In this case, a gain margin of 1.86 and a phase margin of 34.9° are guaranteed.

2.7 Controller Design Methods

Two controller design methods for rational and proper plants, namely the $\mathcal{H}_\infty$ loop shaping method and the closed-loop pole placement method, will be discussed in this section. There is plenty of freedom in these two controller design methods, regarding the choice of loop shaping weighting function for the former and the choice of closed-loop poles for the latter. Robustness (in terms of the gap metric) is the essence of loop shaping design whereas the closed-loop transient performance (in terms of closed-loop pole locations) is the main theme of the pole placement method.

2.7.1 $\mathcal{H}_\infty$ Loop Shaping

The objective of $\mathcal{H}_\infty$ loop shaping design method is to incorporate simple performance/robustness trade-offs obtained in the loop shaping, with guaranteed stability properties of $\mathcal{H}_\infty$ design methods. A typical performance requirement might be that

$$\sigma_{\max}\left((I-PC)^{-1}\right),\ \sigma_{\max}\left((I-PC)^{-1}P\right),\ \sigma_{\max}\left((I-CP)^{-1}\right),\ \sigma_{\max}\left(C(I-PC)^{-1}\right)$$

are made small in some low frequency range, while

$$\sigma_{\max}\left(PC(I-PC)^{-1}\right),\ \sigma_{\max}\left(CP(I-CP)^{-1}\right)$$

are made small in high frequency range, e.g. for robustness and reduction of effects of sensor noise. These requirements, in turn, can be reduced to some desired open-loop shape in the appropriate frequency range:

$$\sigma_{\max}(PC) \gg 1,\ \sigma_{\max}(CP) \gg 1,\ \sigma_{\max}(C) \gg 1$$

at some low frequency range and

$$\sigma_{\max}(PC) \ll 1,\ \sigma_{\max}(CP) \ll 1$$

at some high frequency range. The $\mathcal{H}_\infty$ loop shaping design procedure is described below (see e.g. [MG90, ZDG96]).

$\mathcal{H}_\infty$ Loop Shaping Design Procedure

1. Loop Shape: Use a precompensator W_1 and/or a postcompensator W_2 to shape the singular values of the nominal plant in a desired way as described above. The nominal plant P and the shaping functions W_1, W_2 are combined to form the shaped plant $P_s = W_2 P W_1$. We assume that the formation of P_s does not involve any unstable pole/zero cancellation.

2. Robust Stabilization:

   (a) Calculate the maximum weighted robustness margin

   $$b_{\text{opt}}(P_s) = \sqrt{1 - \left\| \begin{bmatrix} \tilde{N}_s & \tilde{M}_s \end{bmatrix} \right\|_{\mathrm{H}}^2} < 1$$

   where $\tilde{N}_s, \tilde{M}_s$ are the normalized coprime factors of $P_s = \tilde{M}_s^{-1}\tilde{N}_s$. If $b_{\text{opt}}(P_s) \ll 1$, adjust the weights W_1, W_2.

   (b) Select $0 < b < b_{\text{opt}}(P_s)$ and then synthesize a stabilizing controller C_{opt} so that $b_{P_s, C_{\text{opt}}} \geq b$.

3. The final stabilizing feedback controller C is then constructed by combining the shaping functions and the optimal controller C_{opt}:

   $$C = W_1 C_{\text{opt}} W_2.$$

Adopting different weighting functions will result in different controllers for different purposes. For example, a pole at the origin in the weighting function will result in disturbance rejection of a step input in the closed loop. Further investigations on the weighting function will be carried out in subsequent chapters.

2.7.2 Closed-loop Pole Placement

This method requires more effort in symbolic computation of the structure of the controller. The closed-loop pole locations are first selected and then the controller is computed. For simplicity, only SISO plant and controller in Figure 2.1 will be considered.

Write $P(s) = B(s)/A(s)$, where A, B are coprime (i.e. there exist polynomials X and Y such that $XA + YB = 1$) and A is monic. Choose an internal model H (e.g. $H(s) = s$ for d.c. disturbance rejection) in the controller. Then, the controller has the form $C(s) = (S/HR)(s)$, with $\deg(S) \leq \deg(H) + \deg(R)$, with S and R to be determined. With respect to the feedback configuration in Figure 2.1, the closed-loop characteristic polynomial is given by $(AHR-BS)(s)$ and the closed-loop transfer function $P(I - CP)^{-1}(s) = (BHR/(AHR - BS))(s)$. Next we prescribe a characteristic polynomial A_m (e.g. $A_m = (s + \gamma)^k$ for some $k, \gamma > 0$). The degree of A_m can be chosen to be $n + 2\deg(P) - 1$, as suggested in [RS93, HL97]. Then solve the Diophantine equation

$$AHR - BS = A_m$$

for S, R. It is solvable since A, B are coprime and B, H have no common factor. Form the final controller $C(s) = (S/HR)(s)$. In summary:

Closed-loop Pole Placement Design Procedure

1. Write the plant as a quotient of coprime factors $P(s) = B(s)/A(s)$ with $A(s)$ monic.
2. Design the closed-loop characteristic polynomial A_m with degree $n + 2\deg(P) - 1$.
3. Solve the Diophantine equation $A_m(s) = (AHR - BS)(s)$.
4. Form the final controller $C(s) = (S/HR)(s)$.

Internal models in the controller can be selected for different purposes, similar to the loop shaping method. A zero at the origin in the internal model H is used to reject d.c. disturbances. Furthermore, a fast transient decaying rate in the closed loop can be achieved via an appropriate choice of the closed-loop characteristic equation. However, no transparent information on robustness can be derived from closed-loop poles.

3

Linear Repetitive Control Theory

3.1 Introduction

This chapter mainly describes the theoretical development of linear repetitive control theory. Some general prerequisites have been summarized in Chapter 2. A concise literature survey, covering both applications and theoretical developments, is given in Section 3.2. Most of the systems in this chapter are assumed to be SISO rational and proper although some results are applicable to the general MIMO case. Some mathematical preliminaries specifically on repetitive control are given in Section 3.3. Robustness is measured in the gap metric. Section 3.4 presents some theoretical results on asymptotic rejection and asymptotic attenuation of periodic disturbances. A newly defined power-energy induced measure for the transient performance and its relation with robustness can be found in Section 3.5. Finally, we describe two practical controller design methods in Section 3.6 to illustrate the theoretical results derived in this chapter.

3.2 Literature Survey and Motivation of Repetitive Control

Periodic signals (or approximately periodic signals) are common in practical situations where rotating objects or repeated motions such as "picking and placing" are involved. To deal with these situations in an effective way, a new field — *Repetitive Control* — has emerged recently. Repetitive control is applied to achieve asymptotic *reference tracking* and/or *disturbance rejection* of a class of signals comprising a (finite or countably infinite) number of frequencies. In some cases, a subclass of general periodic signals is considered.

The concept of repetitive control was first introduced by Inoue *et al.* [INI81, INK$^+$81] in the early 1980s. Throughout the development of repetitive control, many possible fields of applications have been discovered since then. These applications include rejection of power supply interferences [NH86], problem concerning robotic manipulators [OHN87, TAT88, MGL89, SHKT90, Hor93], tool positioning in a non-circular machining [TT88, TT94], position control for a disk file actuator [TTC88, TTC89, CT90a, CT90b, TCY90, SBK96, Güv96], restoration of periodic signals distorted by nonlinear measurement devices [HHSM92], attitudes stabilization of satellites [BM92, LHP$^+$94], electro-hydraulic material testing [SS93, Güv96], low velocity friction compensation of a machine tool [TUT93a, TUT93b], turning non-circular shapes experiments [AT94], a peristaltic pump [HS94, MH95], digital video/audio disc players [KON95, DSVdHS95, LS98c, LS98b], active noise attenuation/cancellation in finite-length ducts [Hu95, Hu96], vibration suppression of a mechanically coupled loudspeaker [Hil96], and rejection of unknown periodic load disturbances in continuous steel casting processes [MTBR96]. Results have been shown to be fruitful and encouraging.

The theory on repetitive control has been extensively studied since the last decade. It can be divided into continuous-time [FW76, HON85, HY85, HYON88, RO92, LH92, Yam93, CS95, Güv96, Wei96, LS96, HL97, WH97, CS97, LS98c, LS98a], discrete-time [Tom87, TT87, TTC88, TTC89, TCY90, CT90a, CT90b, TN92, SS93, Tom93, Hil94, HS96] and sampled-data [LF94, Lan97] repetitive control. The most primitive issue in repetitive control is the rejection and/or tracking of signals comprising a set of frequencies (countably many and not clustering). This set of frequencies may be finite or infinite (e.g. a subclass of periodic signals having a certain waveform). In the case of infinitely many frequencies, an infinite dimensional linear controller or a nonlinear controller may be used.

Iterative learning control is an area closely related to repetitive control [AKM84, AKMT85, MK85, TY85, TK85, BCG88, MGL89, LB91, HFPM92, Hor93, Yam93, JCHP94]. Some people regard this as repetitive control in a wider sense. The subtle difference between repetitive control and iterative learning control is that the plant in the latter case is always reset to the same initial condition after each cycle (or iteration); whereas in the former case, the control process continues from where it has finished at the end of the preceding cycle. This learning control is mainly applied in robot control of repetitive tasks. In this dissertation, only the former type of repetitive control is considered.

As mentioned previously, a number of practically interesting repetitive control problems (mechanical, electrical or industrial) have been considered. This dissertation was motivated by an audio compact disc (CD) player experiment. Due to the rotation of a compact disc when operating properly, the eccentricity of the disc and the imperfection of the spiral tracks on the disc will generate a periodic disturbance (with dominant components in the first few harmonics) and hence periodic errors in the radial control loop and the focus control loop of a CD player. These persistently exciting periodic error signals can be problematic. These errors have to be suppressed or well attenuated within the allowable tolerance. Detailed descriptions and elaborations of the CD player rig can be found in Chapter 4.

Apart from the practical motivations, repetitive control raises some interesting theoretical problems in its own. One common strategy in repetitive control is the well-known *Internal Model Principle* (IMP) [FW76]. According to this principle, in order to achieve zero tracking error in the steady state or asymptotic disturbance rejection, it is necessary and sufficient that the generators of the reference command signal and disturbance signal are included in the stable closed loop, either incorporated in the plant itself or in the controller. The simplest application of the IMP occurs in the case of a step input. Rejection of a step disturbance requires a simple integrator inside the closed loop. In the case where higher harmonics are involved, a marginally stable internal model rejecting the chosen frequencies has to be used. This principle will be illustrated in this dissertation as system analysis and controller design are carried out. To understand IMP more thoroughly, the following simple but instructive example is considered.

Consider the disturbance rejection of a step in the standard feedback configuration in Figure 2.1, with $u_0 = 1/s$, $y_0 = 0$ and the closed-loop transfer function $P(I-CP)^{-1}$ from u_0 to y_1. Suppose the plant P does not have any zero at the origin. The IMP states that the controller has to have a pole at the origin. The necessity for this can be seen in two ways. Firstly, the infinite controller gain at d.c. together with internal stability implies that the internal signal y_2 (and therefore the plant output y_1) has zero steady state value at that frequency. Secondly, we can see that the stable closed-loop transfer function $P(I-CP)^{-1}$ must have a zero at the origin, attributed to the pole of the controller, in order to cancel the pole of the d.c. disturbance. Thus the d.c. from the input u_0 is blocked.

Now, suppose the controller is moreover to be designed to reject all the sinusoids $\sin(k\omega_0 t)$, $k \in \mathbb{Z}_+ \backslash \{0\}$ and the plant has no zeros at $jk\omega_0$. Applying similar argument as in the d.c. case, all the internal models $s^2 + (k\omega_0)^2$ have to be included in the controller (since $s^2 + (k\omega_0)^2$ is the monic rational minimal annihilating polynomial of $\sin(k\omega_0 t)$). In other words, the factor

$$\frac{1}{s}\prod_{k=1}^{\infty}\frac{(k\omega_0)^2}{s^2 + (k\omega_0)^2}$$

could be incorporated in the controller as an internal model for rejecting all harmonics. However, it can be shown that this infinite product is equal to

$$Te^{-Ts/2}\frac{1}{1-e^{-Ts}}$$

for every $s \in \mathbb{C}$ where $T := 2\pi/\omega_0$ is the fundamental period. Neglecting the delay term, the internal model for rejecting all harmonics $k\omega_0$ (and thus all periodic signals with the same fundamental frequency ω_0, via the consideration of Fourier series) can be chosen to be

$$\frac{1}{1-e^{-Ts}}. \tag{3.1}$$

This infinite dimensional transfer function can be realized by a positive feedback around the time delay T, which was originally used by Inoue [INI81, INK+81]. This periodic generator consists of a positive feedback loop with a delay of period T, which duplicates one cycle and produces a repeated pattern (Figure 3.1).

Another interpretation of the internal model principle is that there should be a signal generator in the closed loop to produce a persistent internal signal (having the same waveform) so as to counteract the persistent exogenous disturbances. It has been pointed out that the infinite dimensional signal generator (3.1) (because of the delay involved in the positive feedback loop) cannot be used for perfect tracking/rejection of periodic signals for some plants [HON85, HY85, HYON88, LS96, LS98c, Lan97]. In [HON85, HY85, HYON88] it was conjectured that a robustly stabilizing repetitive controller (rejecting a general periodic signal completely) cannot exist for a strictly proper plant. This conjecture can be verified and

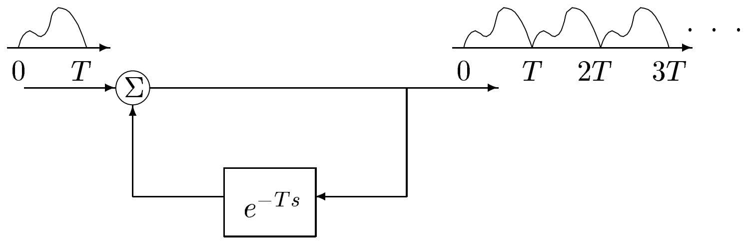

Figure 3.1 *Periodic Signal Generator.*

interpreted in two ways – either by conceptual arguments or by a mathematical proof. The fundamental argument is that robust stability *cannot* be achieved (e.g. for a strictly proper plant) when the periodic signal generator in Figure 3.1 is incorporated in the controller. Two conceptual explanations can be done. Firstly, a strictly proper plant has a zero at infinity while the periodic signal generator has poles at arbitrarily high frequencies and such a pole/zero cancellation on the imaginary axis is not consistent with internal stability of the closed loop. Secondly, the strictly proper plant will perform integration at least once (when viewed in state-space form with zero D-term) and hence the output of the plant will be "smoothed" to some extent, and thereby making it impossible to track/reject an infinitely sharp edge, i.e. arbitrarily high frequency [HYON88]. One remedy is to track/reject low frequency harmonics only, instead of all the harmonics (infinitely many), by putting a low pass filter with infinity norm less than one in the delay term of the signal generator [HON85, HY85, HYON88]. A mathematical explanation of the impossibility of achieving robust asymptotic rejection of all harmonics can be obtained by using a coprime factorization argument [Lan97]. Although these two explanations account for the impossibility of tracking/rejecting periodic signals of arbitrarily high harmonics using a proper LTI controller for a strictly proper plant, there is no *quantitative* description of which frequencies will cause problems in stability.

Some investigations on robust stability in the discrete-time case were carried out in [Hil94], with the delay stability margin as a robustness measure. Recently, the gap metric robustness margin has been adopted (e.g. [BDG+94, GS90]) as a robustness measure in practice. By using this robustness measure, a clear and handy criterion in determining the robustness compromise of tracking/rejecting certain frequencies is obtained [LS96, LS98c]. Details will be described in subsequent sections. It turned out that the analysis is closely related to certain $\mathcal{H}_\infty$ boundary interpolation problems, details of which can be found in [KT85, HS89, HSK92].

In addition to robust stability, a number of other key related issues were also explored in the past. It is known, for instance, that the output of a stable rational and proper system excited by a periodic signal consists of a periodic steady state (of the same fundamental frequency) and a finite energy transient state [LF94, Lan97, Wei96, WH97, LS98c]. In the framework of sampled-data systems, a new induced norm measure with respect to the size of the steady state was proposed [LF94, Lan97]. Similarly, steady state behaviour together with robustness in a discrete-time setting is discussed in [Hil94]. In terms of the gap metric robustness margin, a quantitative trade-off between the steady state and robustness has been given [LS96, LS98c]. Although the consideration of transient state is also important (because for instance a transient state with a slow decaying rate may be problematic), its investigation has been neglected in the past. There were only a few studies in this area concerning for example the placement of closed-loop poles [Hil94] and the time domain transient response [WH97]. Recently, Lee and Smith [LS98c] defined a new power-energy induced measure for the transient output of a stable finite dimensional LTI system excited by a periodic signal. The relation of transient state, expressed by this induced measure, and robustness can also be found in [LS96, HL97, LS98c].

In view of the remarks made above, the following aspects of (continuous-time) repetitive control will be discussed in details later in this chapter:

- the trade-off between asymptotic tracking/rejection of periodic signals and robust stability;
- the steady state behaviour under a certain robust stability requirement;
- the transient performance with respect to robust stability;
- the robust controller design techniques.

3.3 Mathematical Preliminaries

For reasons of convenience, we shall begin with some mathematical preliminaries.

Let a finite set of real numbers (not necessarily harmonic to each other) be given:

$$\Omega_n := \{\omega_1,\ \ldots,\ \omega_n\}.$$

The set of all signals (expressed as a complex Fourier series) under consideration in this chapter and Chapter 4 is

$$\mathcal{S}_n := \left\{ w \;\middle|\; w(t) = \sum_{k=1}^{n} a_k e^{j\omega_k t}, a_k \in \mathbb{C} \right\}.$$

This set $\mathcal{S}_n$ includes some periodic and almost periodic signals [Hal63]. Occasionally, general periodic signals of period T (consisting of infinitely many harmonics) are also considered. The continuous-time periodic signals under consideration are assumed to be continuous and piecewise C^1 on $\mathbb{R}_+$. In the light of Proposition 2.2.14, all these periodic signals are equal to their Fourier series (i.e. the set $\mathcal{S}_n$). In the infinite series case, $\Omega_\infty = \left\{\frac{2\pi}{T}k : k \in \mathbb{Z}\right\}$ and the functions in $\mathcal{S}_\infty$ are assumed to be convergent complex series, i.e. $\sum_{k\in\mathbb{Z}} |a_k|^2 < \infty$. Results analogous to those in this section can also be derived for $\mathcal{S}_\infty$ and will be given in Appendix A, with the technicalities for convergence being taken care of.

The Laplace transform of $u \in \mathcal{S}_n$ is given by

$$\hat{u}(s) = \sum_{k=1}^{n} \frac{a_k}{s - j\omega_k}.$$

Suppose this signal u is fed into a (SISO or MIMO) $\mathscr{L}_2$-stable rational and proper system with transfer function G, the output is equal to

$$\begin{aligned} \hat{y}(s) &= G(s)\hat{u}(s) = \sum_{k=1}^{n} \frac{G(s)a_k}{s - j\omega_k} \\ &= \sum_{k=1}^{n} \frac{G(j\omega_k)a_k}{s - j\omega_k} + \sum_{k=1}^{n} \frac{G(s) - G(j\omega_k)}{s - j\omega_k} a_k \\ &=: \hat{y}_{\text{ss}}(s) + \hat{y}_{\text{tr}}(s). \end{aligned}$$

Note that this $\hat{y}_{\text{tr}}(s)$ is analytic in the closed RHP and belongs to $\mathscr{H}_2$. The time response of the steady state is given by

$$y_{\text{ss}}(t) = \sum_{k=1}^{n} G(j\omega_k) a_k e^{j\omega_k t}.$$

When the system G is written in state-space form $G(s) = D + C(sI - A)^{-1}B$ with stable A, the time response of the transient is given by

$$y_{\text{tr}}(t) = -Ce^{tA} \sum_{k=1}^{n} (j\omega_k I - A)^{-1} B a_k 1_+(t) \in \mathscr{L}_2(\mathbb{R}_+) \tag{3.2}$$

where the function $1_+(\cdot)$ is the Heaviside step function

$$1_+(t) = \begin{cases} 1, & \text{if } t \geq 0, \\ 0, & \text{if } t < 0. \end{cases}$$

Similar decomposition can be performed in the case of some periodic signals passing through a stable rational and proper system. The derivation can be found in Appendix A. This output signal decomposition (inspired by [Lan97]) will be used later.

In this chapter, we will focus solely on SISO rational and proper plants and controllers in the standard feedback configuration (Figure 2.1). We will consider the case of *disturbance rejection* rather than reference tracking since the former necessitates a feedback solution.

3.4 Asymptotic Disturbance Rejection and Attenuation

Consider the feedback configuration in Figure 2.1. Assume the periodic plant input disturbance u_0 is in $\mathcal{S}_n$ and $y_0 = 0$. Asymptotic rejection of such disturbance at y_1 requires that

$$P(I - CP)^{-1}(j\omega_k) = 0 \tag{3.3}$$

for all $\omega_k \in \Omega_n$. For the consideration of robustness under the requirements (3.3), we can define the following optimal gap metric robustness margin:

$$b_{\text{opt}}(P, \Omega_n) := \sup_{C \text{ stblz}} \left\{ b_{P,C} : P(I - CP)^{-1}(j\omega_k) = 0 \quad \forall \omega_k \in \Omega_n \right\}.$$

Using the normalized coprime factorization of the plant and Youla parameterization of the controller (Subsection 2.3.3 and Section 2.4), we have $P(I-CP)^{-1} = N(V+NQ)$, $Q \in \mathcal{RH}_\infty$. (For SISO systems, the left coprime factors coincide with the right coprime factors.) So, the constraints (3.3) can be re-phrased as $Q(j\omega_k) = -(V/N)(j\omega_k)$ if $P(j\omega_k) \neq 0$ (or equivalently, $N(j\omega_k) \neq 0$). No constraint is needed if $P(j\omega_k) = 0$ since the constraint is automatically satisfied in this case. The constrained optimization of the gap metric robustness margin can be re-written as (see Subsection 2.6.1 for some mathematical derivations)

$$b_{\text{opt}}(P,\Omega_n)^{-2} = \inf_{\substack{Q \in \mathcal{RH}_\infty \\ Q(j\omega_k) = Q_k \ \forall \omega_k \in \Omega_n}} \|UM^* + VN^* + Q\|_{\mathcal{L}_\infty}^2 + 1 \tag{3.4}$$

where the constraints $Q(j\omega_k) = -(V/N)(j\omega_k) =: Q_k$ are taken over all $\omega_k \in \Omega_n$ such that $P(j\omega_k) \neq 0$. The following theorem relates the constrained optimal robustness margin to the plant gains at the frequencies in Ω_n.

Theorem 3.4.1. *Let $P(j\omega_k) \neq 0$ for each $\omega_k \in \Omega_n$. Then*

$$b_{\text{opt}}(P,\Omega_n) = \min_{\omega_k \in \Omega_n} \left\{ b_{\text{opt}}(P), \frac{|P(j\omega_k)|}{\sqrt{1+|P(j\omega_k)|^2}} \right\}.$$

Proof. By writing the inner-outer factorization [ZDG96] of $UM^* + VN^* = TB^{-1}$ where $T, B \in \mathcal{RH}_\infty$ and B is the Blaschke product whose zeros are the unstable poles (in RHP) of UM^*+VN^*, we have

$$|UM^* + VN^* + Q|\,(j\omega) = |T + BQ|\,(j\omega)$$

for all $\omega \in \mathbb{R}\bigcup\{\pm\infty\}$. So for each $\omega_k \in \Omega_n$, by using the normalization property $M^*M + N^*N = 1$ and the Bezout identity $MV - NU = 1$, we have

$$\begin{aligned} & |T + BQ|\,(j\omega_k) \\ = & |UM^* + VN^* + Q_k|\,(j\omega_k) \\ = & \left| -\frac{M^*}{N} \right| (j\omega_k) \\ = & \frac{1}{|P(j\omega_k)|}. \end{aligned}$$

The theorem is then proved by using Equation (3.4) and the standard result on boundary interpolation problems [KT85]

$$\begin{aligned} & \inf_{\substack{Q \in \mathcal{RH}_\infty \\ Q(j\omega_k) = Q_k \ \forall \omega_k \in \Omega_n}} \|T_1 + T_2 Q\|_{\mathcal{H}_\infty} \\ = & \max_{\omega_k \in \Omega_n} \left\{ \inf_{Q \in \mathcal{RH}_\infty} \|T_1 + T_2 Q\|_{\mathcal{H}_\infty}, |T_1 + T_2 Q_k|\,(j\omega_k) \right\} \end{aligned} \tag{3.5}$$

where $T_1, T_2 \in \mathcal{RH}_\infty$. □

Remark 3.4.2. *The analogous constraints on $Q \in \mathcal{RH}_\infty$ in the matrix case are $Q(j\omega_k) = -(N^*N)^{-1}N^*V(j\omega_k)$ and we also get*

$$b_{\text{opt}}(P,\Omega_n) = \min_{\omega_k\in\Omega_n}\left\{b_{\text{opt}}(P), \frac{\sigma_{\min}(P(j\omega_k))}{\sqrt{1+\sigma^2_{\min}(P(j\omega_k))}}\right\}$$

if the matrix $P(j\omega_k)$ has full column rank for each $\omega_k \in \Omega_n$. A sketch of the proof can be found in Appendix B.

The quantity $\frac{|P(j\omega_k)|}{\sqrt{1+|P(j\omega_k)|^2}}$ can be interpreted geometrically. A Nyquist graph in the complex plane may be projected as a trajectory on the Riemann sphere $\mathcal{R}$ in $\mathbb{R}^3$ with centre $(0,0,1/2)$ and radius $1/2$ using the stereographic projection $\mathcal{S} : \mathbb{C} \to \mathcal{R}$:

$$\mathcal{S}(s) = \frac{(s_1, s_2, s_1^2+s_2^2)}{1+s_1^2+s_2^2}$$

where $s = (s_1, s_2) = s_1 + js_2$. The inverse of the projection is given by

$$\mathcal{S}^{-1}(x,y,z) = \frac{(x,y)}{1-z} = \frac{x+jy}{1-z}$$

where (x,y,z) satisfies $x^2+y^2+(z-1/2)^2 = 1/4$. It is known that the gap between two plants P_1 and P_2, when less than unity, can be seen as the supremum over frequency of a pointwise distance

$$\kappa(P_1(j\omega), P_2(j\omega)) := \sigma_{\max}\left((I+P_1P_1^*)^{-1/2}(P_2-P_1)(I+P_2^*P_2)^{-1/2}\right)(j\omega).$$

In the scalar case, the pointwise distance is precisely the chordal distance between $P_1(j\omega)$ and $P_2(j\omega)$ when projecting on the Riemann sphere which is equal to

$$\kappa(P_1(j\omega), P_2(j\omega)) = \frac{|P_1(j\omega)-P_2(j\omega)|}{\sqrt{(1+|P_1(j\omega)|^2)(1+|P_2(j\omega)|^2)}}.$$

From this perspective, the quantities $|P(j\omega_k)|/\sqrt{1+|P(j\omega_k)|^2}$ are the chordal distances between the points $P(j\omega_k)$ and the origin on the Riemann sphere. In other words, the maximum gap ball stabilized by the repetitive controller (at the frequency $j\omega_k$) cannot contain the origin (the zero plant). The frequency being rejected is better chosen to be where the plant gain is not close to the origin when projected on the Riemann sphere (i.e. the magnitude is not too small). At the frequency where the plant gain is small, there is no strong reason to completely reject this frequency since the plant itself may have sufficient attenuation. More details on the Riemann sphere interpretation and the gap metric can be found in [Vin93, Vin98].

Theorem 3.4.1 illustrates the impossibility of achieving asymptotic disturbance rejection of general periodic inputs. Indeed, if the plant P is strictly proper, then the robustness margin will be zero if all harmonics are included (also commented in [HYON88]). Even if P is invertible at infinity (unlikely in practice), it is easy to check that the control system fails to be w-stable in the sense of [GS89, GS93]. It can be seen that Condition 2 of Proposition 2.5.4 is not satisfied. Thus, asymptotic rejection for all harmonics is not a practicable possibility. This also explains why the idea of putting a low pass filter into the delay term of the periodic signal generator in Figure 3.1 was proposed. The frequency set to be rejected will then become finite and the plant gains at these frequencies are not likely to be too small. Note that no robustness compromise is required at a given harmonic if $|P(j\omega_k)|/\sqrt{1+|P(j\omega_k)|^2} \geq b_{\mathrm{opt}}(P)$. We mention that the above theorem is closely related to the results in [CS95, CS97] on the regulator problem with robust stability in which a geometric framework was used.

The next result investigates robustness compromises if asymptotic *attenuation* rather than asymptotic rejection of harmonics is required (e.g. when the plant gains at the harmonics are not large enough). The following theorem determines the magnitudes of the plant gains at the harmonics in determining the possibility of asymptotic rejection under a certain gap metric robustness requirement.

Theorem 3.4.3. *Suppose* $0 < \alpha \leq b_{\mathrm{opt}}(P)$. *For any* $\epsilon > 0$ *there exists a* C_ϵ *such that* $b_{P,C_\epsilon} \geq \alpha - \epsilon$ *and*

$$|P(I - C_\epsilon P)^{-1}(j\omega_k)| \leq \xi_k \tag{3.6}$$

for all $\omega_k \in \Omega_n$, *if and only if*

$$\begin{array}{lll} \xi_k & \geq & 0 \qquad\qquad\qquad \textit{when } |P(j\omega_k)| \geq \frac{1}{\sqrt{\alpha^{-2}-1}}, \\ \xi_k & \geq & g(\alpha, |P(j\omega_k)|) \quad \textit{otherwise,} \end{array}$$

where $g(\alpha, x) := \frac{x(1-x\sqrt{\alpha^{-2}-1})}{1+x^2}$.

Proof. The sufficiency part of the proof relies on the following standard boundary interpolation result (similar to the one used in the proof of Theorem 3.4.1).

Lemma 3.4.4. *Let* $T_1, T_2 \in \mathcal{RH}_\infty$ *and let* $\Omega_n = \{\omega_1, ..., \omega_n\} \subset \mathbb{R}$ *be given. Suppose* $T_2(j\omega_k) \neq 0$ *for each* k. *Given a set of numbers* $z_1, ..., z_n \in \mathbb{C}$. *Suppose* $\|T_1 + T_2 Q\|_{\mathcal{H}_\infty} = \alpha$ *for some* $Q \in \mathcal{RH}_\infty$ *and* $|z_k| \leq \alpha$ *for all* k. *Then for each* $\epsilon > 0$, *there exists a* $Q_\epsilon \in \mathcal{RH}_\infty$ *such that*

$$\|T_1 + T_2 Q_\epsilon\|_{\mathcal{H}_\infty} \leq \alpha + \epsilon$$

and

$$(T_1 + T_2 Q_\epsilon)(j\omega_k) = z_k$$

for all $\omega_k \in \Omega_n$.

Proof. This follows from [KT85] and the proof can be found in Appendix C. □

Sufficiency: We first choose a compensator $C_0 = \frac{U+Q_0M}{V+Q_0N}$ such that $b_{P,C_0}^{-1} = \alpha^{-1}$ (or equivalently, $\|UM^* + VN^* + Q_0\|_{\mathcal{L}_\infty} = \sqrt{\alpha^{-2}-1}$). Using the same inner-outer factorization as in the proof of Theorem 3.4.1 (namely, $UM^* + VN^* = TB^{-1}$ for some $T \in \mathcal{RH}_\infty$ and all-pass $B \in \mathcal{RH}_\infty$), we have $\|T + BQ_0\|_{\mathcal{H}_\infty} = \sqrt{\alpha^{-2}-1}$. Define

$$z_k := -\left(\frac{M^*}{N}B\right)(j\omega_k) \qquad \text{for } |P(j\omega_k)|\sqrt{\alpha^{-2}-1} \geq 1, \tag{3.7}$$

$$z_k := -\left(\frac{|P|\sqrt{\alpha^{-2}-1}}{(1+|P|^2)NM}B\right)(j\omega_k) \quad \text{for } 0 < |P(j\omega_k)|\sqrt{\alpha^{-2}-1} < 1. \tag{3.8}$$

Then, we can check that $|z_k| \leq \sqrt{\alpha^{-2}-1}$ for each k. So, for any $\epsilon > 0$, by Lemma 3.4.4, there exists a $Q_\epsilon \in \mathcal{RH}_\infty$ such that

$$\|T + BQ_\epsilon\|_{\mathcal{H}_\infty} \leq \sqrt{\left(\frac{1}{\alpha-\epsilon}\right)^2 - 1} \tag{3.9}$$

and the interpolation constraints

$$(T + BQ_\epsilon)(j\omega_k) = z_k \quad \forall \omega_k \in \Omega_n \tag{3.10}$$

are satisfied. We will now choose

$$C_\epsilon = \frac{U + Q_\epsilon M}{V + Q_\epsilon N}.$$

Then inequality (3.9) is equivalent to $b_{P,C_\epsilon} \geq \alpha - \epsilon$. We will now check that the constraints (3.10) are sufficient for inequality (3.6) to be satisfied. Firstly, we can verify by using the properties of the coprime factors that constraints (3.10) imply

$$(V + Q_\epsilon N)(j\omega_k) = \left(M^* + z_k N B^{-1}\right)(j\omega_k).$$

Thus, if $|P(j\omega_k)|\sqrt{\alpha^{-2}-1} \geq 1$ then (3.7) gives

$$P(I - C_\epsilon P)^{-1}(j\omega_k) = N(V + Q_\epsilon N)(j\omega_k) = 0 \leq \xi_k.$$

If $0 < |P(j\omega_k)|\sqrt{\alpha^{-2}-1} < 1$ then (3.8) gives

$$(V + Q_\epsilon N)(j\omega_k) = \left(\frac{1 - |P|\sqrt{\alpha^{-2}-1}}{(1+|P|^2)\,M}\right)(j\omega_k)$$

which implies that

$$\left|P(I - C_\epsilon P)^{-1}(j\omega_k)\right| = |N(V + Q_\epsilon N)(j\omega_k)| = g(\alpha, |P(j\omega_k)|) \leq \xi_k.$$

Finally, if $P(j\omega_k) = 0$, no interpolation constraint on the controller parameter is required to satisfy $P(I - C_\epsilon P)^{-1}(j\omega_k) = 0$.

Necessity: Clearly, for any $\omega_k \in \Omega_n$ such that $|P(j\omega_k)| \geq 1/(\sqrt{\alpha^{-2}-1})$, there is nothing to prove. So, without loss of generality, assume that $|P(j\omega_k)| < 1/(\sqrt{\alpha^{-2}-1})$ for all $\omega_k \in \Omega_n$. Then for sufficiently small $\epsilon > 0$,

$$|P(j\omega_k)| < \frac{1}{\sqrt{(\alpha-\epsilon)^{-2}-1}}$$

for all $\omega_k \in \Omega_n$. Select such an $\epsilon > 0$ and a C_ϵ such that $b_{P,C_\epsilon} \geq \alpha - \epsilon$. We know, from [Vin93, Lemma V.1] or Appendix D, that

$$\left|P(I-C_\epsilon P)^{-1}(j\omega_k)\right| = \left|\frac{1 + x(j\omega_k)|P(j\omega_k)|\sqrt{(\alpha-\epsilon)^{-2}-1}}{1+|P(j\omega_k)|^2} \cdot P(j\omega_k)\right|$$

for some $|x(j\omega_k)| \leq 1$. Thus,

$$\begin{aligned}
\xi_k &\geq \left|P(I-C_\epsilon P)^{-1}(j\omega_k)\right| \\
&\geq \frac{1-|P(j\omega_k)|\sqrt{(\alpha-\epsilon)^{-2}-1}}{1+|P(j\omega_k)|^2} \cdot |P(j\omega_k)| \\
&= g(\alpha-\epsilon, |P(j\omega_k)|).
\end{aligned}$$

Since this holds for all sufficiently small $\epsilon > 0$, then $\xi_k \geq g(\alpha, |P(j\omega_k)|)$, by the continuity of the function $g(\cdot, |P(j\omega_k)|)$. □

The above theorem gives a minimum modulus for the plant which is consistent with a certain robustness margin. For example if we require $\alpha = 0.3$ (a reasonable level in practice) then asymptotic rejection of a harmonic is possible, provided $|P(j\omega_k)| > 0.315$, otherwise attenuation to less than 7.68% of the disturbance magnitude is always possible as shown by Figure 3.2. Note that $g(\alpha, x)$ has a maximum of $g_{\max} = \frac{\alpha}{2(1+\sqrt{1-\alpha^2})}$ at $x_{\max} = \frac{\alpha}{1+\sqrt{1-\alpha^2}}$, so even with $\alpha = 1$, a 50% reduction is always possible. A similar result has been shown in [Hil94, HS96], namely, that a 50% reduction in the steady state was possible with respect to robustness to time delays.

3.5 Transient Performance

Consider a signal

$$u = \sum_{k=1}^{n} a_k e^{j\omega_k t} \in \mathcal{S}_n$$

which is input to a SISO stable rational and proper system with transfer function $G(s)$ (e.g. $G = P(I-CP)^{-1}$ in our case). Write a state-space form $G(s) = D + C(sI-A)^{-1}B$ with stable A. Let L_0 be the observability gramian with respect to this state-space realization, i.e.

$$L_0 = \int_0^\infty e^{tA^*} C^* C e^{tA}\, dt \geq 0$$

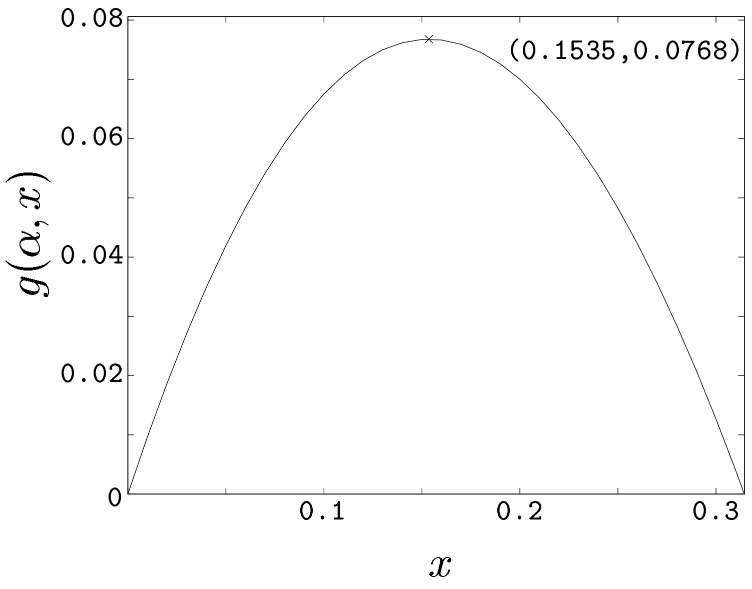

Figure 3.2 *The function $g(\alpha, x)$ for $\alpha = 0.3$.*

and $A^*L_0 + L_0A + C^*C = 0$. Define the vector

$$\mathbf{a} := \begin{pmatrix} a_1 \\ \vdots \\ a_n \end{pmatrix}$$

and the $n \times n$ hermitian non-negative definite matrix

$$\mathcal{M} := \left(B^*(-j\omega_k I - A^*)^{-1} L_0 (j\omega_l I - A)^{-1} B\right)_{1 \le k,\, l \le n}.$$

Using equation (3.2), the square of transient energy can be computed:

$$\begin{aligned} \|y_{\mathrm{tr}}(t)\|_2^2 &= \sum_{k=1}^{n} \sum_{l=1}^{n} a_k^* B^*(-j\omega_k I - A^*)^{-1} L_0 (j\omega_l I - A)^{-1} B a_l \\ &= \mathbf{a}^* \mathcal{M} \mathbf{a}. \end{aligned}$$

Note that

$$\|\mathbf{a}\| = \|u\|_{\mathscr{P}} := \left(\lim_{\gamma \to \infty} \frac{1}{\gamma} \int_0^\gamma |u(t)|^2 \ dt \right)^{\frac{1}{2}}$$

where $\|\mathbf{a}\|$ denotes the Euclidean vector norm. If we define $\|G\|_{\mathrm{tr} \leftarrow \mathcal{S}_n}$ to be the maximal transient energy $\|y_{\mathrm{tr}}(t)\|_2$ for signals $u \in \mathcal{S}_n$ with $\|u\|_{\mathscr{P}} \le 1$, then

$$\|G\|_{\mathrm{tr} \leftarrow \mathcal{S}_n} = \sqrt{\lambda_{\max}(\mathcal{M})}.$$

Our next result shows that, in general, an arbitrarily poor transient performance will result from demanding both *optimal* robustness and asymptotic disturbance rejection simultaneously.

Theorem 3.5.1. *Given* $\Omega_n = \{\omega_1, ..., \omega_n\} \subset \mathbb{R}$. *Suppose* $b_{\text{opt}}(P) < \frac{|P(j\omega_k)|}{\sqrt{1+|P(j\omega_k)|^2}}$ *for all* $\omega_k \in \Omega_n$. *Consider any sequence of stabilizing compensators* C_m, $m \in \mathbb{Z}_+$, *with* $b_{P,C_m} \to b_{\text{opt}}(P)$ *as* $m \to \infty$ *and* $P(1 - C_m P)^{-1}(j\omega_k) = 0$ *for each* $\omega_k \in \Omega_n$ *and each* m. *Then*

$$\left\| P(I - C_m P)^{-1} \right\|_{\text{tr}\leftarrow\mathcal{S}_n} \longrightarrow \infty$$

as $m \to \infty$.

Proof. A direct consequence of the assumed inequalities is that $b_{\text{opt}}(P, \Omega_n) = b_{\text{opt}}(P)$ as seen in Theorem 3.4.1. Next note that

$$\left\| \frac{G(s) - G(j\omega_k)}{s - j\omega_k} \right\|_{\mathcal{H}_2} = (k,k)\text{th entry of } \mathcal{M} \leq \|G\|_{\text{tr}\leftarrow\mathcal{S}_n}$$

where $G = P(I - C_m P)^{-1}$. It will be sufficient to prove that any diagonal entry of $\mathcal{M}$ tends to infinity under the conditions of the theorem.

Suppose on the contrary, there exists a subsequence $C_m = (U+MQ_m)/(V+NQ_m)$ (which we will still refer to as C_m for convenience) such that $b_{P,C_m} \to b_{\text{opt}}(P)$, $P(I-C_m P)^{-1}(j\omega_k) = 0$ $\forall \omega_k$ and there exists a constant $K_1 > 0$ satisfying

$$\left\| \frac{P(I - C_m P)^{-1}}{s - j\omega_k} \right\|_{\mathcal{H}_2} \leq K_1 \tag{3.11}$$

for all m. First, there exists a unique $Q_{\text{opt}} \in \mathcal{H}_\infty$ such that [ZDG96]

$$\|(V, -U) + Q_{\text{opt}}(N, -M)\|_{\mathcal{H}_\infty} = b_{\text{opt}}(P)^{-1}.$$

Next, the set of $\mathcal{H}_\infty$ functions: $\{S_l = (V, -U) + Q_l(N, -M) : l \in \mathbb{Z}_+\}$ is a normal family [Rud87] on the right half plane. Thus, there exists S_{lim} such that $S_l \to S_{\text{lim}}$ uniformly on compact subsets of the right half plane. First note that $S_{\text{lim}} \in \mathcal{H}_\infty$. This follows since $\|S_{\text{lim}}(s)\|$ must be bounded above by $b_{\text{opt}}(P)^{-1}$ on any compact subset of the right half plane. Now define $Q_{\text{lim}} = -S_{\text{lim}} \begin{pmatrix} U \\ V \end{pmatrix} \in \mathcal{H}_\infty$. We claim that

$$\begin{aligned} S_{\text{lim}} &= (V, -U) + Q_{\text{lim}}(N, -M) \\ &= (V, -U) - S_{\text{lim}} \begin{pmatrix} U \\ V \end{pmatrix} (N, -M). \end{aligned} \tag{3.12}$$

This follows since

$$S_l = (V, -U) - S_l \begin{pmatrix} U \\ V \end{pmatrix} (N, -M)$$

for all l, and $S_l \to S_{\text{lim}}$ uniformly on compact subsets of the right half plane. From (3.12) we obtain $\|(V, -U) + Q_{\text{lim}}(N, -M)\|_{\mathcal{H}_\infty} = b_{\text{opt}}(P)^{-1}$ which means that $Q_{\text{lim}} = Q_{\text{opt}}$ since Q_{opt} is unique. A further property of Q_{opt} is that [ZDG96]

$$\left\| \big((V, -U) + Q_{\text{opt}}(N, -M)\big)(j\omega) \right\| = b_{\text{opt}}(P)^{-1}$$

for all $\omega \in \mathbb{R}\bigcup\{\pm\infty\}$. For each k, the condition $P(I - C_{\mathrm{opt}}P)^{-1}(j\omega_k) = 0$ is equivalent to $Q_{\mathrm{opt}}(j\omega_k) = -(V/N)(j\omega_k)$, which implies

$$\begin{aligned} b_{\mathrm{opt}}(P)^{-1} &= \left\|\big((V,-U) + Q_{\mathrm{opt}}(N,-M)\big)(j\omega_k)\right\| \\ &= \sqrt{1 + |(UM^* + VN^* + Q_{\mathrm{opt}})(j\omega_k)|^2} \\ &= \frac{\sqrt{1 + |P(j\omega_k)|^2}}{|P(j\omega_k)|} \\ &< b_{\mathrm{opt}}(P)^{-1}. \end{aligned}$$

Therefore, we must have $P(I - C_{\mathrm{opt}}P)^{-1}(j\omega_k) \neq 0$. In this case, we can find $\sigma > 0$ such that

$$\left\|\frac{P(I - C_{\mathrm{opt}}P)^{-1}}{s - j\omega_k}\right\|_{\sigma,2} \geq K_1 + 2 \tag{3.13}$$

where $\|F\|_{\sigma,2}^2 := \int_{-\infty}^{\infty} |F(\sigma + j\omega)|^2\, d\omega$. We now claim that, for m sufficiently large,

$$\left\|\frac{P(I - C_{\mathrm{opt}}P)^{-1} - P(I - C_mP)^{-1}}{s - j\omega_k}\right\|_{\sigma,2} \leq 1. \tag{3.14}$$

To see this, first note that $|P(I - C_{\mathrm{opt}}P)^{-1}|$ and $|P(I - C_mP)^{-1}|$ are bounded above by $b_{\mathrm{opt}}(P)^{-1} + 1$, for all sufficiently large m. Thus both

$$\int_{\sigma+jK_2}^{\sigma+j\infty} \left|\frac{P(I - C_{\mathrm{opt}}P)^{-1}}{s - j\omega_k}\right|^2 ds$$

and

$$\int_{\sigma-j\infty}^{\sigma-jK_2} \left|\frac{P(I - C_{\mathrm{opt}}P)^{-1}}{s - j\omega_k}\right|^2 ds$$

can be made arbitrarily small (and similarly with C_{opt} replaced by C_m) for sufficiently large K_2. Further

$$\int_{\sigma-jK_2}^{\sigma+jK_2} \left|\frac{P(I - C_{\mathrm{opt}}P)^{-1} - P(I - C_mP)^{-1}}{s - j\omega_k}\right|^2 ds$$

tends to zero as $m \to \infty$, for any fixed K_2. This establishes (3.14). Thus, (3.13) and (3.14) together imply that

$$\begin{aligned} &\left\|\frac{P(I - C_mP)^{-1}}{s - j\omega_k}\right\|_{\mathcal{H}_2} \\ \geq &\left\|\frac{P(I - C_mP)^{-1}}{s - j\omega_k}\right\|_{\sigma,2} \\ \geq &\left\|\frac{P(I - C_{\mathrm{opt}}P)^{-1}}{s - j\omega_k}\right\|_{\sigma,2} - \left\|\frac{P(I - C_{\mathrm{opt}}P)^{-1} - P(I - C_mP)^{-1}}{s - j\omega_k}\right\|_{\sigma,2} \\ \geq &\ K_1 + 1 \end{aligned}$$

for sufficiently large m, which contradicts (3.11). □

Theorem 3.5.1 reveals the fact that a demand for optimal robustness margin is not practical as an arbitrarily bad transient state (sometimes reflected in a slow decaying rate) will result. Both a good robustness margin and a satisfactory transient performance have to be achieved simultaneously. The trade-off between robustness and transient performance will become more transparent in the next section where practical design techniques are discussed.

3.6 Design Techniques

The limitations on the robustness margin, steady state attenuation and transient performance in repetitive control were discussed in the last section. The two design methods mentioned in Section 2.7 will now be used specifically in the repetitive control context. For the loop shaping method estimates, derived from the theorems in Sections 3.4 and 3.5, on the robustness margin and transient performance can be made. For the pole placement method, the transient performance is directly influenced by the closed-loop pole locations. However, there is no apparent relation between the achievable robustness margin and the structure of the closed-loop characteristic equation. Robustness in terms of the gap metric and transient performance in term of the power-energy transient induced measure are discussed. For the sake of illustration, the plant is assumed to be SISO, rational and proper. Certain assumptions are imposed on the structures on the loop shaping weighting function and the closed-loop characteristic equation.

Consider the design of a robust controller for the frequencies

$$\Omega_n = \{\omega_1, \omega_2, ..., \omega_n\} \subset \mathbb{R}$$

in the case of disturbance rejection. We may assume $\Omega_n = -\Omega_n$. Suppose $P(j\omega_k) \neq 0$ for $\omega_k \in \Omega_n$. In order to achieve disturbance rejection for these frequencies, conditions (3.3) have to be satisfied. In other words, the controller has to have poles in Ω_n. So, the (real-rational) internal model

$$H(s) := \prod_{\omega_k \in \Omega_n} (s - j\omega_k) \tag{3.15}$$

is chosen.

3.6.1 $\mathcal{H}_\infty$ Loop Shaping

As described in Section 2.7, the $\mathcal{H}_\infty$ loop shaping method depends heavily on the choice of the loop shaping weighting functions. Here, one weighting function is sufficient because the system is SISO. For simplicity, the following real-rational loop shaping function $W_\beta(s)$ is selected:

$$W_\beta(s) := \frac{H(s+\beta)}{H(s)}, \quad \beta > 0.$$

This weighting function has poles at Ω_n and zeros at $-\beta + j\Omega_n$. For instance, if d.c. and a sinusoid of frequency ω_0 are to be rejected, the weighting function can be taken to be

$$W_\beta(s) = \frac{(s+\beta)}{s} \times \frac{(s+\beta)^2 + \omega_0^2}{s^2 + \omega_0^2}.$$

For small β, the poles and the zeros of $W_\beta(s)$ are close together; and as shown in the sequel, this gives a controller $C_\beta(s)$ with b_{P,C_β} close to the optimal value $b_{\rm opt}(P, \Omega_n)$. When $b_{\rm opt}(P) < |P(j\omega_k)|/\sqrt{1 + |P(j\omega_k)|^2} \quad \forall \omega_k \in \Omega_n$, in the light of Theorem 3.5.1, the transient performance is extremely bad for these small β. This can be reflected in a slow decaying rate of the response. On the other hand, a large value of β gives better transient performance, but at the expense of robustness. This illustrates the *trade-off* between transient performance and robustness. This phenomenon will be elaborated later in this section and in the example of a CD player in Chapter 4.

Using this loop shaping method, the optimal controller (for the weighted plant $W_\beta P$) has order $\deg(W_\beta P) - 1 = n + \deg(P) - 1$, assuming there is no unstable pole/zero cancellation between W_β and P. Thus the final controller, formed by combining the weight and the optimal controller for the weighted plant, has order $2n + \deg(P) - 1$. This extra order (from the internal model) may hinder the use of internal model. However, practically, only a few harmonics (where the plant gain is large) are selected to be rejected. If the plant gains at some frequencies are already small, there is no strong reason to reject these frequencies completely. Furthermore, the order of the final controller can be reduced by a simple model reduction step.

3.6.2 Closed-loop Pole Placement

The closed-loop pole placement method depends on the internal model H and the closed-loop pole locations (see Section 2.7 for details). Using the internal model (3.15) and clustering all closed-loop poles at $-\gamma$ with $\gamma > 0$, the controller can be obtained by solving the Diophantine equation

$$(s+\gamma)^k = AHR - BS$$

where $P = B/A$ with A, B coprime, A monic and $k = \deg(H) + 2\deg(P) - 1$. The controller will then be $C_\gamma = S/HR$.

3.6.3 An Illustration

We illustrate the two controller design methods by using a first order plant

$$P(s) = \frac{\sqrt{2}}{s+1}.$$

Then the normalized coprime factors N, M can be chosen to be

$$N(s) = \frac{\sqrt{2}}{s+\sqrt{3}}, \quad M(s) = \frac{s+1}{s+\sqrt{3}}$$

and the coprime numerator $B(s)$ and denominator $A(s)$ are

$$B(s) = \sqrt{2}, \quad A(s) = s + 1.$$

Suppose $\Omega_1 = \{0\}$ and only d.c. disturbance rejection is considered. So, the internal model is $H(s) = s$. The loop shaping weighting functions are chosen to be

$$W_\beta(s) = \frac{s+\beta}{s}, \quad \beta > 0$$

and the closed-loop characteristic polynomial, having degree 2, is chosen to be $(s+\gamma)^2$, $\gamma > 0$. The loop shaping controller is $C_\beta = W_\beta C_{\text{opt}}$ where C_{opt} is the optimal controller for $W_\beta P$. Solving the Diophantine equation $(s+\gamma)^2 = s(s+1)R - \sqrt{2}S$, we get

$$R(s) = 1, \quad S(s) = -\frac{(2\gamma - 1)s + \gamma^2}{\sqrt{2}}.$$

The closed-loop pole placement controller is therefore

$$C_\gamma(s) = -\frac{(2\gamma - 1)s + \gamma^2}{\sqrt{2}s}.$$

The closed-loop transfer functions from u_0 to y_1 are

$$G(s;\beta) = P(I - C_\beta P)^{-1}$$

and

$$G(s;\gamma) = P(I - C_\gamma P)^{-1}(s) = \frac{\sqrt{2}s}{(s+\gamma)^2}.$$

A nice expression for the power-energy transient induced measure for the pole placement method can be computed:

$$\|G(s;\gamma)\|_{\text{tr}\leftarrow\mathcal{S}_1} = \sqrt{\frac{1}{2\gamma^3}}.$$

Using the (unweighted) gap metric robustness margin and the power-energy induced quantity as the measures for robustness stability and transient performance respectively, the unweighted robustness margins are b_{P,C_β} and b_{P,C_γ} and the measures of the transient performance are $\|G(s;\beta)\|_{\text{tr}\leftarrow\mathcal{S}_1}$ and $\|G(s;\gamma)\|_{\text{tr}\leftarrow\mathcal{S}_1}$. A graph depicting the parameters β, γ and the corresponding robustness margin is shown in Figure 3.3. A similar graph depicting the trade-off between robustness and transient performance is shown in Figure 3.4. Several phenomena can be observed from Figures 3.3 and 3.4. Using the formula given in Theorem 3.4.1, the d.c. rejection is indeed a constraint to the robustness margin. The constrained optimal robustness margin $b_{\text{opt}}(P, \Omega_1)$ is 0.8165, which is equal to the value $|P(0)|/\sqrt{1 + |P(0)|^2}$, while the unconstrained optimal value is 0.8881. From Figure 3.3, the loop shaping method verifies the effect of the constraint when the parameter β is small. The loop shaping graph is flat for small β ($\beta \le 0.2$). On the contrary, for the pole placement method, due to the confined structure of the closed-loop characteristic polynomial, the maximal attainable robustness margin is only 0.7071 and occurs when $\gamma = 1$. From Figure 3.4, similar phenomena due to the disturbance rejection requirement can be observed. Furthermore, the pole placement gives some points lying in the bad region where the power-energy induced measure is large and the robustness margin is small (i.e. top left corner of Figure 3.4). A practically useful region determined from viewpoint of robustness requirement and transient performance, where the robustness margin is acceptable and the power-energy induced measure is sufficiently small, can be selected from Figure 3.4.

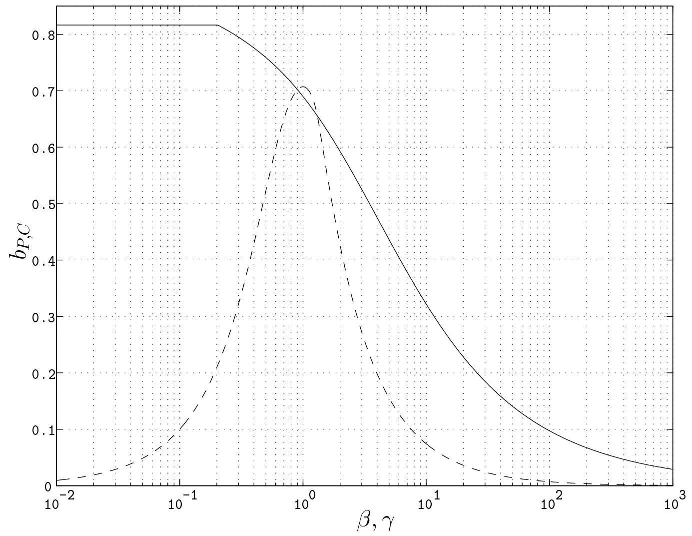

Figure 3.3 *The Relations between* $b_{P,C}$ *and* β, γ. *Loop Shaping: solid "—"; Pole Placement: dashed "- - -".*

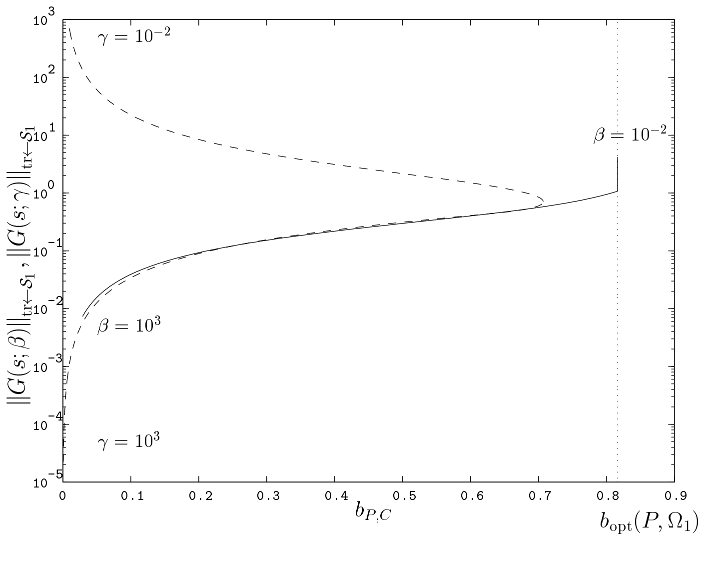

Figure 3.4 *The Relations between the Power-energy Induced Measures and the Robustness Margins, with parameters* β *and* γ. *Loop Shaping: solid "—"; Pole Placement: dashed "- - -".*

4

Application to a CD Player

4.1 Introduction

This chapter gives a practical application of the theory developed in Chapter 3 to a compact disc player system. The controller design methods described there are applied to a Philips CD930 player. Background on the development and full technicalities of compact disc systems can be found in [BBH$^+$85, Dra89, NO92, Poh92]. Therefore, only a concise description of the CD930 player rig (Section 4.2) and the experimental setup (Section 4.3) are given. Lastly, controller designs and implementation results on the CD930 are presented (Section 4.4 and [LS98b]).

4.2 Compact Disc Player System

Storage of information has been shifted from an analog format to a digital format since the 1960s. In the late 1960s and early 1970s, the idea of optical pick-up compact discs by means of *laser* came out and was put into application, initially in the audio industry. Laser could be used in optical reading systems because of its favourable properties, such as monochromaticity and phase coherency. A compact disc (CD) player system is an extremely complicated system consisting of several mechanisms. The main functioning parts are the optical pick-up including error signal generator (for laser position control), data decoding system, digital signal processing system, and digital-to-analog system (for audio output). The core units of the optical pick-up part are the *optical read out unit*, the *radial control unit*, the *focus control unit* and the *rotation speed control unit. For illustration, only the radial control unit is considered in this dissertation.* Descriptions on the other components of a CD player can be found in [BBH$^+$85, Dra89, NO92, Poh92]. All the standards and schematics in this chapter are based on the Philips CD930 model [Dra89].

4.2.1 Radial Control Unit

The Optical Read Out Unit contains a laser generator, a collimator lens, an objective lens and four photo-diode detectors. Signal reading, radial tracking and focus tracking are achieved at the same time. The radial position actuator is designed to follow the track movement and to provide a sufficient positioning accuracy in spite of disc eccentricities, track imperfections and disturbances. These disturbances typically have a magnitude of ± 0.2mm. The maximum allowable radial error is $\pm 0.1\mu$m. (A reduction factor of $2000 = 0.2\text{mm} \div 0.1\mu\text{m}$ has to be achieved by the radial controller.) The photo-diode detectors convert physical radial errors into electrical radial errors. This electrical error signal, after linearization around zero, can be modelled as [BBH+85, Dra89]

$$R_{\text{error}} = R_{\text{offset}} + K_{\text{optics}}\varepsilon \tag{4.1}$$

where ε is the physical radial error between the laser spot and the track, measured from the disc centre. The quantity R_{error} is a fluctuating d.c. signal which *cannot* be used as an indicator signal for control. By inserting an artificial wobble of frequency 600Hz in the radial loop (see [Dra89, Poh92] for details), R_{error} is rectified and a drift-free tracking error signal RE $:= K_{\text{optics}}\varepsilon$ can be obtained. This signal RE will be used as the radial loop control signal. The schematic block diagram for the radial loop is shown in Figure 4.1.

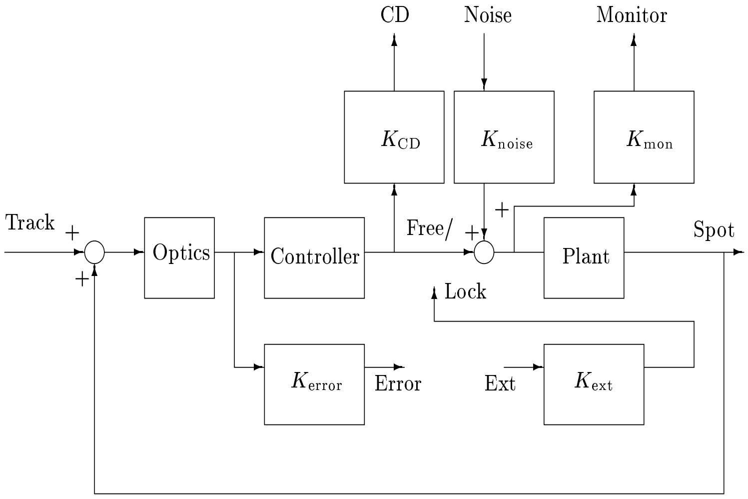

Figure 4.1 *Schematic Block Diagram for the Radial Control Loop of Philips CD930.*

The radial plant consists of an optical element mounted at the end of a balanced radial actuator arm. This actuator is a d.c. motor driven by current. The radial plant is a double integrator with a second order damping system of resonance frequency 3,700Hz. (Detailed derivation can be found in Appendix F.) The open loop nominal bandwidth (as seen from the external controller) is 400Hz [Dra89, DSB92, Swi97]. For simplicity, the nominal radial plant can be taken to be

$$P_{\text{rad}}(s) = \frac{(2\pi \cdot 400)^2}{s^2}. \tag{4.2}$$

The bandwidth may vary around the nominal value due to variations of the optical transfer function gain, the arm transfer function gain and the radial actuator. The variations can be figured out experimentally to have a factor of magnitude between 1/3 and 3 [Dra89]. The (Philips) internal radial controller is a proportional-integral (PI) plus a phase lead compensator. The lead component gives a phase advance, and hence closed-loop stability, as the radial plant P_{rad} has a constant phase of $-180°$. The PI component gives d.c. disturbance rejection. This internal controller was designed to have PI zero at 50Hz, lead zero at 137Hz and lead pole at 1,054Hz. The controller gain was experimentally tested and verified using a digital signal processor (DSP). This controller, when implemented externally (see Figure 4.1 for the schematic), has the transfer function

$$C_{\text{Philips}}^{\text{rad}} = -1.747 \frac{s + 314.5}{s} \frac{s + 862.1}{s + 6622}.$$

The pole and zero of the lead component were chosen so that the maximum phase lead occurs at the frequency 380Hz ($= \sqrt{862.1 \times 6622}/(2\pi)$Hz) and the corresponding phase lead is 50.3°. One can find the above formulas in [FPEN94]. A good phase margin results.

Having described the schematics of the radial control loop of CD930 rig, we will introduce the experimental setup and the procedure for the controller implementation in the next section.

4.3 Descriptions of Experimental Setup

We will start this section with some related issues on the actual controller implementation. In order to allow system identification and external controls (radial position, focus position and turntable speed), there is an extra circuit built in the CD930 experimental rig. It is remarked that the feedback configuration in Figure 4.1 is a positive feedback type whereas the standard feedback configuration in Chapters 2 is of negative feedback type. Signs of the controllers have to be manipulated carefully. Referring to Figure 4.1, internal signals such as internal controller output (`CD`), plant input (`Monitor`) and error (`Error`) can be measured. External input signals such as external controller output (`Ext`) and external noise (`Noise`) can be fed into the CD player. These signals will be used for system identifications and external controls. The constants K_{CD}, K_{noise}, K_{mon}, K_{error} and K_{ext} in Figure 4.1 are transducer gains having the experimentally verified values given in Appendix E and [Dra89, Swi97].

The actual internal analog controller differs from the external controller $C_{\text{Philips}}^{\text{rad}}$ by a constant gain. All the signal measurements, system identification, and controller implementation experiments are performed by the digital signal processor TMS320C40 at a sampling frequency 20kHz. This sampling frequency is fast enough (50 times of the bandwidth of the open loop nominal radial plant) for a good approximation for the designed continuous-time controller and does not incur any downloading problem when the DSP is running. This DSP is capable of performing real-time implementations of controllers and tracings of signals. A series of steps have to be conducted for real-time controller implementation and further data analysis. In short, the steps in the sequential order are:

- design a stabilizing continuous-time robust controller, based on the given nominal plant;
- draw a SIMULINK block diagram (with the selected sampling frequency) for a discrete-time equivalent controller in the state-space form;
- activate the Philips switch box (specially designed for an anti-windup purpose to ensure smooth transitions to external controllers in this experiment) and let the whole system run for a few seconds before the externally implemented controller starts operating;
- generate a C file by the DSP and download the digital controller using the C compiler;
- switch the CD player to the external DSP controller;
- deactivate the switch box after transition to the external controller;
- select the signals (inputs, outputs or internal states of the controller) to be traced and the corresponding time intervals using the `trace` function in the DSP;
- save the traced signals;
- analyse (e.g. using discrete Fourier transform) the recorded data using MATLAB.

A sample SIMULINK block diagram for compilation can be found in Appendix G. Since the input and output signals in the DSP have saturations of ± 10 volts, the transient (e.g. due to the mismatch of the internal analog controller output and the external DSP controller output) when switching to external controller can cause windup of some internal signals, hence possibly instability. (The plant has its saturation but is usually below the saturation limit under normal operating conditions.) For this DSP saturation problem, equalizations of signals from the internal controller and the external controller and a bumpless transfer scheme (regarding to saturations) have to be carried out. An auxiliary "switch box" is used to achieve these purposes. This switch box modifies the error signal RE. The design of the switch box is based on the conventional anti-windup design method [KCMN94] with the circuit

$$\texttt{RE'} = \texttt{RE} - 0.2 \times (\texttt{Rad CD} - \texttt{Rad Ext})$$

where `RE'` is the modified radial error signal fed into the external controller, `RE` the original radial error signal, `Rad CD` the internal radial controller output and `Rad Ext` the external radial controller output (Figure 4.1). The modified error signal will be equal to the original error signal if the internal controller output is equal to the external controller output. Using this anti-windup scheme, the transient due to the inconsistency of the controller outputs is reduced.

4.4 Controller Designs using Loop Shaping and Closed-loop Pole Placement

Controller designs for the radial actuator using $\mathcal{H}_\infty$ loop shaping and closed-loop pole placement will be illustrated. Since the cross interactions between the radial loop and the focus loop are negligible, the radial loop can be treated separately. A Philips eccentric test disc was used in all the experiments. This test disc has the central hole off-centre of about 1mm. Exaggerated radial errors result and better comparisons can be made. Due to the variations of the plant parameters with respect to the track number (see Appendix F), an intermediate track where the variations are smallest was used. A typical radial error, apart from the high frequency noises, can be seen to be roughly periodic (Figure 4.2). At that chosen track, the radial error while the Philips controller $C^{\text{rad}}_{\text{Philips}}$ is implemented externally and its spectrum are shown in Figures 4.2 and 4.3. This spectrum has dominant peaks at harmonics 6Hz, 18Hz and 36Hz. (The peak at d.c. is missing because the d.c. is already rejected by the Philips controller.)

4.4.1 Controller Designs and Implementation Results

Having described the experimental rig, illustrations of the theory developed in Chapter 3 and controller designs are now presented. Based on the spectrum of the physical radial error (Figure 4.3), we will design robust repetitive controllers to reject the frequencies 0Hz, 6Hz, 18Hz and 36Hz. Controllers have to be designed to achieve the following criteria:

- the frequencies 0Hz, 6Hz, 18Hz and 36Hz are rejected;
- satisfactory robustness levels are guaranteed;
- the transient output of the disturbances with respect to the closed-loop transfer function $G = P_{\text{rad}}(I - CP_{\text{rad}})^{-1}$ is small, where the plant P_{rad} is given in equation (4.2).

Define the frequency set $\Omega_7 := \{0, \pm 2\pi 6, \pm 2\pi 18, \pm 2\pi 36\}$. Robustness is measured in the gap metric and the transient performance is measured in the power-energy induced measure, both defined in Chapter 3. It can easily be checked, by using Theorem 3.4.1, that

$$b_{\text{opt}}(P_{\text{rad}}) = b_{\text{opt}}(P_{\text{rad}}, \Omega_7) = 0.3827.$$

Define the internal model

$$H(s) := s\left(s^2 + (2\pi 6)^2\right)\left(s^2 + (2\pi 18)^2\right)\left(s^2 + (2\pi 36)^2\right).$$

Using the method described in Subsection 3.6.1, the set of loop shaping weighting functions

$$W_\beta(s) := \frac{H(s+\beta)}{H(s)}$$

is chosen with parameter $\beta \in [0.5, 15000]$. This parameter will determine the gap metric robustness margin as well as the transient power-energy induced measure. The corresponding graphs can be seen in Figures 4.4 and 4.5. As proved in Theorem 3.5.1, the transient power-energy induced measure will blow up as the robustness margin approaches its optimal value $b_{\text{opt}}(P_{\text{rad}}, \Omega_7)$ (for $\beta \to 0$). This phenomenon is irrespective of design method and can be observed in Figure 4.5. For the robustness requirement $b_{P_{\text{rad}},C} = 0.3$, the loop shaping robust repetitive controller

$$C^{\text{rad}}_{0.3,\text{LS}} = -3.167\frac{(s+128.9\pm j27.47)(s+136.5\pm j98.03)}{s(s+6632)\,(s^2+(2\pi 6)^2)} \times\frac{(s+145.6\pm j205.1)(s+349.7\pm j343.2)}{(s^2+(2\pi 18)^2)\,(s^2+(2\pi 36)^2)}$$

is obtained at $\beta = 156$. Consider the closed loop $G_{LS} := P_{\text{rad}}(I - C^{\text{rad}}_{0.3,\text{LS}}P_{\text{rad}})^{-1}$. The 8th order repetitive controller $C^{\text{rad}}_{0.3,\text{LS}}$ gives a gap metric robustness margin 0.3, the transient power-energy induced measure $\|G_{LS}\|_{\text{tr}\leftarrow\mathcal{S}_7} = 0.1817$ and the closed-loop bandwidth 515.2Hz. The closed-loop poles are located at $\{-150.1\pm j28.11, -155.1\pm j108.9, -156.2\pm j223.7, -190.0, -1765\pm j1789, -1988\}$. A physical radial error and its spectrum are shown in Figures 4.6 and 4.7. As for the Philips controller counterpart, a robustness margin of $b_{P_{\text{rad}},C_{\text{Philips}}} = 0.2054$, a closed-loop bandwidth of 473.0Hz and closed-loop poles at $\{-290.0, -4880, -725.9\pm j1260\}$ are obtained. The closed-loop transfer functions have Bode diagrams in Figure 4.8. From the spectra in Figures 4.3 and 4.7, it can be seen that the frequencies in Ω_7 are rejected and there is a great attenuation of the closed-loop gains at low frequencies by the loop shaping controller.

For the closed-loop pole placement method, the number of closed-loop poles is chosen to be $7+2\times 2-1 = 10$ (suggested in [RS93]). The closed-loop poles are selected at $-a$, $-a$, $-a$ and $-a+j\Omega_7$ for some $a>0$. Using the closed-loop characteristic polynomial

$$A_m(s;a) = (s+a)^4\left((s+a)^2+(2\pi 6)^2\right)\left((s+a)^2+(2\pi 18)^2\right)\left((s+a)^2+(2\pi 36)^2\right),$$

for $a\in[10^2,10^4]$, the robustness requirement $b_{P_{\text{rad}},C^{\text{rad}}_{\text{PP}}} = 0.3$ *cannot* be achieved (see Figure 4.9). The restriction on the locations of the closed-loop poles, namely the same real parts, results in a smaller achievable robustness margin. The closed-loop transfer function $P_{\text{rad}}(I - C^{\text{rad}}_{\text{PP}}P_{\text{rad}})^{-1}$ has the nice form

$$P_{\text{rad}}(I - C^{\text{rad}}_{\text{PP}}P_{\text{rad}})^{-1} = (2\pi 400)^2\frac{(s+10a)H(s)}{A_m(s;a)}.$$

The relationship between the transient power-energy induced measure and the robustness margin with parameter a is shown in Figure 4.5. The maximum robustness margin is 0.1973 and the corresponding pole placement controller is

$$C^{\text{rad}}_{0.1973,\text{PP}} = -4.847\frac{(s+342.7\pm j72.88)(s+330.8\pm j233.6)}{s(s+8249)\,(s^2+(2\pi 6)^2)} \times\frac{(s+292.0\pm j456.9)(s+132.5\pm j930.3)}{(s^2+(2\pi 18)^2)\,(s^2+(2\pi 36)^2)}$$

when $a = 824.9$. Define $G_{PP} := P_{\text{rad}}(I - C^{\text{rad}}_{0.1973,\text{PP}}P_{\text{rad}})^{-1}$. The Bode diagram of G_{PP} is shown in Figure 4.8. The transient power-energy induced measure $\|G_{PP}\|_{\text{tr}\leftarrow\mathcal{S}_7}$ is 0.1697. The closed-loop bandwidth is 558.6Hz. It can be seen from Figure 4.5 that a fast transient decay (in this pole placement design) has unsatisfactory robustness. However, a slow transient does *not* always mean a good robustness (see the top left corner of Figure 4.5). Another observation from

Figure 4.9 is that optimal robustness (or near optimal robustness) may not be attained using pole placement methods. This is due to the confined structure of the closed-loop poles.

In contrast with the loop shaping controller, no physical data can be traced when the pole placement controller $C^{\mathrm{rad}}_{0.1973,\mathrm{PP}}$ is implemented. This is because saturations of internal signals in the DSP occurs immediately after the downloading of the pole placement controller. It seems that the $\mathcal{H}_\infty$ loop shaping method is practically more useful in controller design and has fewer limitations.

It can be seen from Figure 4.8 that the loop shaping controller and the pole placement controller achieve better attenuations at low frequencies. The loop shaping controller is more robust than the Philips internal controller. The d.c., 6Hz, 18Hz and 36Hz frequencies are rejected by both the loop shaping controller and the pole placement controller. On the other hand, these two controllers perform less well in attenuating high frequency disturbances. To sum up, the robustness and performance (with $G = P_{\mathrm{rad}}(I - CP_{\mathrm{rad}})^{-1}$) of the controllers can be summarized as in Table 4.1.

Cont. Type	Freq. Rejection	$b_{P_{\mathrm{rad}},C}$	$\|G\|_{\mathrm{tr}\leftarrow\mathcal{S}_7}$	BW of G	Cont. Ord.
Closed-loop transfer function $G = P_{\mathrm{rad}}(I - CP_{\mathrm{rad}})^{-1}$					
Philips internal	0Hz	0.2054	N/A	473.0Hz	2
Loop Shaping	$0, 6, 18, 36$Hz	0.3000	0.1817	515.2Hz	8
Pole Placement	$0, 6, 18, 36$Hz	0.1973	0.1697	558.6Hz	8

Table 4.1 *Robustness and Performance of Various Controllers.*

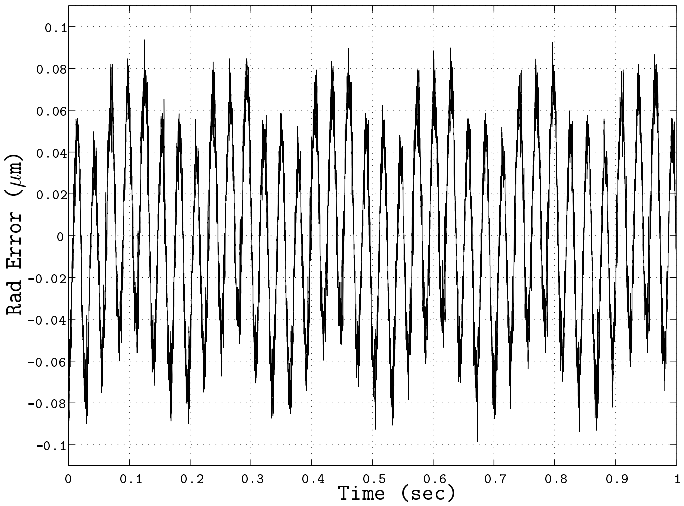

Figure 4.2 *The Physical Radial Error (Rad Error) using the dSPACE implemented Philips Controller* $C^{\mathrm{rad}}_{\mathrm{Philips}}$ *with sampling frequency* $20kHz$.

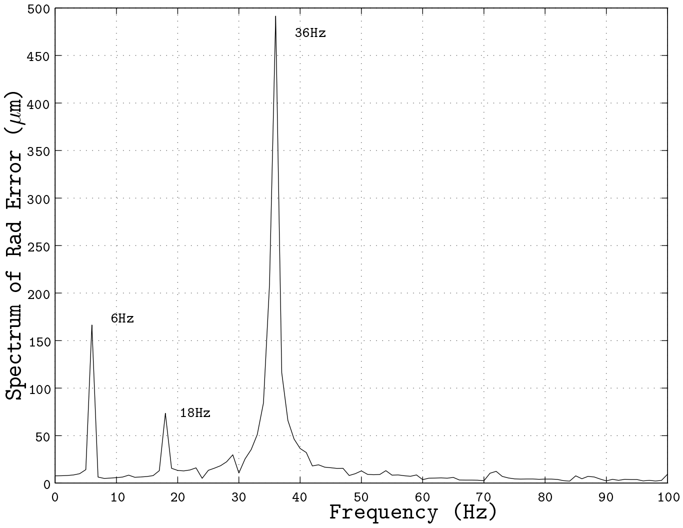

Figure 4.3 *The Spectrum of the Physical Radial Error (Rad Error) using the dSPACE implemented Philips Controller* $C^{\mathrm{rad}}_{\mathrm{Philips}}$ *with sampling frequency* $20kHz$.

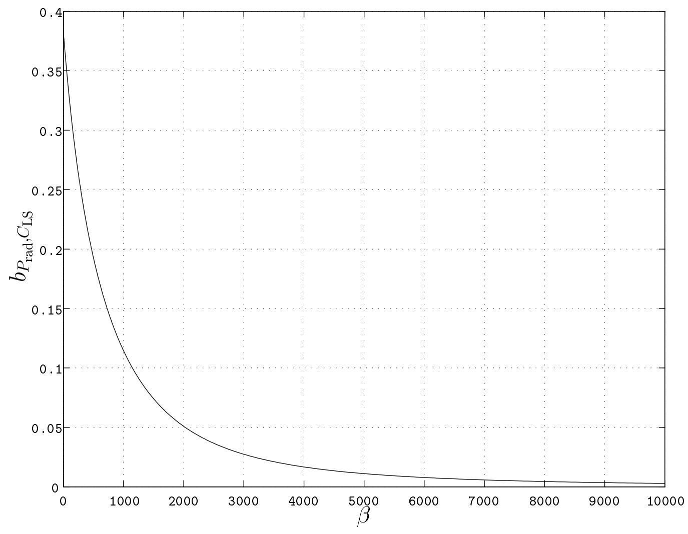

Figure 4.4 *The Relation between $b_{P_{\mathrm{rad}},C_{\mathrm{LS}}}$ and β.*

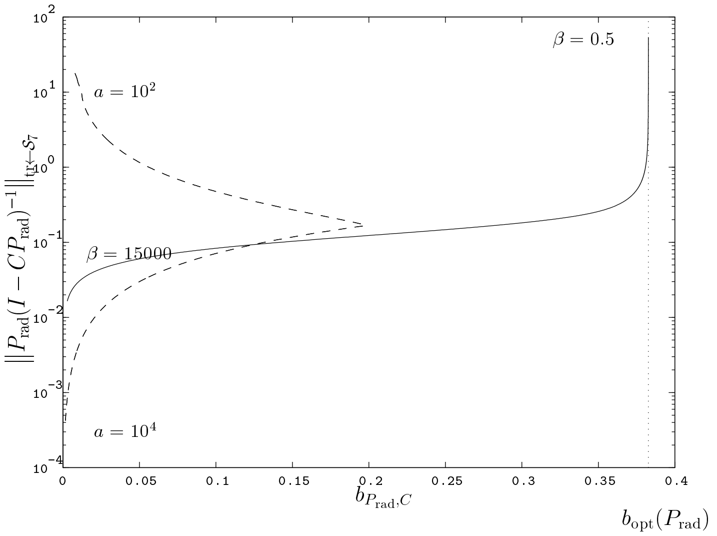

Figure 4.5 *The Relations between the Transient Power-energy Induced Measures and the Robustness Margin with parameters β and a. Loop Shaping: solid "—"; Pole Placement: dashed "- - -".*

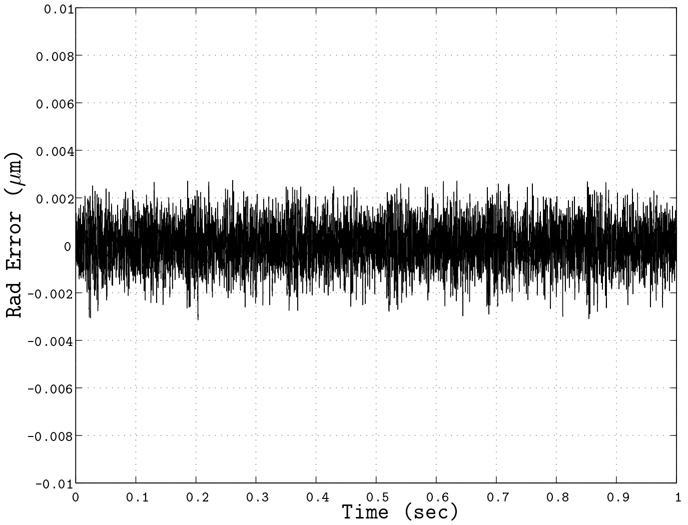

Figure 4.6 *The Physical Radial Error (Rad Error) using the dSPACE implemented Loop Shaping Controller* $C^{\mathrm{rad}}_{0.3,\mathrm{LS}}$ *with sampling frequency* 20*kHz.*

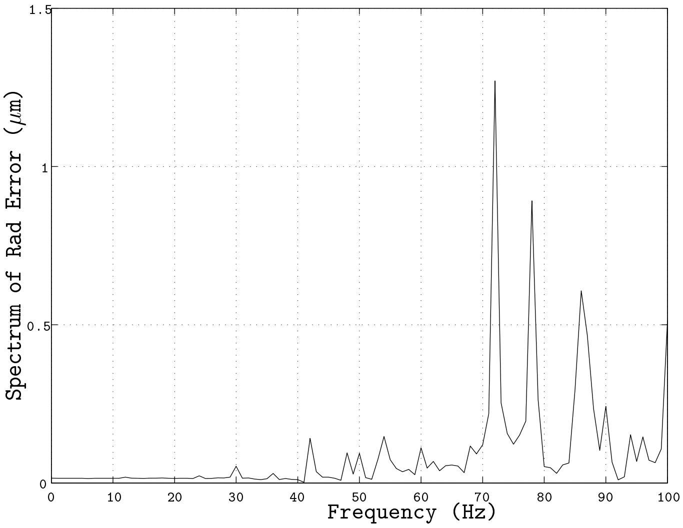

Figure 4.7 *The Spectrum of the Physical Radial Error (Rad Error) using the dSPACE implemented Loop Shaping Controller* $C^{\mathrm{rad}}_{0.3,\mathrm{LS}}$ *with sampling frequency* 20*kHz.*

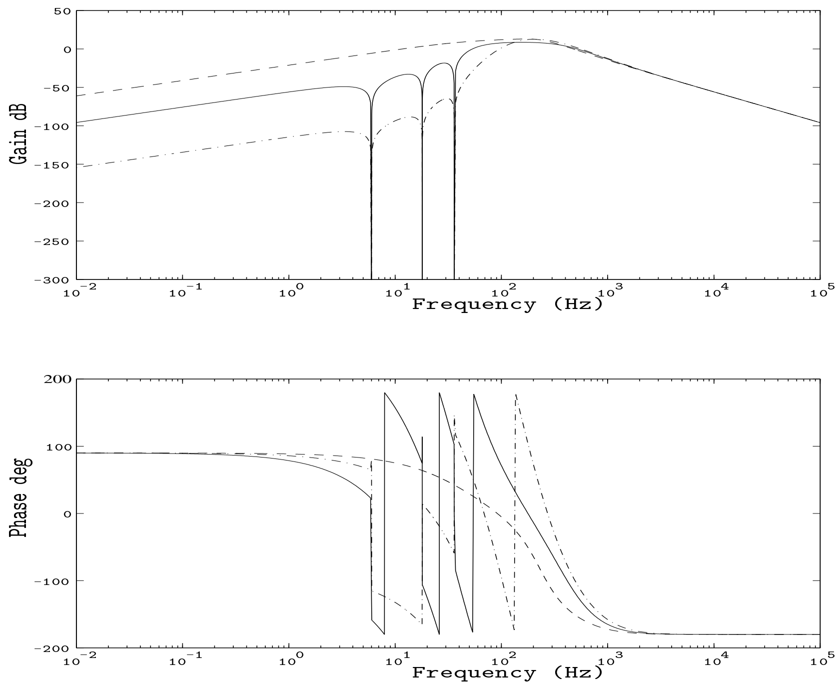

Figure 4.8 *The Bode Diagram for the Closed-loop Transfer Functions.* $P_{\mathrm{rad}}(1-C^{\mathrm{rad}}_{\mathrm{Philips}}P_{\mathrm{rad}})^{-1}$*: dashed "- - -";* $G_{LS} = P_{\mathrm{rad}}(1-C^{\mathrm{rad}}_{0.3,\mathrm{LS}}P_{\mathrm{rad}})^{-1}$*: solid "—";* $G_{PP} = P_{\mathrm{rad}}(1-C^{\mathrm{rad}}_{0.1973,\mathrm{PP}}P_{\mathrm{rad}})^{-1}$*: dashed dot "–·–·–".*

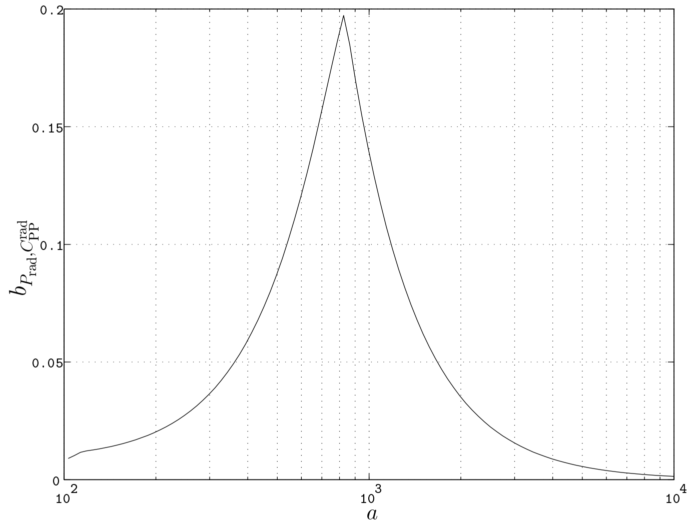

Figure 4.9 *The Relation between* $b_{P_{\mathrm{rad}},C^{\mathrm{rad}}_{\mathrm{PP}}}$ *and* a.

5

Nonlinear Repetitive Control Theory

5.1 Introduction

This chapter explores some theory on the repetitive control of a linear system using a nonlinear controller. It has been seen in Chapter 3 that there are some robustness limitations of linear control when perfect asymptotic rejection of periodic disturbance is sought. The necessity of using a nonlinear controller for robust asymptotic rejection of some periodic disturbances will be discussed in this chapter. The material in this chapter is based on the reference [LS98a]. Motivation of using a nonlinear controller will be given in Section 5.2. A precise problem statement will be formulated in Section 5.3. Section 5.4 describes the construction of a robust nonlinear controller to reject triangular waves for a specific class of linear systems with considerations of asymptotic rejection and robust stability. An example with simulation will be presented in Section 5.5.

5.2 Motivation of Nonlinear Control

The goal of repetitive control is to achieve tracking/rejection of some periodic references/disturbances. The Internal Model Principle [FW76] suggests that the dynamic structure of the reference/disturbance signals has to be incorporated in the linear controller. This means that when a linear controller is used, it needs to have poles (possibly infinitely many) at the harmonics of the periodic signals. It was pointed out by a number of authors that this scheme of complete tracking/rejection of periodic signals lacks robustness [HY85, HYON88]. A similar conclusion making use of the gap metric robustness measure for linear systems is drawn in Theorem 3.4.1 and in [LS96, LS98c], namely, asymptotic rejection of infinitely many harmonics in the case that the plant rolls off at high frequency implies a zero gap metric robustness margin. In fact it can be seen from Proposition 2.5.4 that any such control loop would not be w-stable (e.g. destabilized by an arbitrarily small time delay [LRW96]). Linear control would therefore be impractical in rejecting a class of periodic signals with infinitely many harmonics.

The linear control approach to asymptotic rejection of a periodic waveform with multiple (possibly infinitely many) harmonics necessitates the inclusion of poles in the controller at all frequencies which are harmonics of the periodic signal. Thus, a linear controller would seek asymptotic rejection for *any* periodic signal with the same set of harmonics. Therefore, if it is known that the disturbance is of a specific periodic waveform (e.g. a triangular wave) then such a linear controller would not exploit this fact. The question arises if robust asymptotic rejection is possible with nonlinear control for some particular type of periodic waveform. The answer is in the affirmative, at least for a specific class of plants and triangular wave disturbances. In effect, we illustrate an extension of the Internal Model Principle to a case which necessitates nonlinear control. The notions of the directed gap $\vec{\delta}(\cdot,\cdot)$, the robustness margin $b_{\mathbf{P},\mathbf{C}}$ and the robustness theorem can be found in Section 2.6. These terminologies will be used as the basics of the analysis in the rest of this chapter.

5.3 Problem Statement

We will consider the class of triangular waves of known fundamental period but unknown amplitude and phase. Denote the standard triangular wave of frequency 1 rad/sec with unit amplitude, zero phase and support on $[0,\infty)$ by:

$$f_0(t) := \begin{cases} \frac{2}{\pi}(t-2k\pi), & 2k\pi \leq t < 2(k+1/4)\pi, \\ 2-\frac{2}{\pi}(t-2k\pi), & 2(k+1/4)\pi \leq t < 2(k+3/4)\pi, \\ \frac{2}{\pi}(t-2k\pi)-4, & 2(k+3/4)\pi \leq t < 2(k+1)\pi, \end{cases}$$

where k is any non-negative integer. This wave is piecewise C^1 on $\mathbb{R}_+$ and is equal to its Fourier series (Proposition 2.2.14 and [Fol92]):

$$f_0(t) = \frac{8}{\pi^2}\sum_{n=1}^{\infty}(-1)^{n+1}\frac{\sin(2n-1)\,t}{(2n-1)^2} \quad \forall t \geq 0.$$

This f_0 has infinitely many non-zero Fourier coefficients. Any triangular wave $f(t)$ of fundamental frequency ω_0 rad/sec, amplitude A and phase ϕ can be written as $f(t) = A\,f_0(\omega_0 t+\phi)$. Denote by $\mathcal{T}(\omega_0)$ the set of such triangular waves, i.e.

$$\mathcal{T}(\omega_0) := \{A\,f_0(\omega_0 t+\phi) : A, \phi > 0\}\,.$$

We will restrict attention to scalar plants and controllers in the standard feedback configuration in Figure 2.1. We choose to formulate our repetitive control problem as the asymptotic disturbance rejection of triangular waves $u_0 \in \mathcal{T}(\omega_0)$ at the plant output y_1. We will require that the feedback loop is robustly stable in the sense of having a non-zero gap metric robustness margin $b_{P,C}$. Formally we define our control problem as follows.

Problem 5.3.1. *Consider the feedback configuration in Figure 2.1 with $y_0 = 0$. Given a fundamental frequency ω_0 and a scalar, rational and strictly proper plant $\mathbf{P}$ with $P(j\omega_0) \neq 0$, find a controller $\mathbf{C}$ with $b_{P,C} > 0$ to achieve robust asymptotic rejection at y_1 for any $u_0 \in \mathcal{T}(\omega_0)$.*

We are able to show that Problem 5.3.1 is not soluble with a linear $\mathbf{C}$, assuming that $\mathbf{C}$ belongs to a certain class of linear systems which includes all finite dimensional and some infinite dimensional ones. We first note that the conclusion is trivial if $\mathbf{C}$ is finite dimensional. This follows because any element of $\mathcal{T}(\omega_0)$ contains infinitely many non-zero harmonics and any rational function has finitely many zeros, so the objective of asymptotic disturbance rejection cannot even be achieved. We therefore need to admit controllers which are infinite dimensional. Let us assume $\mathbf{C}$ has transfer function C so that $G := P(I-CP)^{-1} \in \mathcal{H}_\infty^\alpha$ for some $\alpha < 0$, where $\mathcal{H}_\infty^\alpha$ denotes the space of bounded and analytic functions in the right half plane $\Re(s) > \alpha$. It is possible to show using the techniques of Weiss and Häfele 1997 (see Lemma 9 and Proposition 11 of [WH97]) that we can decompose the output y_1, where $\hat{y}_1 = G\hat{u}_0$ for $u_0 = \sum_{k=-\infty}^{\infty} a_k e^{jk\omega_0 t} \in \mathcal{T}(\omega_0)$, uniquely as: $y_1 = y_{1,\mathrm{ss}} + y_{1,\mathrm{tr}}$ where $y_{1,\mathrm{ss}} = \sum_{k=-\infty}^{\infty} G(jk\omega_0) a_k e^{jk\omega_0 t}$ and $y_{1,\mathrm{tr}},\ \dot{y}_{1,\mathrm{tr}} \in \mathscr{L}_2(\mathbb{R}_+)$ (see Appendix A for the proof). The latter implies that $y_{1,\mathrm{tr}} \to 0$ as $t \to \infty$ (as a result of Proposition 5.3.3). So the condition that $y_1 \to 0$ as $t \to \infty$ requires that $G(jk\omega_0) = 0$ for all (infinitely many) k where $a_k \neq 0$. As shown in Chapter 3 and [LS96, LS98c], if asymptotic rejection of a harmonic with frequency ω_1 is sought, then $b_{P,C} < |P(j\omega_1)|/\sqrt{1 + |P(j\omega_1)|^2}$. Since the plant is strictly proper and the triangular wave has infinitely many non-zero harmonics, it is clear that the above problem has no solution with such a linear controller $\mathbf{C}$. The appropriate choices of the underlying signal spaces are $\mathcal{U} = \mathcal{Y} = \mathscr{L}_\infty(\mathbb{R}_+)$ (see Section 2.4 for the feedback configuration). Note that $b_{\mathbf{P},\mathbf{C}}$ is the inverse of the $\mathscr{L}_\infty$-induced norm of the mapping from (u_0, y_0) to (u_1, y_1) in Figure 2.1. It should be noted that, in the linear controller case, the $\mathscr{L}_\infty$-induced version of $b_{\mathbf{P},\mathbf{C}}$ is less than or equal to the $\mathscr{L}_2$-induced version, which is itself equal to $b_{P,C}$. It is because:

$$
\begin{aligned}
& \|K\|_{\mathscr{L}_2\text{-induced}} \\
= \ & \sup_\omega |K(j\omega)| \\
= \ & \sup_\omega \left| \int_0^\infty k(t) e^{-j\omega t}\, dt \right| \\
\leq \ & \sup_\omega \int_0^\infty |k(t)|\, dt \\
= \ & \|K\|_{\mathscr{L}_\infty\text{-induced}}
\end{aligned}
$$

where $\Pi_{\mathcal{G}_\mathbf{P}//\mathcal{G}_\mathbf{C}}$ has the (stable) transfer function

$$
K := \begin{pmatrix} I \\ P \end{pmatrix} (I - CP)^{-1}(I, -C)
$$

and $k(\cdot)$ is the inverse Laplace transform of $K(\cdot)$. Thus Problem 5.3.1 has no solution with a linear controller because the $\mathscr{L}_2$-induced $b_{P,C}$ is zero if all (infinitely many) frequencies are rejected. In order to show that there is a solution for a nonlinear $\mathbf{C}$, we need to adopt the notion of the nonlinear $b_{\mathbf{P},\mathbf{C}}$ with $\mathcal{U} = \mathcal{Y} = \mathscr{L}_\infty(\mathbb{R}_+)$ and make precise the concept of asymptotic rejection.

Definition 5.3.2. *Consider the feedback configuration in Figure 2.1 with $y_0 = 0$. The disturbance u_0 is said to be asymptotically rejected at the plant output y_1 if $\lim_{t\to\infty} y_1(t) = 0$.*

Proposition 5.3.3. *[DV75] If f and $\dot{f} \in \mathscr{L}_2(\mathbb{R}_+)$, then $f \in \mathscr{L}_\infty(\mathbb{R}_+)$ and $|f(t)| \to 0$ as $t \to \infty$.*

Proof. Clearly, we have

$$\frac{1}{2}\big(f^2(b) - f^2(a)\big) = \int_a^b f\dot{f}\, dt \leq \frac{1}{2}\int_a^b (f^2 + \dot{f}^2)\, dt \tag{5.1}$$

for any $a, b \geq 0$. The right hand side is always bounded above by $\big(\|f\|_2^2 + \|\dot{f}\|_2^2\big)/2$. Thus, $f \in \mathscr{L}_\infty(\mathbb{R}_+)$. For the second part, note that for any $\varepsilon > 0$, there exists an $N > 0$ such that

$$\int_a^b f^2\, dt, \int_a^b \dot{f}^2\, dt < \varepsilon$$

whenever $a, b \geq N$ [Rud87]. This fact together with (5.1) implies that the sequence $\{f^2(t_n)\}_{n\in\mathbb{N}}$ for large t_n is Cauchy. By the completeness of $\mathbb{R}$, $\lim_{t\to\infty} f^2(t)$ exists and is zero because $f \in \mathscr{L}_2(\mathbb{R}_+)$. □

5.4 Construction

In this section, a causal nonlinear controller will be given to achieve the asymptotic rejection of inputs $u_0 \in \mathcal{T}(\omega_0)$ at the output y_1 for some given frequency ω_0 with robust stability measured by the nonlinear $b_{\mathbf{P},\mathbf{C}}$. Define a linear controller

$$\tilde{\mathbf{C}} := \begin{pmatrix} \tilde{\mathbf{C}}_1 \\ \tilde{\mathbf{C}}_2 \end{pmatrix}$$

with the transfer function

$$\tilde{C}(s) = \begin{pmatrix} \tilde{C}_1(s) \\ \tilde{C}_2(s) \end{pmatrix} := \begin{pmatrix} -(ks+\gamma)/(s^2+\omega_0^2) \\ -(\gamma s - k\omega_0^2)/(\omega_0(s^2+\omega_0^2)) \end{pmatrix},$$

where $k, \gamma > 0$ are given. Define also the memoryless nonlinear mapping $N : \mathbb{R}^2 \to \mathbb{R}$ as

$$N\begin{pmatrix} x_1 \\ x_2 \end{pmatrix} := \begin{cases} 0, & \text{if } x_1 = x_2 = 0, \\ \frac{2\sqrt{x_1^2+x_2^2}}{\pi}\sin^{-1}\left(\frac{x_1}{\sqrt{x_1^2+x_2^2}}\right), & \text{otherwise,} \end{cases}$$

where $\sin^{-1}(\cdot)$ takes its principal value in the range $-\pi/2$ to $\pi/2$. We will use the notation $\mathbf{N}$ to denote the operator acting on $\mathscr{L}_\infty(\mathbb{R}_+) \times \mathscr{L}_\infty(\mathbb{R}_+)$ and defined by applying N pointwise in time. This nonlinear mapping $\mathbf{N}$ will distort certain vector sinusoids into scalar triangular waves of appropriate amplitudes and phases[1]. Define the (scalar) nonlinear controller $\mathbf{C} := \mathbf{N} \circ \tilde{\mathbf{C}}$

[1] It appears that not every causal nonlinear mapping which converts sinusoids into triangular waves can achieve asymptotic rejection of disturbances in $\mathcal{T}(\omega_0)$. For instance, the nonlinear mapping

$$N(w(t)) = \frac{2\alpha(t)}{\pi}\sin^{-1}\left(\frac{w(t)}{\alpha(t)}\right)$$

where $\alpha(t) := \max_{\tau\in[t-2\pi/\omega_0, t]} |w(\tau)|$ will give a nonlinear controller which seems to produce a bounded but non-zero steady state, as corroborated by simulations.

(see Figure 5.1). The remaining part of this section will show that the controller $\mathbf{C}$ solves

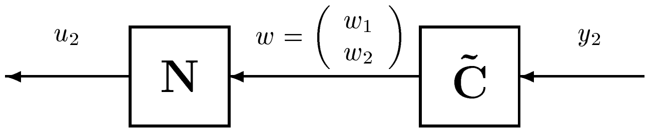

Figure 5.1 *A Nonlinear Controller* $\mathbf{C} := \mathbf{N} \circ \tilde{\mathbf{C}}$.

Problem 5.3.1 under some conditions. The intuition behind the controller is as follows. The linear controller $\tilde{\mathbf{C}}$ can produce in the steady state, for an input which is eventually zero, any pair of sinusoids of the same amplitude and with a $\pi/2$ phase shift between them. If such a signal is applied to $\mathbf{N}$, then the output of $\mathbf{N}$ is, in the steady state, a triangular wave of the same frequency, amplitude and phase as the first component of the output of $\tilde{\mathbf{C}}$. Thus $\mathbf{C}$ plays the role of an internal model in generating suitable signals to counteract the disturbances in $\mathcal{T}(\omega_0)$. In order that $\mathbf{C}$ solves Problem 5.3.1, it is necessary that the operator $\mathbf{H}_{\mathbf{P},\mathbf{C}}$ defined in Section 2.4 is stable. This will be established by showing that the directed gap between $\mathbf{C}$ and some stabilizing linear controller is small enough for Proposition 2.6.2 to apply. To prove additionally that asymptotic disturbance rejection is achieved, the Contraction Mapping Theorem will be used. Two sets of sufficient conditions for the objectives of asymptotic rejection and robust stability will be derived. These will be given in the following subsections.

5.4.1 Asymptotic Rejection

Consider the feedback configuration of Figure 2.1 with $\mathbf{C} = \mathbf{N} \circ \tilde{\mathbf{C}}$. We will assume that $\mathbf{P}$ is stable and that $[\mathbf{P}, \tilde{\mathbf{C}}_1]$ is stable. Let $y_0 = 0$ and consider any $u_0 \in \mathcal{T}(\omega_0)$, say $u_0(t) = A\, f_0(\omega_0 t + \phi)$. Define the corresponding vector signal

$$v_0(t) := \begin{pmatrix} A\sin(\omega_0 t + \phi) \\ A\cos(\omega_0 t + \phi) \end{pmatrix}$$

and observe that

$$u_0 = \mathbf{N} v_0.$$

It can easily be verified that the following equations are satisfied:

$$w = -\tilde{\mathbf{C}}\mathbf{P}(\mathbf{N}v_0 - \mathbf{N}w), \tag{5.2}$$

$$y_1 = \mathbf{P}(\mathbf{N}v_0 - \mathbf{N}w). \tag{5.3}$$

Define the operator

$$\tilde{\mathbf{G}} := -\left(\mathbf{I} - \tilde{\mathbf{C}}\mathbf{P}(1,0)\right)^{-1} \tilde{\mathbf{C}}\mathbf{P}.$$

$\tilde{\mathbf{G}}$ can be shown to have the transfer function

$$\tilde{G} := \frac{-\tilde{C}_1 P}{1 - \tilde{C}_1 P} \begin{pmatrix} 1 \\ \frac{\gamma s - k\omega_0^2}{\omega_0 (ks+\gamma)} \end{pmatrix}. \tag{5.4}$$

By subtracting the term $\tilde{\mathbf{C}}\mathbf{P}(1,0)w$ from both sides of (5.2) and pre-multiplying by the factor $\left(\mathbf{I} - \tilde{\mathbf{C}}\mathbf{P}(1,0)\right)^{-1}$, we obtain the equation $w = \tilde{\mathbf{G}}(\mathbf{N}v_0 - \mathbf{N}w) + \tilde{\mathbf{G}}(1,0)w$. Defining also

$$f := w - v_0,$$

we get

$$f = \tilde{\mathbf{G}}\mathbf{\Gamma}(f) + \left\{\tilde{\mathbf{G}}(1,0) - \mathbf{I}\right\} v_0 \tag{5.5}$$

where the operator $\mathbf{\Gamma}$ is defined as

$$\mathbf{\Gamma}(f) := \mathbf{N}v_0 - \mathbf{N}(v_0 + f) + (1,0)f. \tag{5.6}$$

It is clear that $\mathbf{\Gamma}(0) = 0$. Suppose $P(\pm j\omega_0) \neq 0$, we have

$$\tilde{G}(\pm j\omega_0) = \begin{pmatrix} 1 \\ \pm j \end{pmatrix}$$

and therefore $\left\{\tilde{\mathbf{G}}(1,0) - \mathbf{I}\right\} v_0 \in \mathscr{L}_2(\mathbb{R}_+)$. We will see below that the operator $\mathbf{\Gamma}$ maps the space $\mathscr{L}_2(\mathbb{R}_+)$ into itself. If we can also prove that the incremental gains of $\tilde{\mathbf{G}}$ and $\mathbf{\Gamma}$ satisfy the inequality

$$\|\tilde{\mathbf{G}}\|_\triangle \cdot \|\mathbf{\Gamma}\|_\triangle < 1, \tag{5.7}$$

then (5.5) has a unique solution $\tilde{f} := (\mathbf{I} - \tilde{\mathbf{G}}\mathbf{\Gamma})^{-1} \left\{\tilde{\mathbf{G}}(1,0) - \mathbf{I}\right\} v_0 \in \mathscr{L}_2(\mathbb{R}_+)$, by the Contraction Mapping Theorem [GL95, Kre78]. Under the assumptions that $\mathbf{P}$ is strictly proper and stable then $sP \in \mathcal{H}_\infty$, so that $\frac{d}{dt} \circ \mathbf{P}$ is a bounded operator on $\mathscr{L}_2[0,\infty)$. Thus asymptotic rejection is achieved at the output y_1 by using Proposition 5.3.3 and

$$y_1 = \mathbf{P}\left(\mathbf{N}v_0 - \mathbf{N}(v_0 + \tilde{f})\right) = \mathbf{P}\left(\mathbf{\Gamma}(\tilde{f}) - (1,0)\tilde{f}\right) \in \mathscr{L}_2(\mathbb{R}_+),$$

and

$$\dot{y_1} = \left(\frac{d}{dt} \circ \mathbf{P}\right)\left(\mathbf{\Gamma}(\tilde{f}) - (1,0)\tilde{f}\right) \in \mathscr{L}_2(\mathbb{R}_+).$$

We will now show that $\|\mathbf{\Gamma}\|_\triangle = 2/\pi$ regarding $\mathbf{\Gamma}$ as a mapping from $\mathscr{L}_2(\mathbb{R}_+)$ into $\mathscr{L}_2(\mathbb{R}_+)$. Note that, from the definition in (5.6), for any vector functions f and g on $\mathbb{R}_+$, we have

$$\mathbf{\Gamma}(f) - \mathbf{\Gamma}(g) = \mathbf{N}(v_0 + g) - \mathbf{N}(v_0 + f) + (1,0)\big((v_0 + f) - (v_0 + g)\big).$$

For each $t \geq 0$, write

$$\begin{pmatrix} a_1 \\ b_1 \end{pmatrix} = v_0(t) + g(t), \quad \begin{pmatrix} a_2 \\ b_2 \end{pmatrix} = v_0(t) + f(t).$$

By noting that

$$N\begin{pmatrix} x_1 \\ -x_2 \end{pmatrix} = N\begin{pmatrix} x_1 \\ x_2 \end{pmatrix}$$

and that N is differentiable in $\mathbb{R}^2$ and using the mean value theorem [Rud85], we have

$$\begin{aligned} \left|\big(\mathbf{\Gamma}(f) - \mathbf{\Gamma}(g)\big)(t)\right| &= \left| N\begin{pmatrix} a_1 \\ |b_1| \end{pmatrix} - N\begin{pmatrix} a_2 \\ |b_2| \end{pmatrix} - (a_1 - a_2) \right| \\ &= \left| \left(\frac{\partial N}{\partial x_1}(\underline{\hat{x}}) - 1, \frac{\partial N}{\partial x_2}(\underline{\hat{x}}) \right) \cdot \begin{pmatrix} a_1 - a_2 \\ |b_1| - |b_2| \end{pmatrix} \right| \end{aligned}$$

for some $\underline{\hat{x}} = (\hat{x}_1, \hat{x}_2)^T = \mu(a_1, |b_1|)^T + (1-\mu)(a_2, |b_2|)^T$, $\mu \in (0,1)$. Note that

$$\begin{aligned} \frac{\partial N}{\partial x_1}(\underline{\hat{x}}) &= \frac{2}{\pi}\left(\cos(\hat{\theta}) + \hat{\theta}\sin(\hat{\theta})\right) \\ \frac{\partial N}{\partial x_2}(\underline{\hat{x}}) &= \frac{2}{\pi}\left(\hat{\theta}\cos(\hat{\theta}) - \sin(\hat{\theta})\right) \end{aligned}$$

for some unique $\hat{\theta} \in [-\pi/2, \pi/2]$ where

$$\sin(\hat{\theta}) := \frac{\hat{x}_1}{\sqrt{\hat{x}_1^2 + \hat{x}_2^2}}, \qquad \cos(\hat{\theta}) := \frac{\hat{x}_2}{\sqrt{\hat{x}_1^2 + \hat{x}_2^2}}$$

because $\hat{x}_2 = \mu|b_1| + (1-\mu)|b_2| \geq 0$. For $\theta \in [-\pi/2, \pi/2]$, define

$$h(\theta) := \sqrt{\left(\frac{2}{\pi}(\cos(\theta) + \theta\sin(\theta)) - 1\right)^2 + \left(\frac{2}{\pi}(\theta\cos(\theta) - \sin(\theta))\right)^2},$$

and note that

$$\left|\begin{pmatrix} a_1 - a_2 \\ |b_1| - |b_2| \end{pmatrix}\right| \leq |f(t) - g(t)|,$$

we therefore have

$$\left|\big(\mathbf{\Gamma}(f) - \mathbf{\Gamma}(g)\big)(t)\right| \leq h(\hat{\theta}) \cdot |f(t) - g(t)|$$

for some $\hat{\theta} \in [-\pi/2, \pi/2]$. Since $\max_{\theta \in [-\pi/2, \pi/2]} h(\theta) = h(\pm\pi/2) = 2/\pi$,

$$\left|\big(\mathbf{\Gamma}(f) - \mathbf{\Gamma}(g)\big)(t)\right| \leq \frac{2}{\pi}\,|f(t) - g(t)| \quad \forall t \geq 0.$$

Hence, $\mathbf{\Gamma}$ maps $\mathscr{L}_2(\mathbb{R}_+)$ into itself (since $\mathbf{\Gamma}(0) = 0$) and its incremental gain is less than or equal to $2/\pi$. In fact, $\|\mathbf{\Gamma}\|_\triangle = 2/\pi$. This can be observed by choosing any $\varepsilon > 0$,

$$g := \begin{pmatrix} 1 \\ 0 \end{pmatrix} - v_0, \qquad f := \begin{pmatrix} 1 - \varepsilon \\ \sqrt{2\varepsilon - \varepsilon^2} \end{pmatrix} - v_0$$

and observing that

$$\left|\left(\mathbf{\Gamma}(f) - \mathbf{\Gamma}(g)\right)(t)\right| = \left|1 - \varepsilon - \frac{2}{\pi}\sin^{-1}(1-\varepsilon)\right|$$

and

$$|f(t) - g(t)| = \sqrt{2\varepsilon}.$$

The ratio $\left|\left(\mathbf{\Gamma}(f) - \mathbf{\Gamma}(g)\right)(t)\right| / |f(t) - g(t)|$ has limit $2/\pi$ when ε tends to zero.

Finally we note that $\tilde{\mathbf{G}}$ is linear and therefore the incremental gain of $\tilde{\mathbf{G}}$ acting on $\mathscr{L}_2(\mathbb{R}_+)$ is equal to $\|\tilde{G}\|_{\mathcal{H}_\infty}$. We thus obtain a set of sufficient conditions for asymptotic rejection of disturbances in $\mathcal{T}(\omega_0)$ using the nonlinear controller $\mathbf{C} = \mathbf{N} \circ \tilde{\mathbf{C}}$ as follows.

Sufficient Conditions for Asymptotic Rejection of Disturbances in $\mathcal{T}(\omega_0)$

1. $\mathbf{P}$ is strictly proper, stable and $P(\pm j\omega_0) \neq 0$;
2. $[\mathbf{P}, \tilde{\mathbf{C}}_\mathbf{1}]$ is stable where $\tilde{C}_1(s) = -(ks+\gamma)/(s^2+\omega_0^2)$ for some $k, \gamma > 0$;
3. $\|\tilde{G}\|_{\mathcal{H}_\infty} < \pi/2$ where $\tilde{G}$ is defined in (5.4).

5.4.2 Robust Stability

In this section, we will derive some sufficient conditions for the nonlinear $b_{\mathbf{P},\mathbf{C}}$ with $\mathbf{C} = \mathbf{N} \circ \tilde{\mathbf{C}}$ to be bounded away from zero. We will make use of Proposition 2.6.2 with $[\mathbf{P}, \lambda\tilde{\mathbf{C}}_\mathbf{1}]$ as the nominal closed loop and $[\mathbf{P}, \mathbf{N} \circ \tilde{\mathbf{C}}]$ the perturbed closed loop, for some appropriate $\lambda > 0$, to obtain an upper bound on $b_{\mathbf{P},\mathbf{C}}^{-1} = \left\|\Pi_{\mathcal{G}_\mathbf{P}//\mathcal{G}_\mathbf{C}}\right\|$. We will take the signal spaces to be $\mathcal{U} = \mathcal{Y} = \mathscr{L}_\infty(\mathbb{R}_+)$. We first note that N satisfies the property

$$k_1|x_1| \leq |N(\underline{x})| \leq k_2|x_1| \tag{5.8}$$

for all $\underline{x} = (x_1, x_2)^T \in \mathbb{R}^2$, where $k_1 := 2/\pi > 0$ and $k_2 := 1 < \infty$. (This follows from the inequalities $1 \leq |(\sin^{-1} x)/x| \leq \pi/2$ for $-1 \leq x \leq 1$.) We therefore see that

$$\operatorname{dom}\left(\lambda\tilde{\mathbf{C}}_\mathbf{1}\right) = \operatorname{dom}\left(\mathbf{N} \circ \tilde{\mathbf{C}}\right).$$

For the rest of this section, we use the following (abuse of) notation. Let $F(s)$ be the transfer function of a stable linear system and $y \in \mathscr{L}_\infty(\mathbb{R}_+)$. Then $F(s)y$ denotes the time domain output in $\mathscr{L}_\infty(\mathbb{R}_+)$ of the linear system with input y, i.e. we use Fy to mean $\mathbf{F}y$. We also denote by $\|F(s)y\|_\infty$ the supremum norm of this time domain signal. We now observe that

$$\operatorname{dom}\left(\lambda\tilde{\mathbf{C}}_\mathbf{1}\right) = \left\{\frac{s^2+\omega_0^2}{(s+1)^2}y : y \in \mathcal{Y}\right\} =: \frac{s^2+\omega_0^2}{(s+1)^2}\mathcal{Y}.$$

Thus, the graphs of the two controllers are given by

$$\mathcal{G}_{\lambda\tilde{\mathbf{C}}_\mathbf{1}} = \left\{\begin{pmatrix} \lambda\frac{ks+\gamma}{(s+1)^2}y \\ -\frac{s^2+\omega_0^2}{(s+1)^2}y \end{pmatrix} : y \in \mathcal{Y}\right\}$$

and

$$\mathcal{G}_{\mathbf{N}\circ\tilde{\mathbf{C}}} = \left\{ \begin{pmatrix} \mathbf{N}\left(\left(\frac{ks+\gamma}{(s+1)^2} y, \frac{\gamma s - k\omega_0^2}{\omega_0 (s+1)^2} y \right)^T \right) \\ -\frac{s^2+\omega_0^2}{(s+1)^2} y \end{pmatrix} : y \in \mathcal{Y} \right\}.$$

Define

$$\tilde{F}(s) := \begin{pmatrix} \lambda \frac{ks+\gamma}{(s+1)^2} \\ -\frac{s^2+\omega_0^2}{(s+1)^2} \end{pmatrix}.$$

Then $\mathcal{G}_{\lambda\tilde{\mathbf{C}}_1} = \tilde{F}\,\mathcal{Y}$ and $\|\tilde{F}y\|_\infty \geq \lambda \left\| \frac{ks+\gamma}{(s+1)^2} y \right\|_\infty$. Define also the mapping $\mathbf{\Phi_0} : \mathcal{G}_{\lambda\tilde{\mathbf{C}}_1} \to \mathcal{G}_{\mathbf{N}\circ\tilde{\mathbf{C}}}$ by

$$\mathbf{\Phi_0}(\tilde{F}y) = \begin{pmatrix} \mathbf{N}\left(\left(\frac{ks+\gamma}{(s+1)^2} y, \frac{\gamma s - k\omega_0^2}{\omega_0 (s+1)^2} y \right)^T \right) \\ -\frac{s^2+\omega_0^2}{(s+1)^2} y \end{pmatrix}, \quad y \in \mathcal{Y}.$$

Then this $\mathbf{\Phi_0}$ is causal, bijective and $\mathbf{\Phi_0}0 = 0$. We now choose $\lambda = (k_1 + k_2)/2$. Thus from (5.8),

$$\begin{aligned} \left\| (\mathbf{\Phi_0} - \mathbf{I})\tilde{F}y \right\|_\infty &= \left\| \mathbf{N}\left(\left(\frac{ks+\gamma}{(s+1)^2} y, \frac{\gamma s - k\omega_0^2}{\omega_0 (s+1)^2} y \right)^T \right) - \lambda \frac{ks+\gamma}{(s+1)^2} y \right\|_\infty \\ &\leq \frac{k_2 - k_1}{2} \left\| \frac{ks+\gamma}{(s+1)^2} y \right\|_\infty \leq \frac{k_2 - k_1}{2\lambda} \|Fy\|_\infty . \end{aligned}$$

Hence by the definition of directed gap,

$$\vec{\delta}\left(\mathcal{G}_{\lambda\tilde{\mathbf{C}}_1}, \mathcal{G}_{\mathbf{N}\circ\tilde{\mathbf{C}}} \right) \leq \frac{k_2 - k_1}{k_2 + k_1} = \frac{1 - 2/\pi}{1 + 2/\pi} = 0.2220.$$

On the other hand, the parallel projection operator $\Pi_{\mathcal{G}_{\lambda\tilde{\mathbf{C}}_1}//\mathcal{G}_{\mathbf{P}}}$ has the transfer function

$$\begin{pmatrix} \lambda\tilde{C}_1 \\ 1 \end{pmatrix} (1 - \lambda\tilde{C}_1 P)^{-1}(-P, 1).$$

It is known [ZDG96] that the $\mathscr{L}_\infty$-induced norm for this parallel projection is equal to

$$\begin{aligned} \left\| \Pi_{\mathcal{G}_{\lambda\tilde{\mathbf{C}}_1}//\mathcal{G}_{\mathbf{P}}} \right\| = \max\Bigg\{ & \left\| \mathscr{L}^{-1}\left(\frac{\lambda\tilde{C}_1 P}{1 - \lambda\tilde{C}_1 P} \right) \right\|_1 + \left\| \mathscr{L}^{-1}\left(\frac{\lambda\tilde{C}_1}{1 - \lambda\tilde{C}_1 P} \right) \right\|_1 , \\ & \left\| \mathscr{L}^{-1}\left(\frac{P}{1 - \lambda\tilde{C}_1 P} \right) \right\|_1 + \left\| \mathscr{L}^{-1}\left(\frac{1}{1 - \lambda\tilde{C}_1 P} \right) \right\|_1 \Bigg\} \end{aligned}$$

where $\mathscr{L}^{-1}$ stands for the inverse Laplace transform and

$$\left\| D + C(sI - A)^{-1}B \right\|_1 := |D| + \int_0^\infty \left| Ce^{At}B \right| dt$$

for SISO systems with stable A. Based on Proposition 2.6.2, we can establish a set of sufficient conditions for robust stability of the closed loop $[\mathbf{P}, \mathbf{N} \circ \tilde{\mathbf{C}}]$.

<u>Sufficient Conditions for Robust Stability of the closed loop $[\mathbf{P}, \mathbf{N} \circ \tilde{\mathbf{C}}]$</u>

1. $[\mathbf{P}, \lambda\tilde{\mathbf{C}}_\mathbf{1}]$ is stable, where $\lambda = (k_1 + k_2)/2$;

2. $\frac{k_2 - k_1}{k_2 + k_1} \cdot \left\| \Pi_{\mathcal{G}_{\lambda\tilde{\mathbf{C}}_\mathbf{1}} // \mathcal{G}_\mathbf{P}} \right\| < 1$

where $k_1 = 2/\pi$ and $k_2 = 1$ are the bounds in (5.8).

If these sufficient conditions are satisfied, the (nonlinear) gap metric robustness margin, applying Proposition 2.6.2, has a lower bound

$$b_{\mathbf{P},\mathbf{N}\circ\tilde{\mathbf{C}}} \geq \frac{1 - \frac{k_2 - k_1}{k_2 + k_1} \left\| \Pi_{\mathcal{G}_{\lambda\tilde{\mathbf{C}}_\mathbf{1}} // \mathcal{G}_\mathbf{P}} \right\|}{\left\| \Pi_{\mathcal{G}_\mathbf{P} // \mathcal{G}_{\lambda\tilde{\mathbf{C}}_\mathbf{1}}} \right\|} > 0.$$

5.5 Example and Simulation

This section illustrates the applicability of the conditions derived in the last section with some simulation results. Take the first order plant

$$P(s) = \frac{50}{s + 50} \tag{5.9}$$

and

$$\tilde{C}(s) = \begin{pmatrix} \tilde{C}_1(s) \\ \tilde{C}_2(s) \end{pmatrix} := \begin{pmatrix} -(ks + \gamma)/(s^2 + \omega_0^2) \\ -(\gamma s - k\omega_0^2)/(\omega_0(s^2 + \omega_0^2)) \end{pmatrix}$$

with $k = \gamma = 10$, $\omega_0 = \pi/2$. It is easy to compute that $\|\tilde{G}\|_{\mathcal{H}_\infty} = 1.4936 < \pi/2$ and the 1-norms

$$\left\| \mathscr{L}^{-1}\left(\frac{1}{1 - \lambda\tilde{C}_1 P} \right) \right\|_1 = 2.2682, \quad \left\| \mathscr{L}^{-1}\left(\frac{\lambda\tilde{C}_1}{1 - \lambda\tilde{C}_1 P} \right) \right\|_1 = 1.2697,$$

$$\left\| \mathscr{L}^{-1}\left(\frac{P}{1 - \lambda\tilde{C}_1 P} \right) \right\|_1 = 1.8336, \quad \left\| \mathscr{L}^{-1}\left(\frac{\lambda\tilde{C}_1 P}{1 - \lambda\tilde{C}_1 P} \right) \right\|_1 = 1.2682.$$

These 1-norms were computed using MAPLE with reliable accuracy. So,

$$\begin{aligned} & \vec{\delta}\left(\mathcal{G}_{\lambda\tilde{\mathbf{C}}_\mathbf{1}}, \mathcal{G}_{\mathbf{N}\circ\tilde{\mathbf{C}}} \right) \left\| \Pi_{\mathcal{G}_{\lambda\tilde{\mathbf{C}}_\mathbf{1}} // \mathcal{G}_\mathbf{P}} \right\| \\ \leq\ & 0.2220 \times \max\{1.2682 + 1.2697,\ 1.8336 + 2.2682\} = 0.9106 < 1. \end{aligned}$$

Thus, the closed loop $[\mathbf{P}, \mathbf{N} \circ \tilde{\mathbf{C}}]$ is stable. Similarly, $\Pi_{\mathcal{G}_\mathbf{P} // \mathcal{G}_{\lambda\tilde{\mathbf{C}}_\mathbf{1}}}$ has the transfer function

$$\begin{pmatrix} 1 \\ P \end{pmatrix} (1 - \lambda\tilde{C}_1 P)^{-1} (1, -\lambda\tilde{C}_1)$$

and the $\mathscr{L}_\infty$-induced norm is equal to $\max\{2.2682+1.2697,\ 1.8336+1.2682\} = 3.5379$. Therefore, $b_{\mathbf{P},\mathbf{N}\circ\tilde{\mathbf{C}}} \geq (1-0.9106)/3.5379 = 0.0253$, from Proposition 2.6.2. The closed loop $[\mathbf{P}, \mathbf{N}\circ\tilde{\mathbf{C}}]$ is robustly stable with respect to uncertainties measured by the gap metric. The plant given by (5.9) and the controller $\mathbf{N}\circ\tilde{\mathbf{C}}$ defined above were simulated using SIMULINK for u_0 equal to a unit amplitude triangular wave of period 4 secs, zero phase shift and $y_1 = 0$. The results of the simulation are shown in Figures 5.2 and 5.3, and illustrate the asymptotic rejection property.

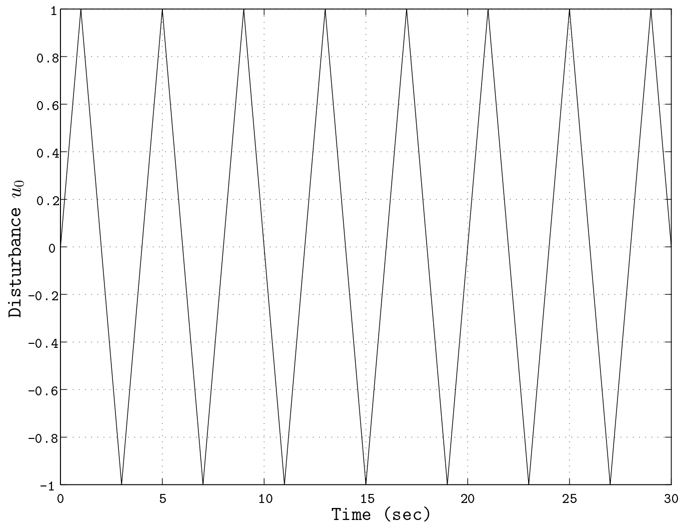

Figure 5.2 *The Triangular Waveform Disturbance* u_0 *of frequency* $\omega_0 = \pi/2$.

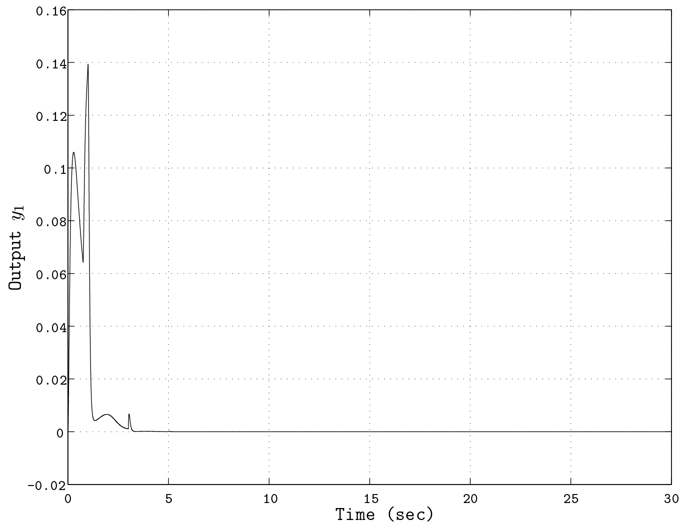

Figure 5.3 *The Plant Output at* y_1.

6

Conclusions

In this final chapter, we will summarize what we feel to be the main contributions of this dissertation and give some possible directions of future research.

6.1 Summary

The central idea of this dissertation is to incorporate the issue of robustness in repetitive control. Robustness is measured by the gap metric robustness margin. The underlying analysis and design techniques illustrate the Internal Model Principle. The main contributions of this dissertation can be roughly divided into results belonging to linear repetitive control theory and those relating to nonlinear repetitive control theory.

Main Contributions:

Linear Repetitive Control

- Under the requirement of asymptotic disturbance rejection, a simple formula computing the constrained optimal gap metric robustness margin was derived (Theorem 3.4.1).
- As a supplement to asymptotic disturbance rejection, the optimal achievable steady state attenuation with respect to a prescribed robustness level was given (Theorem 3.4.3).
- A power-energy induced quantity measuring the transient performance in the repetitive control for a finite set of frequencies was defined. The trade-offs between transient performance and robustness were examined and stated in Theorem 3.5.1. This gives some insight in a robust repetitive controller design. Controller designs should seek a good robustness and a satisfactory transient performance. So, optimal robustness may not be a practical design requirement. A balance between robustness and transient performance has to be considered.

- Two repetitive controller design methods, namely $\mathcal{H}_\infty$ loop shaping and closed-loop pole placement, applying specifically to the context of repetitive control were described.
- The robust repetitive control theory and the design methods were applied to a CD player with satisfactory implementation results.

Nonlinear Repetitive Control

- Limitations of a linear control approach for the robustness in a general repetitive control setup were investigated. A nonlinear control approach was proved to be capable in overcoming some of the limitations of some situations where a linear controller failed. This nonlinear approach also illustrated the extension of the classical Internal Model Principle. Two separate sets of sufficient conditions on the requirements of robust stability and asymptotic disturbance rejection in some situations were derived and illustrated by an example.

6.2 Recommendations of Future Research

We will point out some possible directions of future research in the theory and application of repetitive control.

Linear Repetitive Control Theory

- It would be natural to seek extensions of Theorems 3.4.3 and 3.5.1 to the MIMO case.
- It would be interesting to determine the minimum (or infimum) transient state (with respect to the defined power-energy induced measure) with respect to certain prescribed robustness requirement.

Practical Design Issues

- As a continuation to controller design in the CD player radial loop, it would be interesting to apply similar techniques, may be done in the form of a short term project, to the focus loop and simultaneously download the controllers of both loops.
- Due to the saturations of the DSP and the plant, it is of practical importance to incorporate anti-windup schemes in the robust controller design process.
- Taking the CD player as an example, the frequencies of the periodic disturbances are varying as the CD player is running. So, it would be worthwhile to apply adaptive control techniques in tackling situations with varying periods.

Nonlinear Repetitive Control Theory

- There is a great potential in applying nonlinear techniques (similar to those in Chapter 5) to some other common types of periodic waveform disturbances having infinitely many non-zero Fourier coefficients, e.g. square waves and pulse waves. It would be interesting to find some sufficient conditions to justify if an "internal model" in a causal nonlinear controller is capable to achieve robust asymptotic rejections of such classes of periodic disturbances.

A

Decomposition of Output as a Steady State and a Transient State

This appendix describes the decomposition of the output $y(t)$ as a periodic steady state $y_{\mathrm{ss}}(t)$ and a finite energy transient state $y_{\mathrm{tr}}(t)$ when a periodic input $u(t)$ is fed into a stable LTI system with transfer function $G(s)$. Two cases are discussed separately: the real-rational case and a general case.

A.1 The Real-rational Case: $u \in \mathcal{S}_n, \mathcal{S}_\infty$ and $G \in \mathcal{RH}_\infty$

Denote by T the fundamental period of the input u. Write

$$u(t) = \sum_{k=-\infty}^{\infty} a_k e^{j\frac{2\pi}{T}kt}$$

where

$$a_k = \frac{1}{T}\int_0^T u(t)e^{-j\frac{2\pi}{T}t}\,dt, \quad k \in \mathbb{Z}.$$

Assume that the coefficients a_ks satisfy $\sum_{k\in\mathbb{Z}} |a_k|^2 < \infty$. In the case of $\mathcal{S}_n$, only finitely many coefficients a_ks are non-zero. Define, for each $k \in \mathbb{Z}$, $\omega_k := \frac{2\pi}{T}k$. Then

$$\begin{aligned}
\hat{y}(s) &= G(s)\hat{u}(s) = \sum_{k=-\infty}^{\infty} \frac{G(s)a_k}{s - j\omega_k} \\
&= \sum_{k=-\infty}^{\infty} \frac{G(j\omega_k)a_k}{s - j\omega_k} + \sum_{k=-\infty}^{\infty} \frac{G(s) - G(j\omega_k)}{s - j\omega_k}a_k \\
&=: \hat{y}_{\mathrm{ss}}(s) + \hat{y}_{\mathrm{tr}}(s).
\end{aligned}$$

The time response of the (periodic) steady state is given by

$$y_{\mathrm{ss}}(t) = \sum_{k=-\infty}^{\infty} G(j\omega_k)a_k e^{j\omega_k t}.$$

This steady state has finite power and is bounded above by $\|G\|_\infty \|u\|_{\mathscr{P}}$. Let $G(s)$ be expressed in a state-space form $G(s) = D + C(sI - A)^{-1}B$ with stable A. Using

$$\frac{G(s_1) - G(s_2)}{s_1 - s_2} = -C(s_1 I - A)^{-1}(s_2 I - A)^{-1}B, \quad s_1, s_1 \in \mathbb{C},$$

the time response of the transient can be written as

$$y_{\mathrm{tr}}(t) = -Ce^{tA} \sum_{k=-\infty}^{\infty} (j\omega_k I - A)^{-1} B a_k 1_+(t).$$

To prove that this $y_{\mathrm{tr}}(t) \in \mathscr{L}_2(\mathbb{R}_+)$, the following lemma is used.

Lemma A.1.1. *The series*

$$\sum_{k=1}^{\infty} \left[(j\omega_k I - A)^{-1} + (j\omega_{-k} I - A)^{-1} \right]$$

converges absolutely.

Proof. Let $\|\cdot\|$ be a matrix norm. Using $\omega_{-k} = -\omega_k$, we have

$$\begin{aligned}
(j\omega_k I - A)^{-1} + (j\omega_{-k} I - A)^{-1} &= \frac{1}{j\omega_k} \left\{ \left(I - \frac{A}{j\omega_k} \right)^{-1} - \left(I + \frac{A}{j\omega_k} \right)^{-1} \right\} \\
&= -\frac{2}{\omega_k^2} A \left(I + \frac{A^2}{\omega_k^2} \right)^{-1}.
\end{aligned}$$

For large k, we have $\left\| \frac{A}{\omega_k} \right\| < 1$. So,

$$\begin{aligned}
\left\| (j\omega_k I - A)^{-1} + (j\omega_{-k} I - A)^{-1} \right\| &\leq \frac{2}{\omega_k^2} \cdot \|A\| \cdot \left\| \left(I + \frac{A^2}{\omega_k^2} \right)^{-1} \right\| \\
&\leq 2 \cdot \frac{T^2}{4\pi k^2} \cdot \|A\| \cdot \frac{1}{1 - \left\| \frac{T^2 A^2}{4\pi^2 k^2} \right\|} \\
&\leq c \cdot \frac{1}{k^2}
\end{aligned}$$

for some constant c independent of k. □

Using this Lemma, we know that the quantity

$$\left\| \sum_{k=-\infty}^{\infty} (j\omega_k I - A)^{-1} B a_k \right\|$$

is finite. Thus, $\sum_{k=-\infty}^{\infty}(j\omega_k I - A)^{-1}Ba_k$ converges absolutely and hence $y_{\mathrm{tr}}(t) \in \mathscr{L}_2(\mathbb{R}_+)$. Note that Lemma A.1.1 can be extended to the general frequency set

$$\Omega_\infty = \left\{\omega_k, -\omega_k : k > 0, \sum_{k=1}^{\infty} \frac{1}{\omega_k^2} < \infty\right\}.$$

A.2 A General Case: $u \in \mathcal{T}(\omega_0)$ and $G \in \mathcal{H}_\infty^\alpha$

$\mathcal{H}_\infty^\alpha$ denotes the space of bounded and analytic functions in the open right half plane $\Re(s) > \alpha$. We are going to show that the output of $G \in \mathcal{H}_\infty^\alpha, \alpha < 0$ with a triangular wave input consists of a periodic steady state and a decaying transient state. Define $\mathscr{L}_{2\beta}(\mathbb{R}_+)$ as the space of all functions of the form $v(t) = e^{\beta t}u(t)$, where $u \in \mathscr{L}_2(\mathbb{R}_+)$. Lemma 9 of [WH97] will be used. For the sake of convenience, this Lemma is stated as Lemma A.2.1 below without proof.

Lemma A.2.1. *Let $G \in \mathcal{H}_\infty^\alpha$ for some $\alpha < 0$. Assume that the input function $u \in \mathscr{L}_{2e}(\mathbb{R}_+)$ has the decomposition*

$$u = u_{\mathrm{ss}} + u_{\mathrm{tr}},$$

where u_{ss} is periodic with fundamental frequency ω_0 and $u_{\mathrm{tr}} \in \mathscr{L}_{2\beta}(\mathbb{R}_+)$ with $\alpha \le \beta \le 0$. If y is the corresponding output function, $\hat{y} = G\hat{u}$, then $y \in \mathscr{L}_{2e}(\mathbb{R}_+)$ has a similar decomposition:

$$y = y_{\mathrm{ss}} + y_{\mathrm{tr}},$$

where y_{ss} is periodic with fundamental frequency ω_0 and $y_{\mathrm{tr}} \in \mathscr{L}_{2\beta}(\mathbb{R}_+)$. The decomposition is unique. Moreover, if $\{u_k\}$ and $\{y_k\}$ are the Fourier coefficients of u_{ss} and y_{ss}, i.e.

$$u_{\mathrm{ss}} = \sum_{k\in\mathbb{Z}} u_k e^{jk\omega_0 t}, \quad y_{\mathrm{ss}} = \sum_{k\in\mathbb{Z}} y_k e^{jk\omega_0 t},$$

then $y_k = G(jk\omega_0)u_k$.

For a system $G \in \mathcal{H}_\infty^\alpha, \alpha < 0$ with periodic input $u \in \mathcal{T}(\omega_0)$, the output consists of a steady state y_{ss} with fundamental frequency ω_0 and a transient state $y_{\mathrm{tr}} \in \mathscr{L}_2(\mathbb{R}_+)$, by using Lemma A.2.1 with $\beta = 0$. Note that the derivative $\dot{u}$ is also periodic with the same fundamental frequency ω_0. Applying Lemma A.2.1 again to $\dot{u}$ with $\beta = 0$, we can show that $\dot{y}_{\mathrm{tr}} \in \mathscr{L}_2(\mathbb{R}_+)$. Thus by Proposition 5.3.3, $\lim_{t\to\infty} y_{\mathrm{tr}}(t) = 0$.

B

Theorem 3.4.1 in the MIMO Case

Rewriting the constrained $\mathcal{H}_\infty$ optimization in Nehari problem form (in (2.5)), we have

$$b_{\text{opt}}(P, \Omega_n)^{-2} = \inf_{\substack{Q \in \mathcal{RH}_\infty \\ Q(j\omega_k) = Q_k \ \forall \omega_k \in \Omega_n}} \left\| \tilde{U}\tilde{M}^* + \tilde{V}\tilde{N}^* + Q \right\|_{\mathcal{L}_\infty}^2 + 1.$$

Perform an inner-outer factorization [ZDG96] to obtain $\tilde{U}\tilde{M}^* + \tilde{V}\tilde{N}^* = TB^{-1}$ where $T, B \in \mathcal{RH}_\infty$ and B is inner. Then

$$\left\| \tilde{U}\tilde{M}^* + \tilde{V}\tilde{N}^* + Q \right\|_{\mathcal{L}_\infty} = \|T + BQ\|_{\mathcal{H}_\infty}.$$

Assume $P(j\omega_k)$ has full column rank for each frequency $\omega_k \in \Omega_n$. The rejection requirements (3.3)

$$P(I - CP)^{-1}(j\omega_k) = N(\tilde{V} + Q\tilde{N})(j\omega_k) = 0$$

are soluble and the constraints on the Youla parameter can be chosen to be

$$Q(j\omega_k) = -(N^*N)^{-1}N^*V(j\omega_k) =: Q_k$$

for all k. As in the SISO case, apply the result (3.5) (on page 27) to the matrix case:

$$\begin{aligned} &\inf_{\substack{Q \in \mathcal{RH}_\infty \\ Q(j\omega_k) = Q_k \ \forall \omega_k \in \Omega_n}} \|T_1 + T_2 Q\|_{\mathcal{H}_\infty} \\ &= \max_{\omega_k \in \Omega_n} \left\{ \inf_{Q \in \mathcal{RH}_\infty} \|T_1 + T_2 Q\|_{\mathcal{H}_\infty}, \sigma_{\max}\big(T_1(j\omega_k) + T_2(j\omega_k)Q_k\big) \right\}. \end{aligned}$$

The proof is completed by showing that

$$\sigma_{\max}\big(T(j\omega_k) + B(j\omega_k)Q_k\big) = 1/\sigma_{\min}(P).$$

It is noted that

$$\begin{aligned} &\sigma_{\max}\big(T(j\omega_k) + B(j\omega_k)Q_k\big) \\ = \ &\sigma_{\max}\big((\tilde{U}\tilde{M}^* + \tilde{V}\tilde{N}^* + Q_k)(j\omega_k)\big) \\ = \ &\sigma_{\max}\big((\tilde{U}\tilde{M}^* + \tilde{V}\tilde{N}^* - (N^*N)^{-1}N^*V)(j\omega_k)\big). \end{aligned}$$

Using the Bezout identity and the normalization property of the coprime factors of P, we have

$$\begin{aligned}
& \tilde{U}\tilde{M}^* + \tilde{V}\tilde{N}^* - (N^*N)^{-1}N^*V \\
= \; & (N^*N)^{-1}\big(N^*N\tilde{U}\tilde{M}^* + N^*N\tilde{V}\tilde{N}^* - N^*V\big) \\
= \; & (N^*N)^{-1}\big(N^*V\tilde{M}\tilde{M}^* - N^*\tilde{M}^* + N^*V\tilde{N}\tilde{N}^* - N^*V\big) \\
= \; & -(N^*N)^{-1}N^*\tilde{M}^* \\
= \; & -M^{-1}(P^*P)^{-1}P^*\tilde{M}^*.
\end{aligned}$$

So, at each $j\omega_k$,

$$\begin{aligned}
& \sigma^2_{\max}\big(M^{-1}(P^*P)^{-1}P^*\tilde{M}^*\big) \\
= \; & \sigma^2_{\max}\left(\begin{pmatrix} M \\ N \end{pmatrix} M^{-1}(P^*P)^{-1}P^*\tilde{M}^*\right) \\
= \; & \sigma^2_{\max}\left(\begin{pmatrix} I \\ P \end{pmatrix} (P^*P)^{-1}P^*\tilde{M}^*\right) \\
= \; & \lambda_{\max}\left(\tilde{M}P(P^*P)^{-1}(I+P^*P)(P^*P)^{-1}P^*\tilde{M}^*\right) \\
= \; & \lambda_{\max}\left(P(P^*P)^{-1}(I+P^*P)(P^*P)^{-1}P^*\tilde{M}^*\tilde{M}\right) \\
= \; & \lambda_{\max}\big(P(P^*P)^{-1}(I+P^*P)(P^*P)^{-1}P^*(I+PP^*)^{-1}\big) \\
= \; & \lambda_{\max}\big((P^*P)^{-1}\big) \\
= \; & 1/\sigma^2_{\min}(P).
\end{aligned}$$

C

Proof of Lemma 3.4.4

For convenience, Lemma 3.4.4 is stated below as Lemma C.0.2. This lemma is a slight modification of the standard boundary interpolation result in Equation (3.5) on page 27 and in [KT85].

Lemma C.0.2. *Let $T_1, T_2 \in \mathcal{RH}_\infty$ and let $\Omega_n = \{\omega_1, ..., \omega_n\} \subset \mathbb{R}$ be given. Suppose $T_2(j\omega_k) \neq 0$ for each k. Given a set of numbers $z_1, ..., z_n \in \mathbb{C}$. Suppose $\|T_1 + T_2 Q\|_{\mathcal{H}_\infty} = \alpha$ for some $Q \in \mathcal{RH}_\infty$ and $|z_k| \leq \alpha$ for all k. Then for each $\epsilon > 0$, there exists a $Q_\epsilon \in \mathcal{RH}_\infty$ such that*

$$\|T_1 + T_2 Q_\epsilon\|_{\mathcal{H}_\infty} \leq \alpha + \epsilon$$

and

$$(T_1 + T_2 Q_\epsilon)(j\omega_k) = z_k$$

for all $\omega_k \in \Omega_n$.

Proof. Suppose that $Q_0 \in \mathcal{RH}_\infty$ satisfies the assumptions in Lemma C.0.2. Hence, we may define

$$Q_k := \frac{z_k - T_1(j\omega_k)}{T_2(j\omega_k)}$$

for each k. Then the quantities $\inf_{Q \in \mathcal{RH}_\infty} \|T_1 + T_2 Q\|_{\mathcal{H}_\infty}$, $|T_1(j\omega_k) + T_2(j\omega_k) Q_k|$ are not greater than α. So, by (3.5), we have

$$\inf_{\substack{Q \in \mathcal{RH}_\infty \\ Q(j\omega_k) = Q_k \ \forall \omega_k \in \Omega_n}} \|T_1 + T_2 Q\|_{\mathcal{H}_\infty}$$

not greater than α. Thus, for any $\epsilon > 0$, by definition of the infimum, there exists $Q_\epsilon \in \mathcal{RH}_\infty$ such that the conditions of the Lemma are satisfied. $\square$

D

A Lemma

In this appendix, a lemma relating the sensitivity function and the gap metric robustness margin is stated and proved. Only the SISO rational and proper case is considered. For the MIMO case, the reader is referred to [Vin93, Vin98].

Define $\rho(P,C)$ as the pointwise version of $b_{P,C}$:

$$\begin{aligned}
& \rho\big(P(j\omega), C(j\omega)\big) \\
:= \;& \sigma_{\max}^{-1}\left(\begin{pmatrix} I \\ P(j\omega) \end{pmatrix} \big(I - C(j\omega)P(j\omega)\big)^{-1}\big(I, -C(j\omega)\big)\right) \\
= \;& \sigma_{\max}^{-1}\big((I + C^*C)^{1/2}(I - PC)^{-1}(I + PP^*)^{1/2}\big)(j\omega),
\end{aligned}$$

thus, $b_{P,C} = \inf_\omega \rho\big(P(j\omega), C(j\omega)\big)$ provided $[P,C]$ is stable. The following lemma characterizes the best possible bound for the sensitivity function in terms of the plant gain and a bound of $\rho(P,C)$.

Lemma D.0.3. *Given a scalar, rational and proper plant P with $P(j\omega) \neq 0$, then $\rho\big(P(j\omega), C(j\omega)\big) \geq 1/\gamma$ if and only if*

$$\frac{1}{1 - P(j\omega)C(j\omega)} = \frac{x(j\omega)|P(j\omega)|\sqrt{\gamma^2 - 1} + 1}{1 + |P(j\omega)|^2}$$

for some $x(j\omega)$ with $|x(j\omega)| \leq 1$.

Proof. For the reason of brevity, we suppress the argument $j\omega$ in this proof. Define $S := (1 - PC)^{-1}$ and

$$H := \frac{\sqrt{1 + |C|^2}\sqrt{1 + |P|^2}}{1 - PC}.$$

So, $\rho(P,C) \geq 1/\gamma$ if and only if $|H| \leq \gamma$. It is observed that

$$(1 + |C|^2)|S|^2 = \left(1 + \frac{1}{|P|^2}\right)\left|S - \frac{1}{1 + |P|^2}\right|^2 + \frac{1}{1 + |P|^2}$$

and therefore

$$|H|^2 - 1 = \frac{(1+|P|^2)^2}{|P|^2} \left| S - \frac{1}{1+|P|^2} \right|^2 .$$

It follows that $\rho(P, C) \geq 1/\gamma$ if and only if

$$\frac{(1+|P|^2)}{|P|} \left(S - \frac{1}{1+|P|^2} \right) = x\sqrt{\gamma^2 - 1}$$

for some $|x| \leq 1$. The proof is then completed by writing S in terms of x. $\square$

E

Specifications of a Compact Disc and the Philips CD930 Model

In this appendix, specifications of a typical compact disc and the Philips CD930 model are given.

<u>Disc Parameters</u>

– Playing time, single side, two channels	approx. 60 min.
– Linear scanning velocity (2 channels)	$1.2 - 1.4$m/sec.
– Sense of rotation seen from the reading side	counterclockwise when viewed from readout surface.
– Rotation frequency of the disc	3.3Hz (outermost track) to 8.3Hz (innermost track).
– Diameter of the disc	120mm.
– Thickness of the disc	1.2 ± 0.1mm.
– Weight of the disc	$14 - 33$g.
– Diameter of centre hole	15mm.
– Recording area	$46 - 117$mm.
– Signal area	$50 - 116$mm.
– Refractive index of the plastic transparent substrate (e.g. polycarbonate)	1.55 ± 0.1.
– Thickness of the plastic transparent substrate	1.2 ± 0.1mm.
– Metal used for the reflective film	aluminium, silver or gold.
– Thickness of the reflective metal film	$0.05 - 0.1\mu$m.
– Track pitch	$1.6 \pm 0.1\mu$m.
– Minimum pit length	0.833μm (1.2m/sec) to 0.972μm (1.4m/sec).
– Maximum pit length	3.05μm (1.2m/sec) to 3.56μm (1.4m/sec).
– Pit depth	$0.12 \pm 0.01\mu$m.
– Pit width	0.4μm.

Optical system

– Laser diode type	AlGaAs.
– Wavelength of laser	0.76 to 0.82μm.
– Focal depth	$\pm 2\mu$m.
– Diameter of laser spot shining on the metal film	1μm.

Signal format

– Number of channels	2 and/or 4 simultaneously sampled.
– Quantization	16 bits linear/channel.
– Quantizing timing	concurrent for all channels.
– Sampling frequency	44.1kHz.
– Channel bit rate	4.3218Mb/sec.
– Data bit rate	2.0338Mb/sec.
– Data-to-channel bit ratio	8 : 17.
– Error correction code	cross interleave Reed-Solomon code (with 25% redundancy).
– Modulation system	eight-to-fourteen modulation.

Typical Disturbances and Allowable Errors

– Maximum deflection and up-and-down movement	± 0.5mm.
– Allowable focus error	$\pm 2\mu$m.
– Radial eccentricity	± 0.2mm.
– Allowable radial error	$\pm 0.1\mu$m.

Control loops of CD930

– Bandwidth of focus control loop	800Hz.
– Resonance frequency of the damping system in the focus control loop	40Hz.
– Bandwidth of radial control loop	400Hz.
– Resonance frequency of the damping system in the radial control loop	$3,700$Hz.

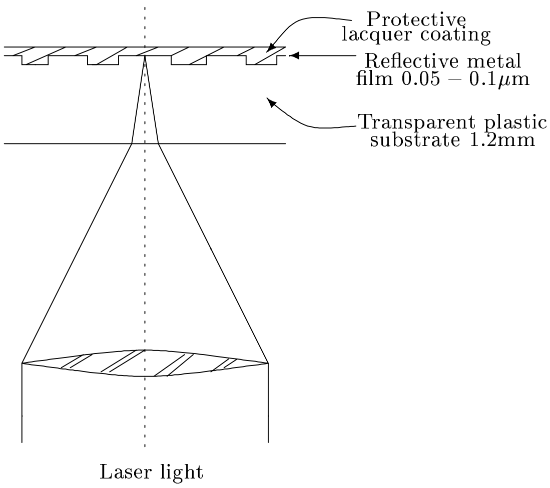

Figure E.1 *Cross Section of a Compact Disc.*

	Radial	Focus
K_{CD}	$10^5 \pm 0.2\%$	$3.9 \times 10^4 \pm 0.2\%$
K_{noise}	$10^{-5} \pm 0.2\%$	$10^{-5} \pm 0.2\%$
K_{mon}	$-10^5 \pm 0.2\%$	$-10^5 \pm 0.5\%$
$K_{\mathrm{error}} \times K_{\mathrm{optics}}$	$7.5 \times 10^6 \mathrm{V/m} \pm 10\%$	$1.5 \times 10^4 \mathrm{V/m} \pm 20\%$
K_{ext}	$10^{-5} \pm 0.2\%$	$10^{-5} \pm 0.2\%$

Table E.1 *The Transducer Gains for the Radial and Focus Loops of Philips CD930.*

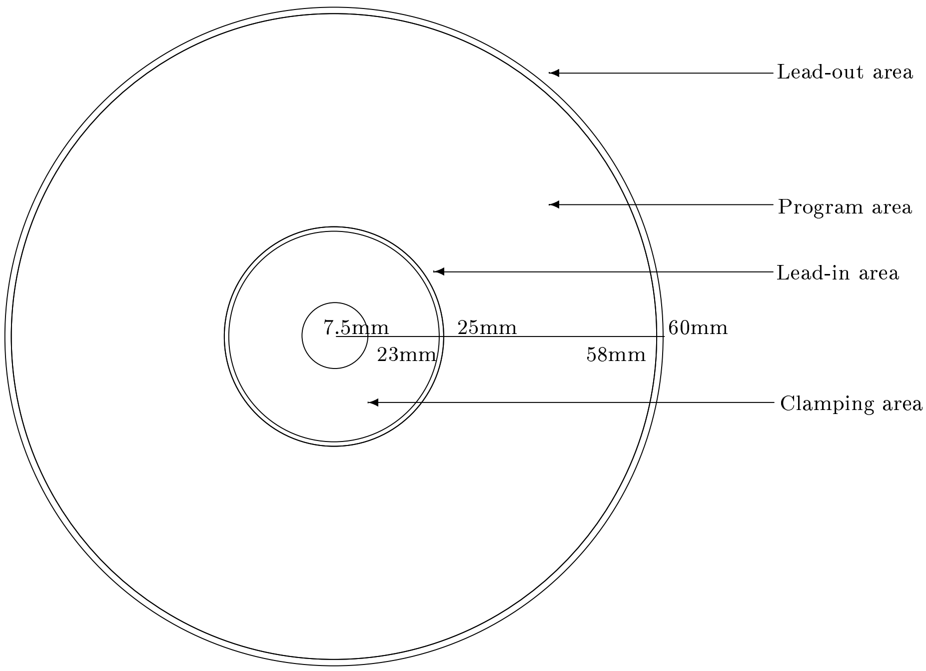

Figure E.2 *A Typical Compact Disc.*

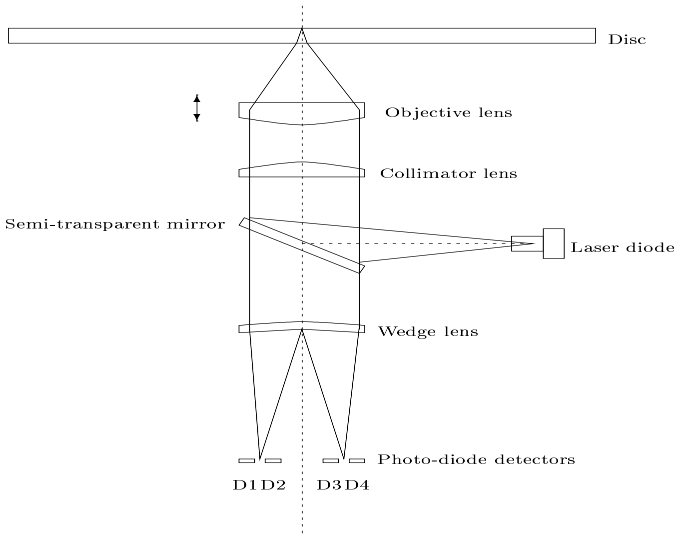

Figure E.3 *Schematics of the Optical Read Out Unit in the Philips CD930 player.*

F

Derivation of the Radial Transfer Function

A simplified radial transfer function is derived from the geometry of a CD in this appendix. The radial transfer function is the transfer function from the input of the d.c. motor (i.e. the current I_{rad}) to the input of the controller.

The optical element is mounted at the end of the balanced radial actuator arm. The actuator arm is a d.c. motor. When a current I_{rad} is sent to the motor, the coil and the magnet of the motor create a torque on the arm:

$$T_{\text{arm}} = K_{\text{motor}} I_{\text{rad}}$$

where T_{arm} is the torque, K_{motor} the proportionality factor and I_{rad} the radial control current. The torque results in an angular acceleration, inversely proportional to the moment of inertia of the arm:

$$\ddot{\phi}_{\text{arm}} = \frac{T_{\text{arm}}}{J_{\text{arm}}}.$$

Thus, the transfer function from the radial current to the angle of the radial arm is:

$$\frac{\phi(s)}{I_{\text{rad}}} = \frac{K_{\text{act}}}{s^2}$$

where the actuator proportionality constant K_{act} is equal to $K_{\text{motor}}/J_{\text{arm}}$. Due to the fact that the spot is at the end of the arm with finite length, the movement across tracks, as the angle ϕ grows, will not be perpendicular to the track direction. The geometry of the radial actuator is given in Figure F.1. For the computation of the transfer function from the radial arm angle to the laser spot position, we linearize the following equation around an angle ϕ_0

$$\begin{aligned} x_{\text{spot}}(\phi) &= \sqrt{(d - R_{\text{arm}}\sin(\phi))^2 + (R_{\text{arm}}\cos(\phi))^2} \\ &= \sqrt{d^2 + R_{\text{arm}}^2 - 2dR_{\text{arm}}\sin(\phi)} \end{aligned}$$

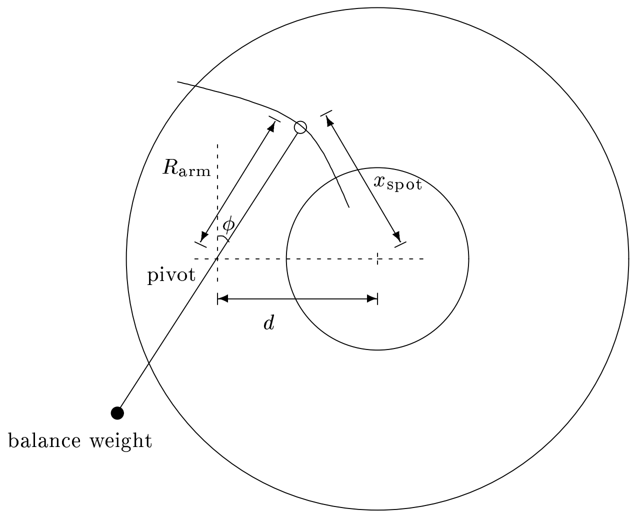

Figure F.1 *The Geometry of the Radial Actuator.*

where R_{arm} is the radius of the radial actuator arm, d the axis between the pivot of the radial actuator and the axis of the disc rotation, and ϕ the rotation angle. Then, for $\phi \approx \phi_0$ where ϕ_0 is the radial position of the nearest reference track,

$$\begin{aligned} x_{\mathrm{spot}}(\phi) - x_{\mathrm{spot}}(\phi_0) &\approx -\frac{dR_{\mathrm{arm}}\cos(\phi_0)}{\sqrt{d^2 + R_{\mathrm{arm}}^2 - 2dR_{\mathrm{arm}}\sin(\phi_0)}} \cdot (\phi - \phi_0) \\ &=: K_{\mathrm{arm}}(\phi_0) \cdot (\phi - \phi_0). \end{aligned}$$

Since $\phi_0 \in (-15^\circ, 40^\circ)$, we have $0.77 \leq K_{\mathrm{arm}}/R_{\mathrm{arm}} \leq 1$. This K_{arm} varies according to the arm radial position (i.e. ϕ_0). Consider the local behaviour around the reference track ϕ_0. As a whole, the governing equation of the local behaviour from the current input I_{rad} to the difference between the laser spot position and the nearest track ε is

$$\varepsilon := \triangle x_{\mathrm{spot}} = \frac{K_{\mathrm{act}} K_{arm}}{s^2} \cdot I_{\mathrm{rad}}$$

The actual signal feeding into the controller is RE $:= K_{\mathrm{optics}}\varepsilon$ (see (4.1)), after the d.c. offset rectification. Thus, the radial plant (apart from the second order damping system) is a double integrator with the transfer function

$$P_{\mathrm{rad}} = \frac{K_{\mathrm{opt}} K_{\mathrm{act}} K_{\mathrm{arm}}}{s^2}.$$

G

A dSPACE SIMULINK Block Diagram for a Controller Implementation

Take the loop shaping controller $C^{\mathrm{rad}}_{0.3,\mathrm{LS}}$ for the radial control loop as an example:

$$
\begin{aligned}
C^{\mathrm{rad}}_{0.3,\mathrm{LS}} \quad = \quad & -3.167\frac{(s+128.9\pm \jmath 27.47)(s+136.5\pm \jmath 98.03)}{s(s+6632)\,(s^2+(2\pi 6)^2)} \\
& \times \frac{(s+145.6\pm \jmath 205.1)(s+349.7\pm \jmath 343.2)}{(s^2+(2\pi 18)^2)\,(s^2+(2\pi 36)^2)}.
\end{aligned}
$$

The digital controller input "`Rad Error`" is the modified radial error `RE'` and the digital controller output "`Rad Ext`" is the external radial input of the CD player (see Section 4.3). In generating all the necessary files for implementation, the function `real-time option` in the SIMULINK mode is used.

System matrices for the discrete-time equivalent are:

$$
A = \begin{bmatrix}
0.9999 & -0.0113 & 0 & 0 & 0 & 0 & 0 & 0 \\
0.0113 & 0.9999 & 0 & 0 & 0 & 0 & 0 & 0 \\
0.0352 & 0.0416 & 1.0000 & -0.0057 & 0 & 0 & 0 & 0 \\
0.0001 & 0.0001 & 0.0057 & 1.0000 & 0 & 0 & 0 & 0 \\
0.0355 & 0.0419 & 0.0146 & 0.0223 & 1.0000 & -0.0019 & 0 & 0 \\
0.0000 & 0.0000 & 0.0000 & 0.0000 & 0.0019 & 1.0000 & 0 & 0 \\
0.0304 & 0.0359 & 0.0125 & 0.0191 & 0.0116 & 0.0303 & 0.7178 & 0 \\
0.0000 & 0.0000 & 0.0000 & 0.0000 & 0.0000 & 0.0000 & 0.0000 & 1.0000
\end{bmatrix};
$$

$$B = \begin{bmatrix} 0.5000 \\ 0.0028 \\ 0.5088 \\ 0.0014 \\ 0.5125 \\ 0.0005 \\ 0.4399 \\ 0.0000 \end{bmatrix} \times 10^{-4};$$

$$C = \begin{bmatrix} -0.2215 & -0.2645 & -0.0922 & -0.1413 & -0.0865 & -0.2253 & 2.0187 & -5.5010 \end{bmatrix} \times 10^{4};$$

$$D = -3.1670.$$

A sample SIMULINK block diagram is shown in Figure G.1.

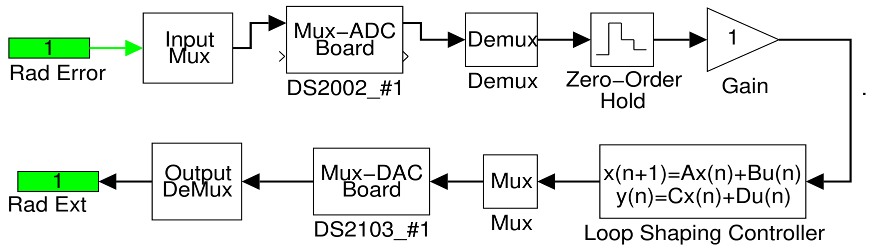

Figure G.1 *The SIMULINK Block Diagram for a Real-time Implementation of an External Controller.*

Bibliography

[AKM84] S. Arimoto, S. Kawamura, and F. Miyazaki. Bettering operation of robots by learning. *Journal of Robotic Systems*, 1(2):123–140, 1984.

[AKMT85] S. Arimoto, S. Kawamura, F. Miyazaki, and S. Takami. Learning control theory for dynamical systems. In *Proceedings of IEEE Conference on Decision and Control*, pages 1375–1380, 1985.

[AT94] D.M. Alter and T.C. Tsao. Two-dimensional exact model matching with application to repetitive control. *ASME Journal of Dynamic Systems, Measurement, and Control*, 116:2–9, 1994.

[BBH+85] G Bouwhuis, J. Braat, A. Huijser, J. Pasman, G. van Rosmalen, and K. Schouhamer Immink. *Principles of Optical Disc Systems.* Adam Hilger Ltd., 1985.

[BCG88] B. Bondi, G. Casalino, and L. Gambardella. On the iterative learning control theory for robotic manipulators. *IEEE Journal of Robotics and Automation*, 4:14–22, 1988.

[BDG+94] G.J. Balas, J.C. Doyle, K. Glover, A. Packard, and R. Smith. *μ-Analysis and Synthesis Toolbox User's Guide: For Use with MATLAB.* The MathWorks, Inc., 1994.

[BM92] H.L. Broberg and R.G. Molyet. Correction of periodic errors in a satellite servo using repetitive control. In *Proceedings of the First IEEE Conference on Control Applications*, pages 682–683, 1992.

[CS95] M.K.K. Cevik and J.M. Schumacher. The regulator problem with robust stability. *Automatica*, 31:1393–1406, 1995.

[CS97] M.K.K. Cevik and J.M. Schumacher. The robust regulation problem with robust stability. Preprint, 1997.

[CT90a] K.-K. Chew and M. Tomizuka. Digital control of repetitive errors in disk drive systems. *IEEE Control Systems Magazine*, 10:16–19, 1990.

[CT90b] K.-K. Chew and M. Tomizuka. Steady-state and stochastic performance of a modified discrete-time prototype repetitive controller. *ASME Journal of Dynamic Systems, Measurement, and Control*, 112:35–41, 1990.

[DFT92] J.C. Doyle, B.A. Francis, and A.R. Tannenbaum. *Feedback Control Theory.* Macmillan Publishing Company, 1992.

[Dra89] W. Draijer. Adaptive control of the philips compact disc radial servo system. Technical Report Nr. 136/89, Philips NAT. LAB., 1989.

[DSB92] W. Draijer, M. Steinbuch, and O.H. Bosgra. Adaptive control of the radial servo system of a compact disc player. *Automatica*, 28:455–462, 1992.

[DSVdHS95] H.G.M. Dötsch, H.T. Smakman, P.M.J. Van den Hof, and M. Steinbuch. Adaptive repetitive control of a compact disc mechanism. In *Proceedings of IEEE Conference on Decision and Control*, pages 1720–1725, 1995.

[DV75] C.A. Desoer and M. Vidyasagar. *Feedback Systems: Input-Output Properties.* Academic Press, 1975.

[Fol92] G.B. Folland. *Fourier Analysis and its Applications.* Brooks/Cole Publishing Company, 1992.

[FPEN94] G.F. Franklin, J.D. Powell, and A. Emami-Naeini. *Feedback Control of Dynamic Systems.* Addison-Wesley Publishing Company, 1994.

[Fra87] B.A. Francis. *A Course in $\mathcal{H}_\infty$ Control Theory*, volume 88. Springer-Verlag, 1987.

[FW76] B.A. Francis and W.M. Wonham. The internal model principle of control theory. *Automatica*, 12:457–465, 1976.

[GL95] M. Green and D.J.N. Limebeer. *Linear Robust Control.* Prentice-Hall, 1995.

[GS89] T.T. Georgiou and M.C. Smith. w-stability of feedback systems. *Systems Control Letter*, 13:271–277, 1989.

[GS90] T.T. Georgiou and M.C. Smith. Optimal robustness in the gap metric. *IEEE Transactions on Automatic Control*, 35(6):673–686, 1990.

[GS93] T.T. Georgiou and M.C. Smith. Graphs, causality, and stabilizability: Linear, shift-invariant systems on $\mathscr{L}_2[0,\infty)$. *Mathematics of Control, Signals, and Systems*, 6:195–223, 1993.

[GS97] T.T. Georgiou and M.C. Smith. Robustness analysis of nonlinear feedback systems: An input-output approach. *IEEE Transactions on Automatic Control*, 42(9):1200–1221, 1997.

[Güv96] L. Güvenç. Stability and performance robustness analysis of repetitive control systems using structured singular values. *ASME Journal of Dynamic Systems, Measurement, and Control*, 118:593–597, 1996.

[Hal63] J.K. Hale. *Oscillations in Nonlinear Systems*. Dover Publications, Inc., 1963.

[HFPM92] G. Heinzinger, D. Fenwick, B. Paden, and F. Miyazaki. Stability of learning control with disturbances and uncertain initial conditions. *IEEE Transactions on Automatic Control*, 33(7):110–114, 1992.

[HHSM92] T.K. Hamrita, B.S. Heck, and A.P. Sakis Meliopoulos. Application of repetitive control for restoration of periodic signals distorted by nonlinear measurement devices. In *Proceedings of the American Control Conference*, pages 2681–2685, 1992.

[Hil94] G. Hillerström. *On Repetitive Control*. PhD thesis, Luleå University of Technology, September 1994.

[Hil96] G. Hillerström. Adaptive suppression of vibrations – a repetitive control approach. *IEEE Transactions on Control System Technology*, 4:72–78, 1996.

[HL97] G. Hillerström and R.C.H. Lee. Trade-offs in repetitive control. Technical Report CUED/F-INFENG TR 294, University of Cambridge, June 1997.

[HON85] S. Hara, T. Omata, and M. Nakano. Synthesis of repetitive control systems and its applications. In *Proceedings of IEEE Conference on Decision and Control*, pages 1387–1392, 1985.

[Hor93] R. Horowitz. Learning control of robot manipulators. *ASME Journal of Dynamic Systems, Measurement, and Control*, 115:402–411, 1993.

[HS89] S. Hara and T. Sugie. $\mathcal{H}_\infty$-suboptimal control problem with boundary constraints. *Systems Control Letter*, pages 93–99, 1989.

[HS94] G. Hillerström and J. Sternby. Application of repetitive control to a peristaltic pump. *ASME Journal of Dynamic Systems, Measurement, and Control*, pages 786–789, 1994.

[HS96] G. Hillerström and J. Sternby. Robustness properties of repetitive controllers. *Internal Journal of Control*, 65(6):939–961, 1996.

[HSK92] S. Hara, T. Sugie, and R. Kondo. $\mathcal{H}_\infty$ control problem with $j\omega$-axis zeros. *Automatica*, 28:55–70, 1992.

[Hu95] J.-S. Hu. Active sound attenuation in finite-length ducts using closed-form transfer function models. *ASME Journal of Dynamic Systems, Measurement, and Control*, 117:143–154, 1995.

[Hu96] J.-S. Hu. Active noise cancellation in ducts using internal model-based control algorithms. *IEEE Transactions on Control System Technology*, 4(2):163–170, 1996.

[HY85] S. Hara and Y. Yamamoto. Stability of repetitive control systems. In *Proceedings of IEEE Conference on Decision and Control*, pages 326–327, 1985.

[HYON88] S. Hara, Y. Yamamoto, T. Omata, and M. Nakano. Repetitive control system: A new type servo system for periodic exogenous signals. *IEEE Transactions on Automatic Control*, 33(7):659–668, 1988.

[INI81] T. Inoue, M. Nakano, and S. Iwai. High accuracy control of servomechanism for repeated contouring. In *10th Annual Symp. on Incremental Motion Control Systems and Devices*, pages 285–292, 1981.

[INK+81] T. Inoue, M. Nakano, T. Kubo, S. Mutsumoto, and H. Baba. High accuracy control of a proton synchrotron magnet power supply. In *Proceedings of 8th World Congress of IFAC*, pages 216–221, 1981.

[JCHP94] Y.A. Jiang, D.J. Clements, T. Hesketh, and J.S. Park. Adaptive learning control of robot manipulators in task space. In *Proceedings of the American Control Conference*, pages 207–211, 1994.

[KCMN94] M.V. Kothare, P.J. Campo, M. Morari, and C.N. Nett. A unified framework for the study of anti-windup designs. *Automatica*, 30:1869–1883, 1994.

[KON95] T. Katayama, M. Ogawa, and M. Nagasawa. High-precision tracking control system for digital video disk players. *IEEE Transactions on Consumer Electronics*, 41(2):313–321, 1995.

[Kre78] E. Kreyszig. *Introductory Functional Analysis with Applications.* John Wiley & Sons, 1978.

[KT85] P.P. Khargonekar and A. Tannenbaum. Non-Euclidean metrics and the robust stabilization of systems with parameter uncertainty. *IEEE Transactions on Automatic Control*, 30:1005–1013, 1985.

[Lan97] A. Langari. *Sampled-Data Repetitive Control Systems.* PhD thesis, University of Toronto, 1997.

[LB91] K.H. Lee and Z. Bien. Initial condition of learning control. *IEE Proceedings-D*, 136(6):525–528, 1991.

[LF94] A. Langari and B.A. Francis. Sampled-data repetitive control systems. In *Proceedings of the American Control Conference*, pages 3234–3235, 1994.

[LH92] C.A. Lin and S.J. Ho. Controller design for linear multivariable systems with periodic inputs. *IEE Proceedings-D*, 139(1):1–8, 1992.

[LHP+94] D.A Lawrence, T.E. Holden, F. Padieu, P. Axelrad, and M. Malone. Disturbance learning control for small satellites. In *Proceedings of the American Control Conference*, pages 2882–2886, 1994.

[LRW96] H. Logemann, R. Rebarber, and G. Weiss. Conditions for robustness and nonrobustness of the stability of feedback systems with respect to small delays in the feedback loop. *SIAM Journal of Control and Optimization*, 34:572–600, 1996.

[LS96] R.C.H. Lee and M.C. Smith. Some remarks on repetitive control systems. In *Proceedings of IEEE Conference on Decision and Control*, pages 2023–2024, Kobe, Japan, 1996.

[LS98a] R.C.H. Lee and M.C. Smith. Necessity of nonlinear control for robust rejection of periodic disturbances. *Submitted*, 1998.

[LS98b] R.C.H. Lee and M.C. Smith. Repetitive control experiments for a CD player. *To appear in American Control Conference*, 1998.

[LS98c] R.C.H. Lee and M.C. Smith. Robustness and trade-offs in repetitive control. *To appear in Automatica*, 34, 1998.

[MG90] D.C. McFarlane and K. Glover. *Robust Controller Design Using Normalized Coprime Factor Plant Descriptions*, volume 138 of *Lecture Notes in Control and Information Sciences*. Springer-Verlag, 1990.

[MGL89] R.H. Middleton, G.C. Goodwin, and R.W. Longman. A method for improving the dynamic accuracy of a robot performing a repetitive task. *The International Journal of Robotic Research*, 8(5):67–74, 1989.

[MH95] A. Medvedev and G. Hillerström. An external model control system. *Control Theory and Advanced Technology*, 10(4):1643–1665, 1995.

[MK85] T. Mita and E. Kato. Iterative control and its application to motion control of robot arm. In *Proceedings of IEEE Conference on Decision and Control*, pages 1393–1398, 1985.

[MTBR96] T.J. Manayathara, T.-C. Tsao, J. Bentsman, and D. Ross. Rejection of unknown periodic load disturbances in continuous steel casting process using learning repetitive control approach. *IEEE Transactions on Control System Technology*, 4(3):259–265, 1996.

[NH86] M. Nakano and S. Hara. Microprocessor based repetitive control. In *Microprocessor based control systems*, pages 279–296. D. Reidel Publishing Company, 1986.

[NO92] H. Nakajima and H. Ogawa. *Compact Disc Technology.* IOS Press, 1992.

[OHN87] T. Omata, S. Hara, and M. Nakano. Nonlinear repetitive control with applications to trajectory control of manipulators. *Journal of Robotic Systems*, 4:631–652, 1987.

[Poh92] K.C. Pohlmann. *The Compact Disc Handbook.* Oxford University Press, 1992.

[RO92] E. Rogers and D.H. Owens. *Stability Analysis for Linear Repetitive Processes*, volume 175 of *Lecture Notes in Control and Information Sciences.* Springer-Verlag, 1992.

[RS93] S. Rönnbäck and J. Sternby. A design algorithm for anti-windup compensators – polynomial approach. In *Proceedings IFAC World Congress*, volume VIII, pages 509–514, 1993.

[Rud85] W. Rudin. *Principles of Mathematical Analysis.* McGraw-Hill, 1985.

[Rud87] W. Rudin. *Real and Complex Analysis.* McGraw-Hill, 1987.

[SBK96] A. Sacks, M. Bodson, and P. Khosla. Experimental results of adaptive periodic disturbance cancellation in a high performance magnetic disk drive. *ASME Journal of Dynamic Systems, Measurement, and Control*, 118:416–424, 1996.

[SHKT90] N. Sadegh, R. Howowitz, W.-W, Kao, and M. Tomizuka. A unified approach to the design of adaptive and repetitive controllers for robotic manipulators. *ASME Journal of Dynamic Systems, Measurement, and Control*, 112:618–629, 1990.

[SS93] F.-R. Shaw and K. Srinivasan. Discrete-time repetitive control system design using the regeneration spectrum. *ASME Journal of Dynamic Systems, Measurement, and Control*, 115:228–237, 1993.

[Swi97] S.J. Swift. Identification and control of a CD player. Master's thesis, University of Cambridge, 1997.

[TAT88] M.-C. Tsai, G. Anwar, and M. Tomizuka. Discrete time repetitive control for robot manipulators. In *IEEE Conference on Robotics and Automation*, pages 1341–1346, 1988.

[TCY90] M. Tomizuka, K.-K. Chew, and W.-C. Yang. Disturbance rejection through an external model. *ASME Journal of Dynamic Systems, Measurement, and Control*, 112(4):559–564, 1990.

[TK85] M. Tsutomu and E. Kato. Iterative control and its application to motion control of robot arm – a direct approach to servo-problems. In *Proceedings of IEEE Conference on Decision and Control*, pages 1393–1398, 1985.

[TN92] T.-C. Tsao and M. Nemani. Asymptotic rejection of periodic disturbances with uncertain period. In *Proceedings of the American Control Conference*, pages 2696–2699, 1992.

[Tom87] M. Tomizuka. Zero phase error tracking algorithm for digital control. *ASME Journal of Dynamic Systems, Measurement, and Control*, 109(1):65–68, 1987.

[Tom93] M. Tomizuka. On the design of digital tracking controllers. *ASME Journal of Dynamic Systems, Measurement, and Control*, 115(2B):412–418, 1993.

[TT87] Tsao T.-C. and M. Tomizuka. Adaptive zero phase error tracking algorithm for digital control. *ASME Journal of Dynamic Systems, Measurement, and Control*, 109(4):349–354, 1987.

[TT88] T.-C. Tsao and M. Tomizuka. Adaptive and repetitive digital control algorithms for noncircular machining. In *Proceedings of the American Control Conference*, pages 115–120, 1988.

[TT94] T.-C. Tsao and M. Tomizuka. Robust adaptive and repetitive digital tracking control and applications to hydraulic servo for noncircular machining. *ASME Journal of Dynamic Systems, Measurement, and Control*, 116:24–32, 1994.

[TTC88] M. Tomizuka, T.-C. Tsao, and K.-K. Chew. Discrete-time domain analysis and synthesis of repetitive controllers. In *Proceedings of the American Control Conference*, pages 860–866, 1988.

[TTC89] M. Tomizuka, T.-C. Tsao, and K.-K. Chew. Analysis and synthesis of discrete-time repetitive controllers. *ASME Journal of Dynamic Systems, Measurement, and Control*, 111(3):353–358, 1989.

[TUT93a] E.D. Tung, Y. Urushisaki, and M. Tomizuka. Algorithm for high-speed control of machine tools. In *Proceedings of the American Control Conference*, pages 1966–1970, 1993.

[TUT93b] E.D. Tung, Y. Urushisaki, and M. Tomizuka. Low velocity friction compensation for machine tool feed devices. In *Proceedings of the American Control Conference*, pages 1932–1936, 1993.

[TY85] M. Togai and O. Yamano. Analysis and design of an optimal learning control scheme for industrial robots: A discrete system approach. In *Proceedings of IEEE Conference on Decision and Control*, pages 1399–1404, 1985.

[Vid85] M. Vidyasagar. *Control System Synthesis: A Factorization Approach*. MIT Press, 1985.

[Vin93] G. Vinnicombe. *Measuring the Robustness of Feedback Systems*. PhD thesis, University of Cambridge, 1993.

[Vin98] G. Vinnicombe. *Uncertainty and Feedback – $\mathcal{H}_\infty$ Loop-shaping and the ν-gap Metric.* Imperial College Press, 1998. In Press.

[Wei91] G. Weiss. Representation of shift-invariant operators on $\mathscr{L}_2$ by $\mathcal{H}_\infty$ transfer functions: An elementary proof, a generalization to $\mathscr{L}_p$, and a counterexample for $\mathscr{L}_\infty$. *Mathematics of Control, Signals, and Systems*, 4:193–203, 1991.

[Wei96] G. Weiss. Repetitive control systems: Old and new ideas. In *Mathematical Theory of Networks and Systems.* Birkhäuser-Verlag, 1996.

[WH97] G. Weiss and M. Häfele. Repetitive control of MIMO systems using $\mathcal{H}_\infty$ design. Preprint, 1997.

[Wil71] J.C. Willems. *The Analysis of Feedback Systems.* M.I.T. Press, 1971.

[Yam93] Y. Yamamoto. Learning control and related problems in infinite-dimensional systems. In H.L. Trentelman and J.C. Willems, editors, *Essays on Control: Perspective in the Theory and its Applications*, pages 191–222. Birkhäuser, 1993.

[ZDG96] K. Zhou, J.C. Doyle, and K. Glover. *Robust and Optimal Control.* Prentice-Hall, 1996.